MOLECULAR INTERACTION
OF Ca-PUMP ATPase
IN SARCOPLASMIC RETICULUM MEMBRANE

KAZUO YAMASAKI

DEPARTMENT OF BIOLOGY

FACULTY OF SCIENCE

OSAKA UNIVERSITY

1992

CONTENTS

ABBREVIATIONS

AMP-PNP	adenyl-5'-imidodiphosphate
$C_{12}E_8$	octaethylene glycol monododecylether
$C_{12}E_9$	polyoxyethylene-9-laurylether
DMSO, Me_2SO	dimethyl sulfoxide
DOC	deoxycholate
DTNB	5,5'-dithiobis(2-nitrobenzoic acid)
EDTA	Ethylenediaminetetraacetic acid
EGTA	ethylene glycol bis(β-aminoethyl ether) -N,N,N',N'-tetraacetic acid
EP	phosphoenzyme
FITC	fluorescein isothiocyanate
IAEDANS	N-iodoacetyl-N'-(5-sulfo-1-naphtyl) ethylenediamine
LDS	lithium dodecyl sulfate
PBM	N,N'-(1,4-phenylene)bismaleimide
SDS	sodium dodecyl sulfate
SR	sarcoplasmic reticulum
TFA	trifluoroacetic acid.
TES	N-Tris(hydroxymethyl)methyl -2-aminoethane sulfonate.

GENERAL INTRODUCTION

The contraction and relaxation cycle of muscle cells is regulated by intracellular Ca^{2+} concentration. In the relaxed state, concentration of free Ca^{2+} in the cell is maintained below 1 μM. Ca^{2+} concentration is modulated by a complex membrane system in the muscle cell which consists of the two components of the plasma membrane, which contains tubular infoldings (the transfer system, "T-system") running transverse to the fiber axis, and the intracellular membrane network known as the sarcoplasmic reticulum (SR) (1). The T-system and terminal cisternae of the SR are interconnected through a feet protein in a structure called "triad" (Fig. 1). When the muscle cell is excited, the depolarization at plasma membrane is transferred to interior of the cell via the T-system, which then induces Ca^{2+} release from the SR. Subsequently, myofibrils are activated by the released Ca^{2+}, and muscle contraction is induced. This process is called "excitation-contraction coupling." During the relaxation phase, the intracellular Ca^{2+} is reabsorbed into the SR lumen by the Ca^{2+}-pump protein in its longitudinal section, and intracellular Ca^{2+} concentration decreases.

The principal protein of the SR membrane is a Ca^{2+}-dependent ATPase that consists of a single type of polypeptide chain having molecular weight of approximately 115,000 (3). The Ca^{2+}-ATPase protein accounts for more than 70% of the total SR protein. Reconstituted vesicles obtained from purified Ca^{2+}-ATPase and excess lipid exhibit marked Ca^{2+} accumulation in the presence of ATP (4), suggesting that Ca^{2+}-ATPase is the key enzyme involved in active transport of Ca^{2+} across the SR membrane.

It has been established by a number of investigators that

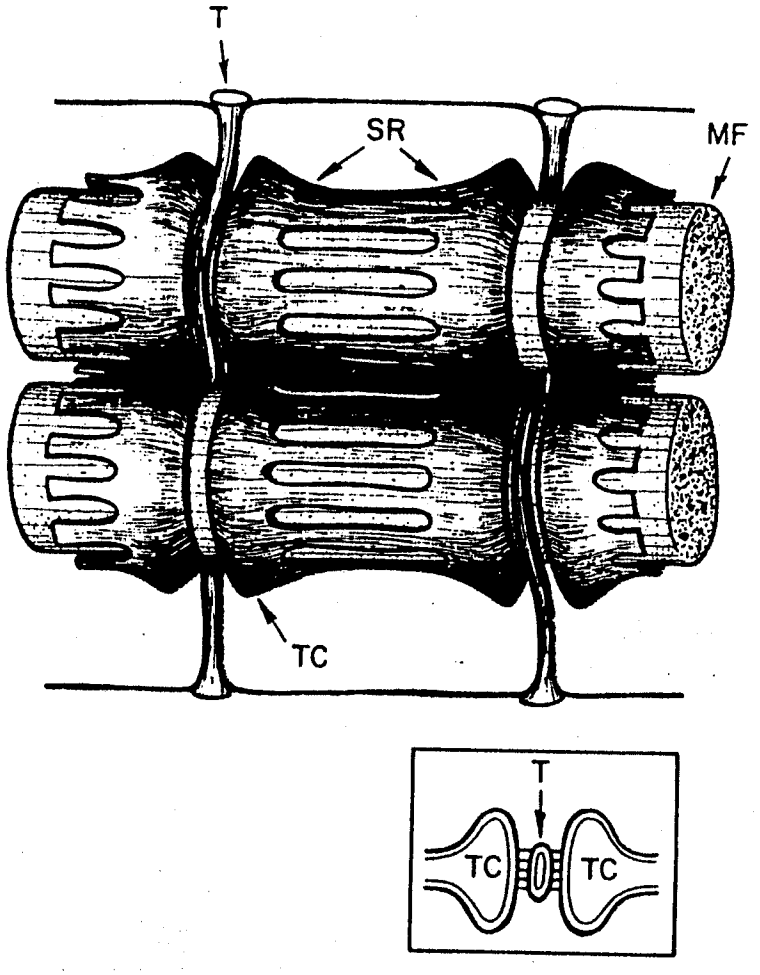

Fig. 1 Schematic representation of the relationship between sarcoplasmic reticulum (SR), T-System (T), and Myofibrils (MF), TC, terminal cisternae. The inset is a representation of the triad. From Ref. 2.

SR membrane transports 2 mol Ca^{2+} per 1 mol ATP hydrolyzed (5). Based on kinetic analysis of partial and overall reactions of Ca^{2+}-ATPase, the reaction scheme described below has been proposed as the mechanism of coupling of ATP hydrolysis to Ca^{2+}-transport (Fig. 2). The reaction cycle of ATP hydrolysis by Ca^{2+}-ATPase proceeds via two kinds of phosphorylated intermediates (E_1P and E_2P) and with two free enzyme states (E_1 and E_2)(6). In the E_1 state, Ca^{2+}-ATPase has high affinity Ca^{2+}-binding sites (Kd-10^{-7}M) oriented toward the cytoplasmic side of the SR, while, in the E_2 state, it has low affinity Ca^{2+} binding sites (Kd>10^{-3} M) oriented toward the luminal side of the SR. The first step of Ca^{2+} transport cycle of Ca^{2+}-ATPase is binding of Ca^{2+} and ATP to E_1 state Ca^{2+}-ATPase. E_1 state Ca^{2+} ATPase has two Ca^{2+} binding sites per one catalytic site, and its binding exhibits co-operative behavior (5,7-13). In the second step, an ADP-sensitive phosphoenzyme (E_1P) is formed by transfer of the ATP terminal phosphate to an aspartyl residue of the catalytic site (14-19). At the same time, the bound Ca^{2+} is occluded by this enzyme (13,20-23). E_1P is instantaneously consumed when large amounts of EGTA and ADP are added simultaneously; this is accompanied by formation of ATP in the reverse reaction from E_1P and ADP (24-30). In the third step, E_1P converts into ADP-insensitive phosphoenzyme (E_2P) (24,31-35). During the conversion from E_1P into E_2P, Ca^{2+}-binding sites of Ca^{2+}-ATPase markedly decrease in affinity for Ca^{2+}. At the same time,the orientation of the Ca^{2+} binding sites changes from the cytoplasmic to luminal side of the SR membrane. As a result, 2 moles of Ca^{2+} are released on the luminal side of SR (33). In the fourth step, E_2P is hydrolyzed to

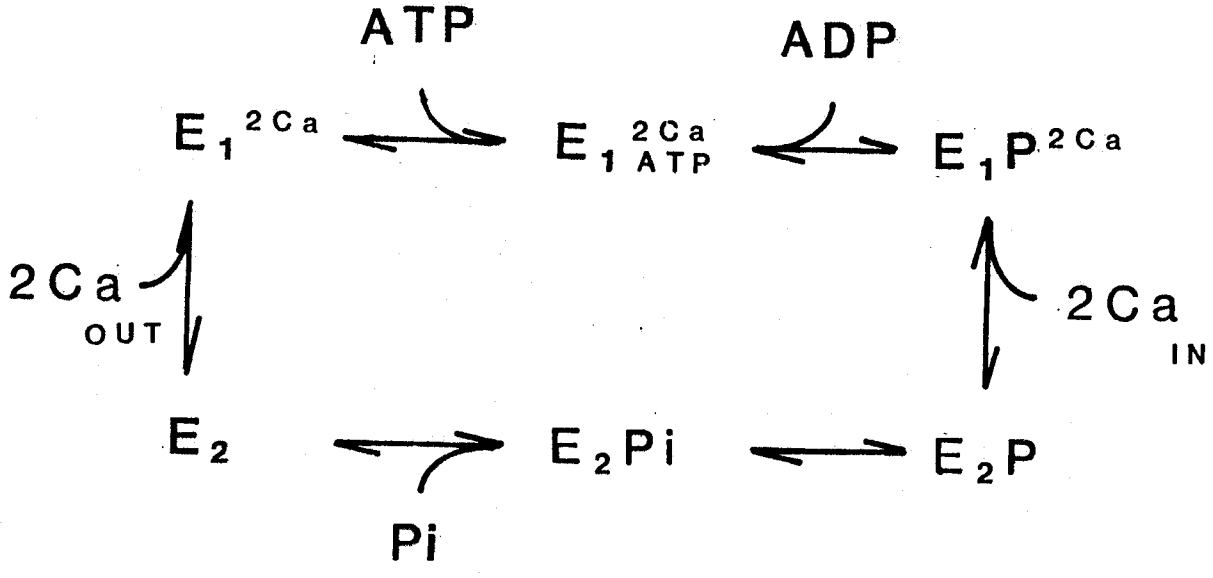

Fig. 2 Catalytic cycle of Ca^{2+}-ATPase----- E_1 and E_2 are enzyme forms capable of reacting with ATP and Pi, respectively. E_1P indicates the ADP-sensitive phosphoenzyme. E_2P indicates the ADP-insensitive phosphoenzyme. E_2Pi indicates the enzyme-phosphate complex

form inorganic phosphate (Pi) and the free enzyme (E_2.) At the last step of this catalytic cycle, Ca^{2+}-ATPase converts from E_2 to E_1. The catalytic cycle of Ca^{2+}-ATPase is completely reversible. When EGTA, Pi and ADP are added to medium containing SR vesicles that have been loaded with Ca, Ca^{2+} is released from the vesicles into the outer medium. This Ca^{2+} efflux is coupled to the formation of ATP at the ratio of $2Ca^{2+}$/ATP (36-39). Therefore, the overall free-energy requirement for ATP is attributed to dissipation of the transmembrane Ca^{2+} gradient. Such reversal of the Ca^{2+} transport cycle includes formation of a phosphorylated intermediate (E_2P) by incorporation of Pi into the enzyme (40,41). This phosphoenzyme is chemically equivalent to that formed by utilization of ATP in the forward reaction.

To understand the molecular mechanism of active transport, it is essential to know the structural features of the protein that allow coupling between the spatially distinct sites of nucleotide hydrolysis and ion transport. Ca^{2+}-ATPase (115,000 daltons) is digested by trypsin into A and B fragments with respective molecular weights of about 55,000 and 45,000 (42-46). Further digestion results in the cleavage of A fragment into A_1 and A_2 with respective molecular weights of about 30,000 and 20,000. The phosphorylation site is located on the A_1 tryptic fragment (43), and the fluorescein isothiocyanate (FITC) binding site, which is considered to be a nucleotide binding site is located the B fragment (47). The entire amino acid sequence of Ca^{2+}-ATPase has been deduced from its complementary DNA sequence (48). MacLennan, Green and co-workers proposed the model of the secondary and tertiary structures of this enzyme shown in Fig. 3

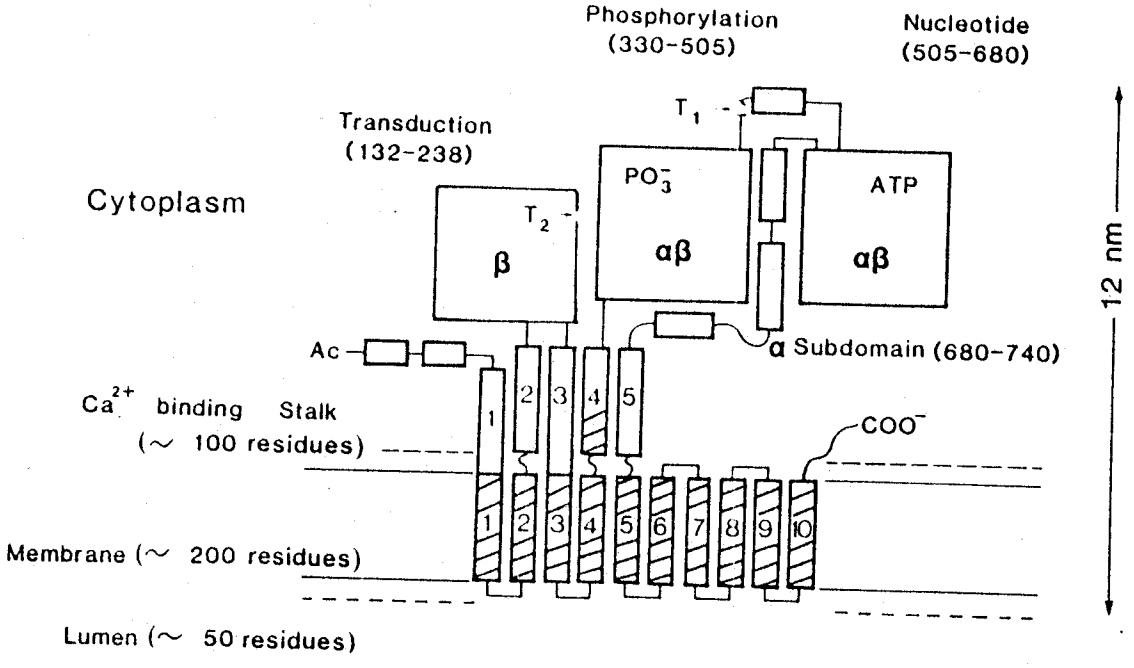

Fig. 3 Model of the secondary and tertiary structures of the Ca^{2+}-ATPase peptide based on the amino acid sequence. The globular domain projecting into the cytoplasm forms three distinct subdomains that are connected with ten transmembrane helices through five amphipatic 'stalk' helices. T_1 and T_2 indicate two accessible tryptic cleavage sites (at Arg-505 and Arg-198, respectively). From Ref. 49.

(49). In this model, Ca^{2+}-ATPase has ten transmembrane segments (M_1-M_{10}) and three large cytoplasmic subdomains. The phosphorylation site (Asp-351) and FITC binding site (Lys-515) are located on separate cytoplasmic subdomains located between M_4 and M_5. Residues forming amphiphatic helices are arranged in a 'stalk' connecting the transmembrane domain with the globular cytoplasmic domain. Residues involved in high-affinity Ca^{2+} binding to Ca^{2+}-ATPase were identified through site-directed mutagenesis (50). These residues are located on the transmembrane segments M_4-M_6 and M_8.

One of the major problems in understanding the molecular basis for the Ca^{2+}-pump is the quaternary structure of Ca^{2+}-ATPase; the question of whether an oligomer or a monomer of Ca^{2+}-ATPase functions as the structural unit for the Ca^{2+}-transport in the the intact SR membrane is still controversial. Many observations suggest that Ca^{2+}-ATPase is an oligomer in the SR membrane. Observation by freeze-fracture electron microscopy has indicated that the surface particles are present 2-4 times higher average density than the intramembranous particle (51-54). Vanderkooi and co-worker, who observed fluorescence-energy transfer between probes attached to different Ca^{2+}-ATPase molecules in the same vesicle, suggested that the energy transfer takes place within oligomeric complexes (55). Peptide cross-linking with bifunctional reagents has led to demonstration of dimers as well as tetramers (56-58). Peptide-peptide interaction in the membrane is suggested by observation of immobilization of spin-labels attached to Ca^{2+}-ATPase (59,60). Ca^{2+}-ATPase has a tendency to form an oligomer even when the Ca^{2+}-ATPase is

solubilized by detergents such as Triton X-100, deoxycholate, and $C_{12}E_8$ (61). However, it has not been determined whether molecular interaction of Ca^{2+}-ATPase plays an important role in the Ca^{2+}-transport cycle. A finding that has been considered support the concept interaction between catalytic sites on subunits is the relatively low maximum level of steady state phosphorylation. The EP levels most commonly reported in the literature correspond to 3-4 nmol per mg of total SR protein. Stoichiometry of 3-4 nmol/mg is less than would be expected (7-8 nmol/mg) based on the properties of SDS gel, in which a band including the 115,000 dalton ATPase chain accounts for most of the protein (62-64). This observation would accord with the idea that only one subunit of a dimer can exist in a phosphorylated form (half of the site reactivity). Recently, Suzuki et al. observed that one high affinity ATP binding site and one low affinity ATP binding site are present per every one phosphorylatable site (65). The other observations also suggest the coupling of molecular interaction with Ca^{2+}-transport. It was observed that the molecular interaction of Ca^{2+}-ATPase changes during the transport cycle. The Ca^{2+}-ATPase forms a two-dimensional crystal on the SR membrane surface under certain condition (66). Incubation of the SR membrane with vanadate as a phosphate analogue (or with phosphate at acid pH) under Ca^{2+}-free condition leads to two dimensional crystallization with a dimeric Ca^{2+}-ATPase as the unit cell. On the other hand, Ca^{2+} as well as lanthanide ions induce membrane crystals with a monomer as the minimum asymmetric unit. HPLC studies of $C_{12}E_8$-solubilized Ca^{2+}-ATPase present in reversible monomer-oligomer equilibrium have been carried out in

the presence of various ligands and during turnover (61). Under these conditions, ATP, vanadate and phosphoenzyme turnover shift the equilibrium toward monomers.

However, some workers consider that the catalytic function of Ca^{2+}-transport can be performed by ATPase as a monomer, Ca^{2+}-ATPase monomerized by detergent possesses all fundamental Ca^{2+}-dependent ATPase activities. It was directly demonstrated by 'active enzyme centrifugation' that the catalytic activity in predominantly monomeric Ca^{2+}-ATPase preparation sediments at the same rate as the monomeric peptide did (67). In addition, it has been shown that the monomeric Ca^{2+}-ATPase peak observed by HPLC splits ATP during its passage down the column. Those reconstituted vesicles with excess phospholipid (lipid to protein weight ratio 800-900:1) show Ca^{2+} accumulation (68). In these vesicles, Ca^{2+}-ATPase is assumed to exist as a monomer.

Therefore, definition of the minimal functional unit for the Ca^{2+}-ATPase coupled with Ca^{2+}-pump represents a major challenge in structural and functional studies of SR.

The present study is a continuation of attempts to obtain direct evidence for the coupling between the molecular interactions of Ca^{2+}-ATPase and Ca^{2+}-transport in the SR membrane. This study consists of four parts as follows:
Part I: The first approach is to analyze vanadate binding to membrane bound Ca^{2+}-ATPase under a variety of conditions. I found that 0.5 mol of high affinity and 0.5 mol of low affinity vanadate binding sites are present per 1 mol of Ca^{2+}-ATPase. When SR membrane was solubilized by a nonionic detergent, $C_{12}E_9$, only 1 mol of single sites exists per 1 mol of Ca^{2+}-ATPase. These

results strongly suggest that, in intact SR membrane, the Ca^{2+}-ATPase exists in dimeric form, and that a catalytic site can be formed by the interaction between the ATPase molecules in the dimer.

Part II: I investigated inhibition of E_2P formation by vanadate was investigated in detail. The vanadate binding to low-affinity sites resulted in the competitive inhibition of E_2P formation. This inhibition was easily reversed when vanadate concentration was reduced by dilution. Vanadate binding to high-affinity sites also inhibited E_2P formation. However, the phosphorylation activity was restored very slow when the vanadate effect was reversed by chelation of Mg^{2+} with EDTA.

Part III: Ca^{2+}-ATPase was cross-linked by N,N'-(1,4-phenylene) bismaleimide (PBM). The intermolecular cross-linking was greatly affected by the binding of AMP-PNP or vanadate to Ca^{2+}-ATPase. Under ligand free condition, high-order oligomeric ATPase was formed by cross-linking without accumulation of any particular oligomer. When SR was reacted with PBM under the condition where nucleotide binding site was occupied by the ATP analogue AMP-PNP, predominantly dimeric Ca^{2+}-ATPase was formed. Under this condition, ATPase molecules were cross-linked through an SH-group in the A_1 region of the enzyme. When SR was reacted with PBM in the presence of vanadate, oligomerization of Ca^{2+}-ATPase by PBM was strongly inhibited.

Part IV: The primary structure of the cross-linking site on the Ca^{2+}-ATPase was determined after modification of SR with PBM. Under ligand free condition, Ca^{2+}-ATPase was cross-linked with PBM at Cys-377 and Cys-614 to form high order oligomer. On the

other hand, Ca^{2+}-ATPase was cross-linked with PBM at Cys-377 to form a dimer only in the presence of AMP-PNP. These results suggest that the molecular interaction of the Ca^{2+}-ATPase in the intact SR membrane may alter during the reaction cycle. In conclusion, ATPase-ATPase interaction plays an important role in Ca^{2+}-transport across the SR membrane.

REFERENCES

1. Peachey,L.D., & Franzini-Armsyrong,C. (1983) in "Handbook of Physiology; Skeletal Muscle" (Peachey,L.D., & Adrian,R.H. eds.) pp. 23-72, American Physiological Society, Bethesda.
2. deMeis,L (1981) in The Sarcoplasmic Reticulum. John Wiley & Sons, New York
3. MacLennan,D.H. (1970) J.Biol.Chem. 245, 4508-4518
4. Racher,E. (1972) J.Biol.Chem. 247, 8198-8200
5. Hasselbach,W. (1964) Prog.Biophys.Mol.Chem. 14, 167-222
6. deMeis,L. & Vianna,A. (1979) Ann.Rev.Biochem. 48, 275-292
7. Kanazawa,T., Yamada,S., Yamamoto,T., & Tomomura,Y. (1971) J.BioChem. 70, 95-123
8. Meissner,G. (1973) Biochim.Biophys.Acta 298, 906-926
9. Inesi,G., Kurzmack,M., Coan,C., & Lewis,D.E. (1980) J.Biol.Chem. 3025-3031
10. Dupont,Y. (1982) Biochim.Biophys.Acta 688, 75-87
11. Champeil,P., Gingold,M.P., Guillan,F. & Inesi,G. (1983) J.Biol.Chem. 255, 3025-3031
12. Nakamura,J. (1986) Biochim.Biophys.Acta 870, 495-501
13. Inesi,G. (1987) J.Biol.Chem. 262, 16338-16342
14. Makinose,M. (1969) Eur.J.Biochem. 10, 74-82
15. Ymamoto,T., & Tomomura,Y. (1968) J.Biochem. 64, 137-145
16. Degani,C., & Boyer,P.D. (1973) J.Biol.Chem. 248, 8222-8226
17. Froehlich,J.P., & Taylor,E.W. (1975) J.Biol.Chem. 250, 2013-2021
18. Allen,G., & Green,N.M. (1976) FEBS Lett. 63, 188-192
19. Stahl,N., & Jencks,W.P. (1987) Biochemistry 26, 7654-7667

20. Sumida,M., & Tomomura,Y. (1974) J.Biochem. 75, 283-297

21. Kuzmack,M., Verjovski-Almeida,S., & Inesi,G. (1977) Biochem.Biophys.Res.Commun. 78, 772-776

22. Dupont,Y. (1980) Eur.J.Biochem. 109, 231-238

23. Takisawa,H., & Makinose,M. (1981) Nature 290, 271-273

24. Takisawa,H., & Makinose,M. (1983) J.Biol.Chem. 258, 2986-2992

25. Sigekawa,M., & Dougherty,J.P. (1978) J.Biol.Chem. 253, 1458-1464

26. Takisawa,H., & Tomomura,Y. (1979) J.Biochem. 86, 425-441

27. Yamada,S., & Ikemoto,N. (1980) J.Biol.Chem. 255, 3108-3119.

28. Shigekawa,M., Wakabayashi,S., & Nakamura,H. (1983) J.Biol.Chem. 258, 14157-14161

29. Andersen,J.P., Jørgensen,P.L., & Møller,J.V. (1985) Proc. Natl.Acad.Sci.US 82, 4573-4577

30. Andersen,J.P., Lassen,K., & Møllar,J.V. (1985) J.Biol.Chem. 260, 371-380

31. Makinose,M. (1973) FEBS Lett. 37, 140-143

32. Ikemoto,N. (1986) J.Biol.Chem. 251, 7275-7277

33. Nakamura,Y. & Tonomura,Y (1982) J.Biochem. 91, 449-461

34. deMeis,L., & Inesi,G. (1985) Biochemistry 25,7623-7633

35. Khananshivili,D., & Jencks,W.P. (1988) Biochemistry 27, 2943-2952

36. Makinose,M., & Hasselbach,W. (1971) FEBES Lett. 12, 271-272

37. Yamada,S., Sumida,M., & Tonomura,Y. (1972) J.Biochem. 72, 1537-1548

38. Knowles,A.F., & Racker,E. (1975) J.Biol.Chem. 250, 1949-1951

39. deMeis,L., & Tume,R.K. (1977) Biochemistry 16, 4455-4463

40. Masuda,H. & deMeis,L. (1973) Biochemistry 12, 4581-4585

41. Kanazawa,T. & Boyer,P.D. (1973) J.Biol.Chem 248,3163-3172

42. Migala,A., Agostini,B., & Hasselbach,W. (1973) Z.Naturforsch 28c, 178-182

43. Thorlry-Laowson,D.A., & Green,N.M. (1973) Eur.J.Biochem. 40,403-413

44. Ikemoto,N., Sreter,F.A., & Gargely,J. (1971) Arch.Biochem. Biophys. 147, 571-582

45. Inesi,G., & Scales,D. (1974) Biochemistry 13, 3298-3306

46. Stweart,P.S. & MacLennan,D.H. (1974) J.Biol.Chem. 249, 985-993

47 Mitchinson,C., Wilderspin,A.F., Trinnaman,B.J. & Green,N.M. (1982) FEBS Lett. 146, 87-92

48. Brandl,C.J., Green,N.M. Korczak,B. & MacLennan, D.H. (1986) Cell 44, 597-607

49. MacLennan,D.H., Brandl,C.J., Korczak,B., & Green,N.M. (1985) Nature 316, 696-700

50. Clarke,D.M., Loo,T.W., Inesi,G., MacLennan,D.H. (1989) Nature 339, 476-478

51. Jilka,R.L., Martonosi,A.N., & Tillack,J.W. (1975) J.Biol. Chem. 250, 7511-7524

52. Scales,D. & Inesi,G. (1976) Biophys.J. 16, 735-751

53. Wang,C.T.,Saito,A. & Fleischer,S. (1979) J.Biol.Chem. 254, 9209-9219

54. Napolitano,C.A., Cooke,P., Segalman,K. & Herbette,L. (1983) Biophys.J. 42, 119-125

55. Vanderkooi,J.M., Ierokomas,A. Nakamura,H., & Marutonosi,A. (1977) Biochemistry 16, 1262-1267

56. Louis,C.F.,& Shooter,E.M. (1972) Arch.Biochem.Biophys. 153,

641-655

57. Baskin,R.J. & Hanna,S. (1979) Biochim.Biophys.Acta 576, 61-70

58. Murphy,A.J. (1976) Biochem.Biophys.Res.Commun. 70, 160-166

59. Anderson,J.P., LeMaire,M., & Møllar,J.V. (1980) Biochim. Biophys.Acta 603,84-100

60. Anderson,J.P., Fellmann,P., Møllar,J.V. & Devaux,P.F. (1981) Biochemistry 20, 4928-4936

61. Anderson,J.P., & Vilsen,B. (1985) FEBS Lett. 189, 13-17

62. Froehlish,J.P., & Taylor,E.W. (1975) J.Biol.Chem. 261, 3654-3660

63. Verjovski-Almeida,S. Kurzmack,M. & Inesi,G. (1978) Biochemistry 17, 5006-5013

64. Ferreira,S.T. & Verjovski-Almeida,S. (1988) J.Biol.Chem. 263, 9973-9980

65. Suzuki,H., Kubota,T., Kubo,K., & Kanazawa,T. (1990) Biochemistry 29, 7040-7045

66. Dux,L., Taylor,K.A., Ting-Beall,H.P. & Martomosi,A. (1985) J.Biol.Chem. 260,11730-11743

67. Martin,D.W. (1983) Biochemistry 22, 2276-2282

68. Heegaard,C.W., LeMaire,M., Gulik-Krzywick,T., & Møllar,J.V. (1990) J.Biol.Chem. 265, 12020-12028

Part I

Existence of High- and Low-Affinity Vanadate-Binding Sites on Ca^{2+}-ATPase of the Sarcoplasmic Reticulum

SUMMARY

The binding of vanadate to isolated sarcoplasmic reticulum (SR) membranes was measured colorimetrically by equilibrium sedimentation and ion exchange column filtration. The concentration dependence of vanadate binding exhibited a biphasic curve with two phases of equal amplitude. A similar biphasic curve of the vanadate dependence was observed with the purified Ca^{2+}-ATPase prepared by deoxycholate extraction. Sites of vanadate binding could be classified into two distinct species based on apparent affinity; the high-affinity binding sites have a dissociation constant below 0.1 μM, and the low-affinity sites one of 36 μM. The maximum amount of vanadate bound to each of the high- or low-affinity sites was estimated to be 2.6 - 3.6 nmol/mg SR protein, which corresponds to approximately 0.5 mol of vanadate bound per mol of Ca^{2+}-ATPase. These results indicate that one mol of Ca^{2+}-ATPase contains 0.5 mol of high-affinity vanadate-binding sites as well as 0.5 mol of low-affinity vanadate-binding sites. Vanadate binding to the low-affinity sites was competitively inhibited by inorganic phosphate, while vanadate binding to the high-affinity sites resulted in a non-competitive inhibition of the phosphoenzyme formation from inorganic phosphate. When SR membranes were solubilized with polyoxyethylene-9-laurylether ($C_{12}E_9$), the vanadate binding exhibited a monophasic concentration dependency curve with a dissociation constant of 13 μM. The number of vanadate-binding sites was estimated to be 7.2 nmol/mg SR protein which represents about one mol of site per mol of Ca^{2+}-ATPase. Vanadate binding to

the solubilized Ca^{2+}-ATPase was competitively inhibited by inorganic phosphate. When the detergent was removed to reconstitute SR membrane, vanadate binding again exhibited a biphasic concentration dependency curve. These results indicate that interactions between the ATPase molecules in intact SR membranes may involve the cooperative binding of vanadate to the enzyme.

INTRODUCTION

The Ca^{2+}-ATPase of SR plays an important role in Ca^{2+} transport across the membrane (1). The reaction mechanism by which ATP hydrolysis is coupled to Ca^{2+} transport has been investigated extensively based on kinetic measurements (1,2) as well as on structural studies (3-6). To obtain a better understanding of the molecular basis of active transport, more detailed information is needed concerning the structural features of the ATPase molecules in the SR membrane. A number of investigators have suggested that ATPase molecules exist in the SR membrane in an oligomeric form (7-15), though the functional role of the interaction between the ATPase molecules has not been defined well. There are several reports which indicate that two ATPase units in a dimer may interact to form half of the reactive site. This model is supported by the fact that only a half mole of the ATPase was phosphorylated by ATP even under the optimum conditions (16-18). Furthermore, evidence for changes in the ATPase-ATPase interaction in the Ca^{2+}-pump cycle have been obtained by analyzing the two-dimensional crystal structures of the enzyme molecules on SR membrane in the transition of the enzyme state between a phosphate-reactive form (E_2) and a nucleoside triphosphate-reactive form (E_1) (6), by measuring rotational motion of the enzyme in the phosphorylation step using saturation-transfer electron paramagnetic resonance (19), or by examining the effect of ligand binding on the oligomerization of the ATPase using molecular sieve HPLC (20). Previously we observed that cross-linking between the ATPase

molecules through PBM was markedly affected by incubation of the SR vesicles with PBM in the absence and presence of AMP-PNP or vanadate (21), and that Cys_{377} and Cys_{614} on the ATPase peptide seemed to be involved in the cross-linking between the ATPase molecules in the SR membrane (22).

In the present study, as an extension of previous work on the ATPase-ATPase interaction, we measured the binding of vanadate to Ca^{2+}-ATPase under Ca^{2+}-free conditions. We observed that high- and low-affinity vanadate binding sites exist equally at 0.5 mol per 1 mol of Ca^{2+}-ATPase in intact SR membrane, while only 1 mol of a single site per 1 mol of the ATPase exists after solubilization of the SR membrane by $C_{12}E_9$.

EXPERIMENTAL PROCEDURES

Materials------Sarcoplasmic reticulum (SR) was isolated from rabbit dorsal and hind limb white muscles by a method described previously (23). SR vesicles suspended in 60 mM KCl, 20% glycerol and 10 mM Tris-maleate (pH 7.0) were divided into small portions, rapidly frozen using liquid nitrogen and stored at -80° C. The Ca^{2+}-ATPase was partially purified from intact SR vesicles by deoxycholate extraction according to Meissner et al. (24). Monovanadate was prepared from V_2O_5 according to Goodno (25). AMP-PNP was obtained from Sigma. 4-(2-Pyridylazo)resorcinol was obtained from Dojin. $C_{12}E_9$ was obtained from Nikko Chemical. Bio-Beads SM-2 was obtained from Bio-Rad.

Measurement of vanadate binding to SR------Vanadate binding to SR vesicles was carried out at 23° C in assay medium containing 0.2-2.5 mg/ml SR protein, 0.1 M KCl, 20 mM TES (pH 7.2), 1 mM $MgCl_2$, 1 mM EGTA, 10% Me_2SO and 0-100 μM vanadate. After incubation, the SR vesicles were precipitated by centrifugation for 10 min at 100,000xg. The pellet was resuspended in 1 ml of 1% SDS for the determination of free vanadate concentration. The concentration of vanadate was measured by the method of Goodno using the metallochromic dye 4-(2-pyridylazo)resorcinol as an indicator (25). Vanadate binding to solubilized SR was carried out in medium containing 2.5 mg/ml SR, 30 mg/ml $C_{12}E_9$, 0.1 M KCl, 100 mM TES (pH 7.2), 1 mM $MgCl_2$, 1 mM EGTA, 10% Me_2SO and 0-100 μM vanadate. SR vesicles were solubilized with $C_{12}E_9$ immediately before addition of vanadate. The SR mixture (0.2 ml) was passed through a Dowex 2x8 (100-200 mesh) short column (about 0.2 ml) to

remove free vanadate. The eluted SR protein was denatured by 1% SDS for the determination of free vanadate concentration.

Phosphorylation Assay------Phosphorylation of SR by inorganic phosphate was performed in the medium containing 0.1 mg/ml SR, 0.1 M KCl, 20 mM TES (pH 7.2), 1 mM $MgCl_2$, 1 mM EGTA, 10% Me_2SO and 0-4 mM [^{32}P]phosphate. After incubation for 10 min at 23° C, the phosphorylation was quenched with 5% trichloroacetic acid containing 10 mM nonradioactive phosphate. The amount of phosphoenzyme (EP) formed was determined as described elsewhere (26).

RESULTS

Binding of Vanadate to SR Vesicles------The binding of vanadate to SR vesicles was measured at the protein concentration of 0.5 mg/ml by equilibrating the microsomes with an assay medium of 0.1 M KCl, 20 mM TES (pH 7.2), 1 mM $MgCl_2$, 1 mM EGTA, 10% Me_2SO and 0-100 μM vanadate at 23° C. After the incubation, the SR vesicles were sedimented by centrifugation at 100,000xg for 10 min and the amount of vanadate bound to the SR vesicles was determined as described in "EXPERIMENTAL PROCEDURES". As shown in Fig. 1A, the dependence of vanadate binding to SR vesicles on the added vanadate concentration showed a biphasic curve. In the low concentration range of vanadate, the affinity of vanadate to microsomes was extremely high, so that almost all the added vanadate was bound to SR vesicles. This high-affinity vanadate binding to SR vesicles was almost saturated with vanadate lower than 2 μM. Above this concentration, the amount of vanadate bound to SR also increased with increasing vanadate concentration, but the affinity was much lower than that in the low vanadate concentration range. These observations suggest that there exist two classes of vanadate-binding sites having greatly different affinities. In the presence of 1 mM AMP-PNP and 2 mM $CaCl_2$, the amount of vanadate binding was reduced to a very low level (Fig. 1A closed symbols). This level was proportional to the vanadate concentration and did not show a saturation curve at least under the conditions tested. When 10 mM EDTA was added to the reaction mixture, the amount of vanadate bound to SR vesicles was decreased to the same level as that obtained in the presence of

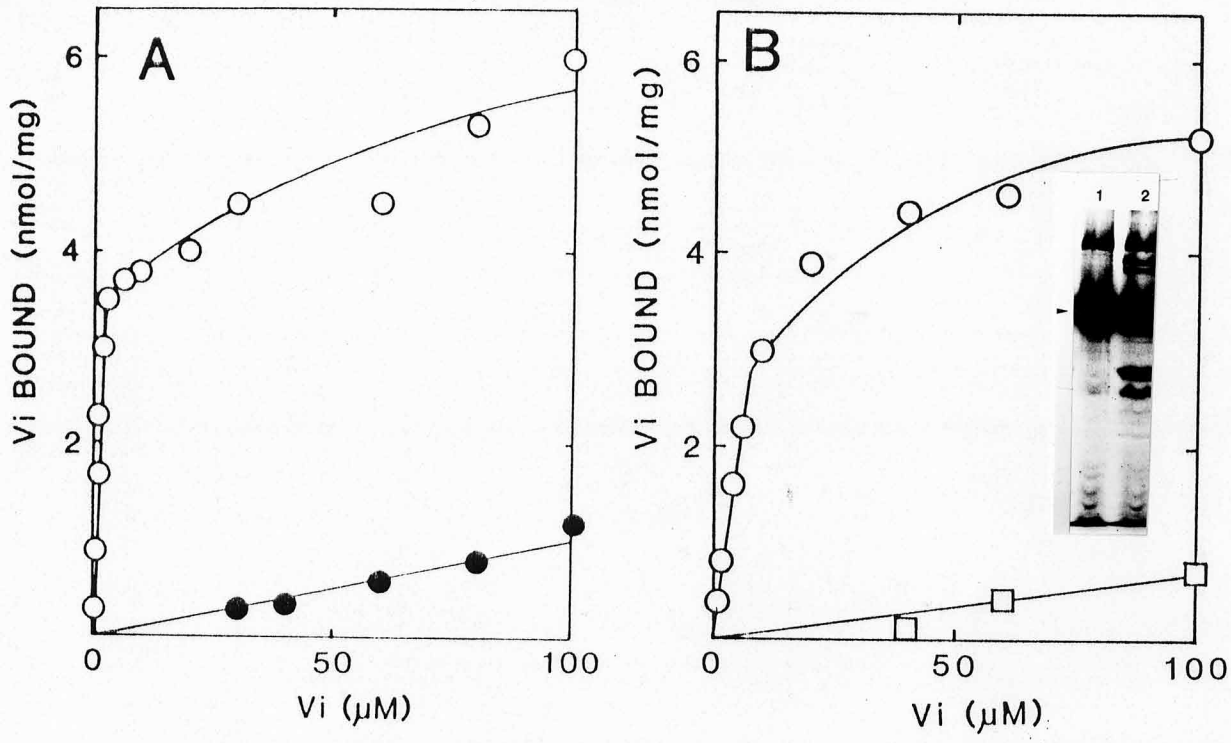

Fig.1 Vanadate binding to SR vesicles and purified Ca^{2+}ATPase----Panel A: SR vesicles (0.5 mg/ml) were incubated in assay medium containing 20 mM TES (pH 7.2), 0.1 M KCl, 1 mM $MgCl_2$, 1 mM EGTA and 0-100 μM vanadate in the absence (○) or presence (●) of 1 mM AMP-PNP and 2 mM $CaCl_2$. SR vesicles were sedimented by centrifugation, and bound vanadate was measured as described in "EXPERIMENTAL PROCEDURE." Panel B: Vanadate binding to the purified Ca^{2+}-ATPase (2.5 mg/ml) in the absence (○) or presence (□) of 10mM EDTA were measured as described above. The inset shows the SDS-PAGE pattern of purified Ca^{2+}-ATPase (lane 1) and native SR (lane 2). The arrowhead indicates the Ca^{2+}-ATPase band. The SDS-PAGE was performed on 7.5% gel according to the method of Laemmli (27).

AMP-PNP and Ca^{2+} (data not shown). We regarded the vanadate binding in the presence of AMP-PNP and Ca^{2+} or EDTA as a nonspecific one. In the following experiments, the specific amount of vanadate binding was expressed as the difference between the amounts of bound vanadate in the presence and absence of AMP-PNP and Ca^{2+}. In order to test the possibility that some SR protein(s) other than the Ca^{2+}-ATPase might be involved in the biphasic vanadate binding, the Ca^{2+}-ATPase was partially purified as described by Meissner et al.(24) and vanadate binding was measured under the same conditions as described above except for the protein concentration. Polyacrylamide gel electrophoresis of the purified enzyme preparation showed an essentially single band of Ca^{2+}-ATPase with a minor band of aggregated ATPase (see Ref. 24) and the content of SR proteins other than the Ca^{2+}-ATPase was negligibly small compared with that of the intact SR (Fig. 1B inset). Figure 1B showed that the dependence of vanadate binding to the purified enzyme preparation exhibited a biphasic curve similar to that obtained for the intact SR vesicles. These observations strongly suggest that these two different kinds of vanadate-binding sites are located on the Ca^{2+}-ATPase.

In Fig. 2, the amount of vanadate bound to the SR vesicles was plotted against the concentration of free vanadate. The high-affinity vanadate binding was almost saturated at a free vanadate concentration of about 0.2 μM, and the dissociation constant of high- affinity vanadate binding was too low to estimate (<0.1 μM). On the other hand, the vanadate binding to the low-affinity sites increased in the range of free vanadate concentration above 10 μM. As can be seen in the Fig. 2 inset, the Scatchard plot of

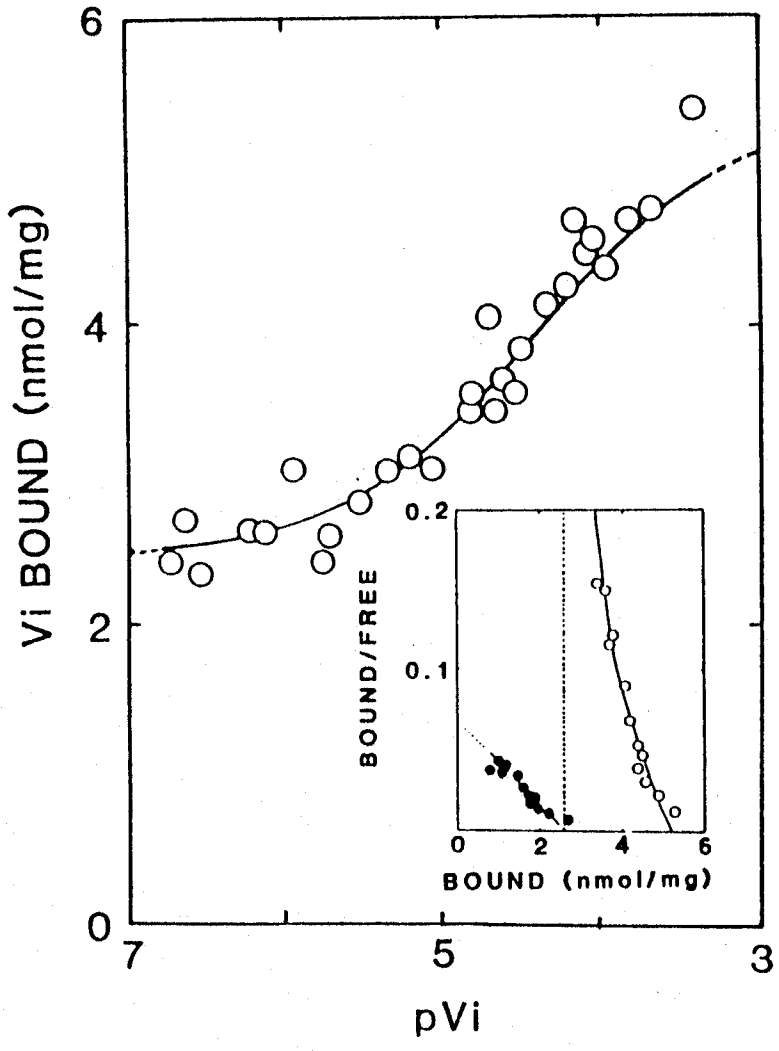

Fig. 2 Concentration dependence of vanadate binding to SR vesicles----Vanadate binding to SR vesicles (0.2-2.5 mg/ml protein) was measured as in Fig. 1. Free vanadate concentration given on the abscissa was determined from that of the supernatant after centrifugation of the SR mixture. The inset shows the Scatchard plot of vanadate binding in the range of free vanadate concentration above 10 μM (○). Closed symbols indicate low-affinity vanadate binding. The amounts of low affinity vanadate binding were determined on the assumption that the maximum amount of high affinity-vanadate binding was 2.6 nmol/mg SR protein with a dissociation constant of below 0.1 μM (dotted line).

low-affinity vanadate binding yielded a straight line (closed symbols) when we assumed that the number of the high-affinity sites was 2.6 nmol/mg SR protein and that the apparent dissociation constant for vanadate was below 0.1 μM. From this straight line, the maximum amount and dissociation constant of low-affinity vanadate binding were estimated as 2.6 nmol/mg SR protein and 36 μM, respectively. These data indicated that there exist equal numbers of high- and low-affinity vanadate binding sites on the Ca^{2+}-ATPase. The amount of bound vanadate varied from one preparation to another between 2.6 and 3.6 nmol/mg SR protein, which corresponds to approximately 0.5 mol of the binding site per mol of Ca^{2+}-ATPase, if we assume that 115,000-dalton ATPase accounts for 60-80% of the weight of the total SR proteins. With our SR preparation, 2.9-3.9 nmol E_1P/mg SR protein was formed by the reaction with ATP under optimum conditions, which corresponds to approximately 0.5 mol of phosphorylation site per mol of ATPase. This value agrees reasonably well with the number of high- or low-affinity vanadate- binding sites. From these observations, we concluded that 1 mol of the Ca^{2+}-ATPase contains 0.5 mol of high-affinity vanadate- binding site as well as 0.5 mol of low-affinity vanadate-binding site.

Effects of Phosphate on Vanadate Binding to SR Vesicles-----Many investigators have suggested that vanadate ion serves as an analogue of inorganic phosphate in the reaction of the E_1,E_2-type ATPases including the Ca^{2+}-ATPase (28,29). Therefore, it is of interest to examine the effects of phosphate on vanadate binding to the high- and low-affinity sites of the ATPase. Figure 3 shows the concentration dependence of vanadate binding at various

concentrations of phosphate. SR vesicles (2.5 mg/ml) were preincubated with 0, 0.5, and 1 mM phosphate at 23° C. Immediately after addition of vanadate, the SR mixture was centrifuged at 100,000xg for 10 min. The broken line in panel A shows the curve of vanadate binding to a site to which all the added vanadate is bound. If the affinity of the site for vanadate is very high, the amounts of bound vanadate will apparently increase as a linear function of the added ion until this site is saturated. If a low-affinity vanadate-binding site also exists in SR, an additional saturation curve with a low Kd for vanadate will be seen which crosses the broken line at the intercept, which indicates the maximum amount of vanadate bound to the high-affinity binding site. Therefore, the amount of vanadate bound to the low-affinity site can be obtained by subtracting the value of the intercept from the total bound vanadate at a given concentration. The data shown in Panel A indicate that the apparent dissociation constant of vanadate binding to the low-affinity site increased from 25 to 170 μM when the phosphate concentration in the reaction mixture was increased from 0 to 1 mM. The double-reciprocal plot of the low-affinity vanadate binding revealed that vanadate binding to the low-affinity site seemed to be competitively inhibited by phosphate (Fig. 3B). The data shown in Fig. 3A indicated that phosphate seemed to affect not only low- but also high-affinity vanadate binding. The maximum amount of vanadate bound to the high-affinity site as estimated from the intercept of the binding curve at the broken line was markedly decreased when phosphate concentration was increased. However, the phosphate effect on the high-affinity vanadate binding was

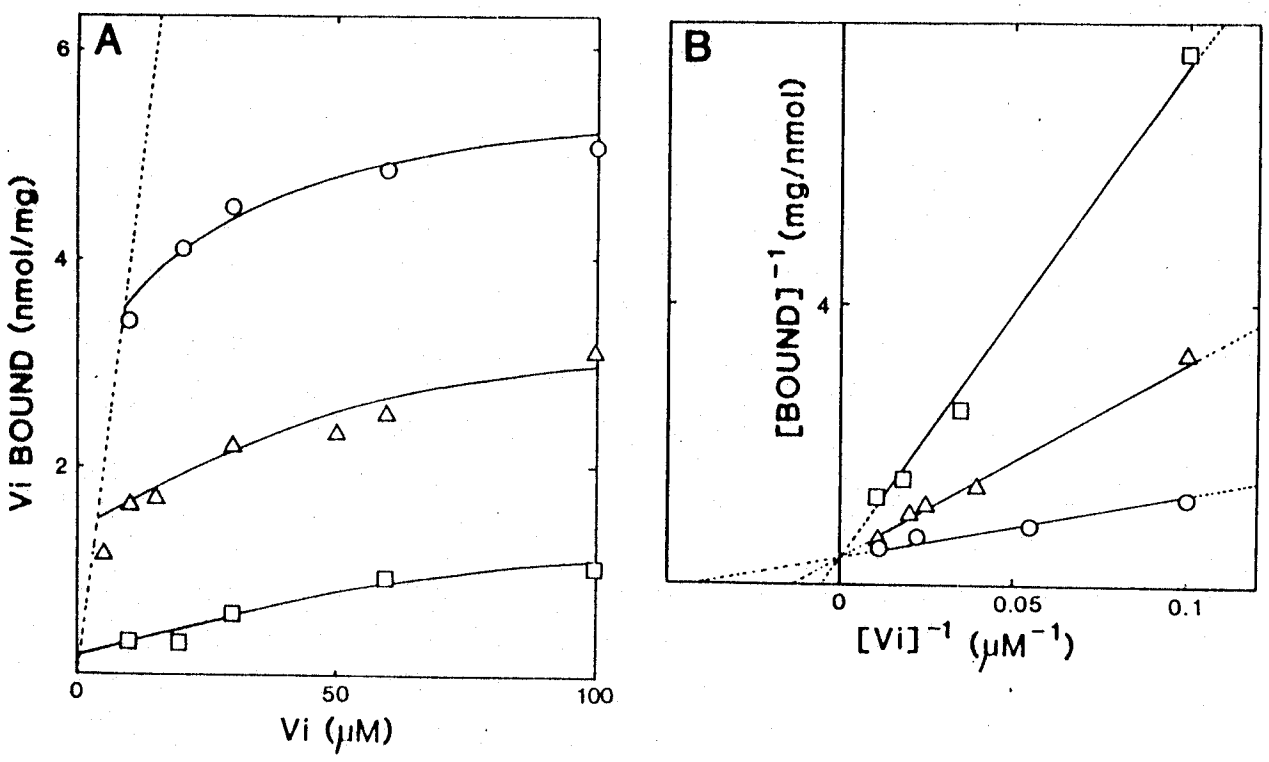

Fig. 3 Competitive inhibition of the low-affinity vanadate binding by inorganic phosphate.----Panel A: SR vesicles (2.5 mg/ml) were preincubated with 0 (○), 0.5 (△), or 1 mM (□) sodium phosphate in a solution containing 0.1 M KCl, 20 mM TES (pH 7.2), 1 mM $MgCl_2$, 1 mM EGTA and 10% Me_2SO. SR vesicles were incubated with 0-100 μM vanadate, then quickly centrifuged. The broken line indicates the amount of added vanadate (see text). Panel B: Double-reciprocal plot of the low-affinity vanadate binding. The amount of low-affinity vanadate binding was calculated by assuming that the amount of high-affinity vanadate binding was 3.3 (○), 1.5(△), and 0.2 nmol/mg(□), in the presence of 0, 0.5, and 1 mM phosphate, respectively.

complex, because regardless of the phosphate concentration, the intercept increased slowly and reached the control level in the absence of phosphate at about 10 min after the addition of vanadate (data not shown). On the other hand, the inhibition of the low-affinity vanadate binding by phosphate was not affected by changing the incubation time after the addition of vanadate. The cause of the slow change in the intercept remains unknown, but it is considered that the rate of vanadate binding to the high-affinity site may be much lower than that to the low-affinity sites.

Figure 4 shows the dependence of EP formation on the phosphate concentration at 0, 2, and 5 μM vanadate. SR vesicles (0.1 mg/ml) were incubated with various concentrations of phosphate at 23° C. Five minutes later, vanadate was added to the indicated concentration, and SR was further incubated for 10 min, then the reaction was terminated by the addition of 5% trichloroacetic acid. As shown in Fig. 4 A, the maximum level of E_2P at a saturating concentration of phosphate decreased from 1.9 to 0.2 nmol/mg protein when the vanadate concentration was increased from 0 to 5 μM. On the other hand, the Lineweaver-Burk plot of the data from Panel A revealed that the apparent Km for phosphate (1.4 mM) was not altered by vanadate at least up to 5 μM (Panel B in Fig. 4). At these low concentrations of vanadate, its binding to the low-affinity site of SR can be neglected (Fig. 2). Therefore, vanadate binding to the high-affinity sites of the ATPase seems to result in the non-competitive inhibition of E_2P formation.

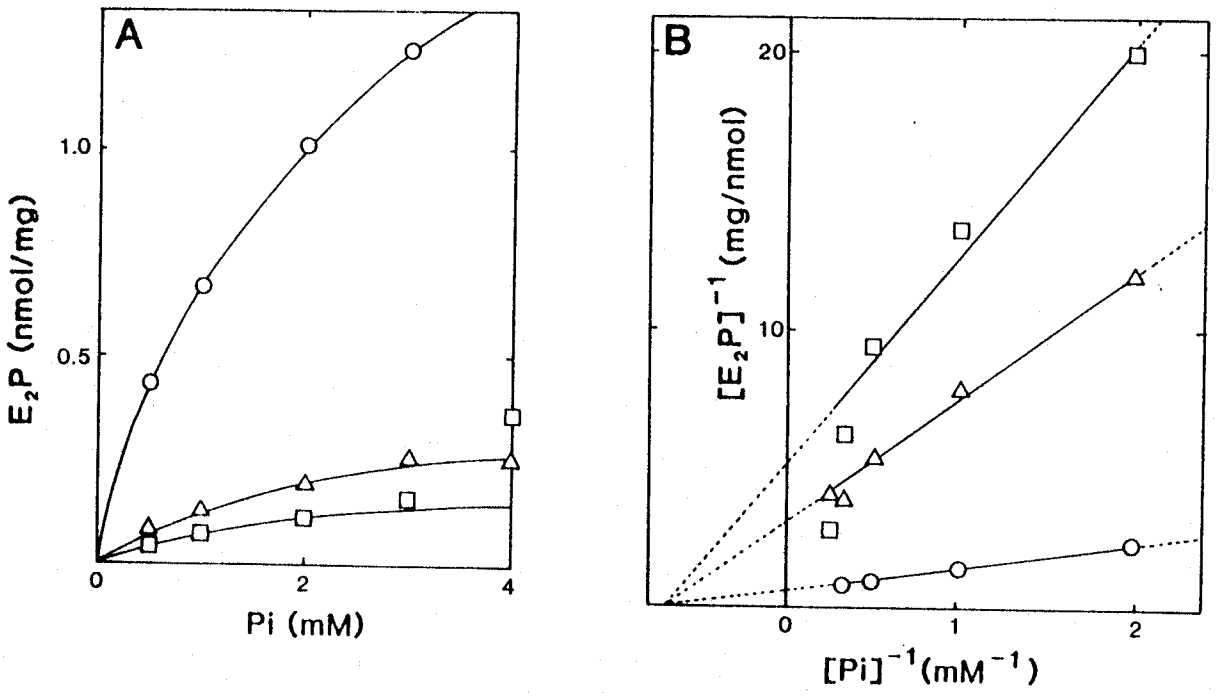

Fig. 4 Non competitive inhibition of E_2P formation by high-affinity vanadate binding-----Panel A: SR vesicles (0.1 mg/ml) were preincubated with 0-4 mM sodium phosphate in a medium of 0.1 M KCl, 20 mM TES (pH 7.2), 1 mM $MgCl_2$, 1 mM EGTA and 10% Me_2SO for 5 min. Vanadate was added at concentrations of 0(○), 2(△) and 5 μM (□). After 10 min incubation, E_2P formation was quenched by 5% TCA and the amount of E_2P was determined as described in "EXPERIMENTAL PROCEDURE." Panel B: Lineweaver-Burk plot of E_2P formation at the indicated concentrations of vanadate. The data came from Panel A.

Binding of Vanadate to Solubilized Ca^{2+}-ATPase---

As described in the preceding section, there exist 0.5 mol of high-affinity vanadate-binding sites as well as 0.5 mol of low-affinity vanadate-binding sites per mol of Ca^{2+}-ATPase. These results can be interpreted as indicating that SR vesicles contain two distinct types of Ca^{2+}-ATPase which have different affinities for vanadate, or that the affinity of the enzyme for vanadate changes due to interactions between the enzyme molecules in the SR membrane. To test these hypotheses, we tried to measure the vanadate binding to solubilized SR. When SR membranes are solubilized with a high concentration of nonionic detergent, such as $C_{12}E_9$ or $C_{12}E_8$, the interaction between the Ca^{2+}-ATPase molecules is disrupted and the enzyme exists mainly in a monomeric form (30). For measurements of vanadate binding to the $C_{12}E_9$-solubilized ATPase, we employed a new method as described below. After incubation of the solubilized SR with various concentrations of vanadate, the reaction mixture was rapidly passed through a Dowex 2x8 column to remove free vanadate. The amount of vanadate released from the ATPase during passage through the column was found to be negligibly small. The concentration dependence of vanadate binding to SR vesicles, which was measured using the Dowex column, agreed well with that measured by the centrifugation method (Fig. 5). Since AMP-PNP significantly inhibits the trapping of free vanadate with Dowex resin, nonspecific binding was measured in the presence of 1 mM Ca^{2+} alone. The nonspecific binding measured by the Dowex column method was three times larger than that measured by the centrifugation method.

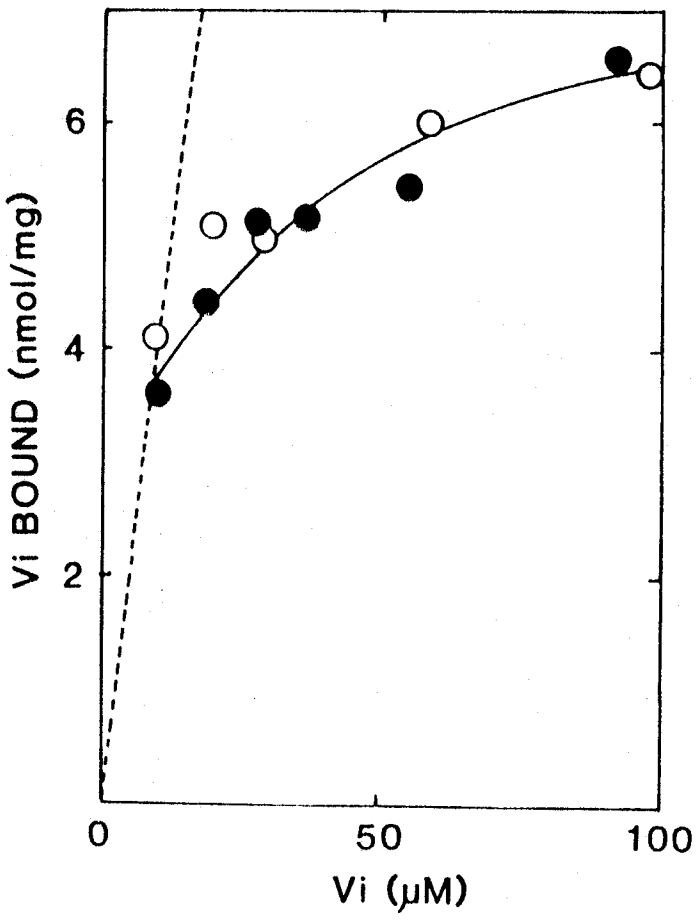

Fig. 5 Comparison between two methods for measurement of vanadate binding------SR vesicles were incubated in assay medium containing 0.1 M KCl, 20 mM TES (pH 7.2), 1 mM $MgCl_2$, 1 mM EGTA, 10% Me_2SO and 0-100 μM vanadate. Vanadate binding was measured by a centrifugation method (○) as well as by the Dowex column method (●) as described in "EXPERIMENTAL PROCEDURE."

In the experiment shown in Fig. 6, vanadate binding to the solubilized SR was compared with that to SR vesicles at different concentrations of vanadate. SR vesicles (2.5 mg/ml) were solubilized by 30 mg/ml $C_{12}E_9$ in the presence of 0.1 M KCl, 0.1 M TES (pH 7.2), 1 mM $MgCl_2$, 1 mM EGTA and 10% Me_2SO. The reaction was started by addition of vanadate to the assay medium. After a while, the SR mixture was passed through a Dowex column, and the eluate was used to measure the vanadate concentration. As a control, vanadate binding to SR vesicles was measured under the same conditions, except for the use of $C_{12}E_9$. Clearly, the amount of vanadate bound to the solubilized SR increased depending on the vanadate concentration in the medium without showing a biphasic curve such as that observed with the intact SR vesicles. The Scatchard plot of the vanadate binding to the solubilized SR was linear, indicating that the vanadate-binding site of the solubilized SR was homogeneous, and that its apparent dissociation constant and the number of sites were 13 μM and 7.2 nmol/mg protein, respectively. The number of vanadate-binding sites of solubilized SR was almost equal to the sum of high- and low-affinity vanadate-binding sites for the SR vesicles. One possible explanation is that these data indicate that the biphasic character of vanadate binding to SR vesicles may be interpreted as a consequence of the interaction between the Ca^{2+}-ATPase molecules in the SR membrane, because the biphasic binding curve was not observed when the enzyme was solubilized to a monomeric form with a high concentration of $C_{12}E_9$ (30). It is known that when Ca^{2+}-ATPase is solubilized with nonionic detergents in the absence of Ca^{2+}, the enzyme activity decreases

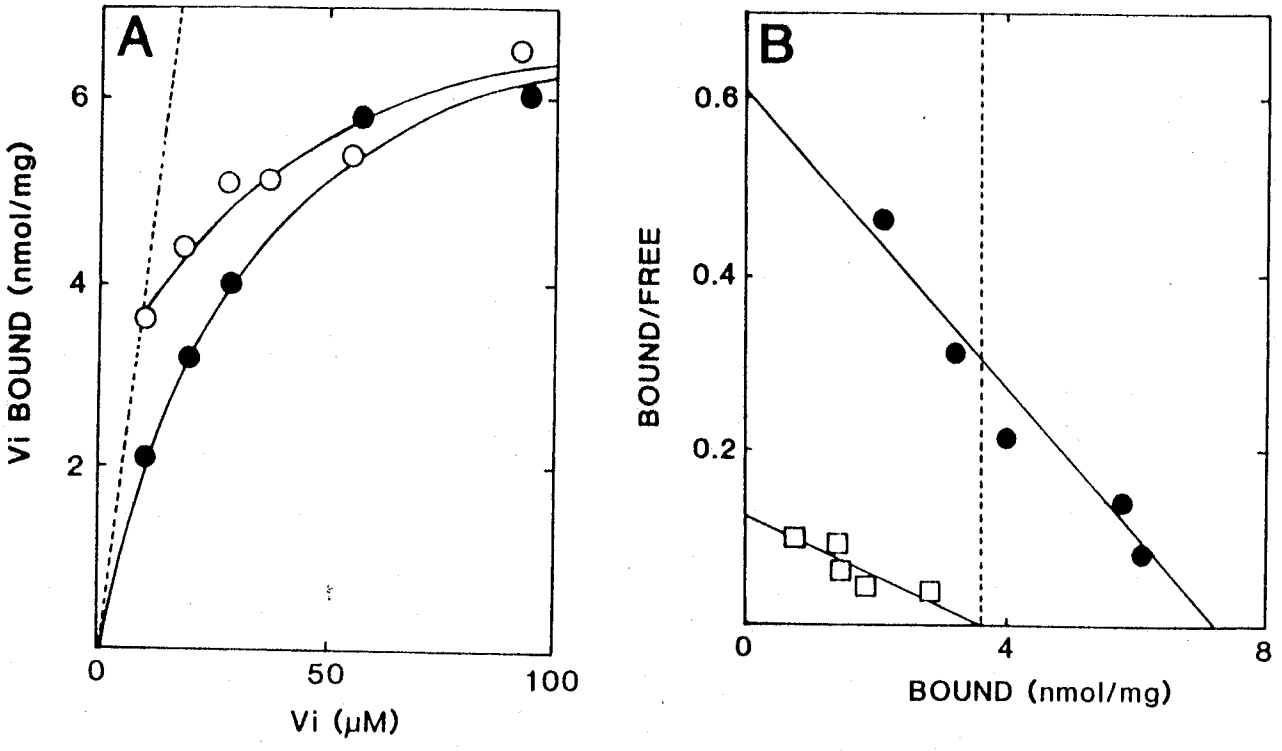

Fig. 6 Vanadate binding to solubilized SR-----Panel A: SR vesicles (2.5 mg/ml) were incubated with 0-100 μM vanadate in the presence of 0.1 M KCl, 100 mM TES (pH 7.2), 1 mM $MgCl_2$, 1 mM EGTA and 10% Me_2SO. The mixture was passed through a Dowex column and the amount of vanadate bound was measured as in Fig. 5 (open circles). Nonspecific vanadate binding was determined in the standard medium containing 2 mM $CaCl_2$. SR vesicles were solubilized by 30 mg/ml $C_{12}E_9$ in the standard medium. The reaction was started by addition of 0-100 μM vanadate to the medium. The amount of vanadate binding was determined as described above (closed circles). Panel B: Scatchard plots of vanadate binding to solubilized (●) and intact SR vesicles (□). The amounts of low-affinity vanadate binding were determined on the assumption that the maximum amount of high-affinity vanadate binding and its dissociation constant were 3.6 nmol/mg and below 0.1 μM, respectively (dotted line). The data came from Panel A.

with time (31). In the experiment shown in Fig. 6, the time interval between the addition of $C_{12}E_9$ to solubilize SR and the passing of the reaction mixture through the Dowex column was less than 5 min. Under these conditions, capability of E_1P formation of Ca^{2+}-ATPase remained constant up to at least 5 min after its solubilization (data not shown). Therefore, $C_{12}E_9$-induced change in the concentration dependence of vanadate binding from a biphasic to a monophasic pattern is not likely to have been caused by enzyme inactivation by the detergent.

Figure 7 shows the vanadate binding to solubilized SR in the absence or presence of 0.5 mM phosphate. SR vesicles (2.5 mg/ml) were preincubated with phosphate for several min at 23° C, then they were solubilized with $C_{12}E_9$. Vanadate binding to SR, measured as described in Fig. 6, was competitively inhibited by phosphate in a manner similar to that observed for the low-affinity vanadate binding in SR vesicles (Fig. 3B).When SR vesicles were reconstituted from the solubilized ATPase by the addition of Bio-beads SM-2 to remove $C_{12}E_9$, the vanadate binding to the reconstituted SR again exhibited a biphasic concentration dependency curve (Fig. 8). This result excludes the possibility that the vanadate-binding region of the Ca^{2+}-ATPase was irreversibly modified by $C_{12}E_9$. Therefore it is possible that the biphasic vanadate binding strictly depends on the membrane structure of SR. It should be noted that in the reconstituted membrane, the numbers of high- and low-affinity binding sites simultaneously decreased to approximately half of those in intact SR. This may be in part due to random orientation of ATPase molecules in the reconstituted membrane.

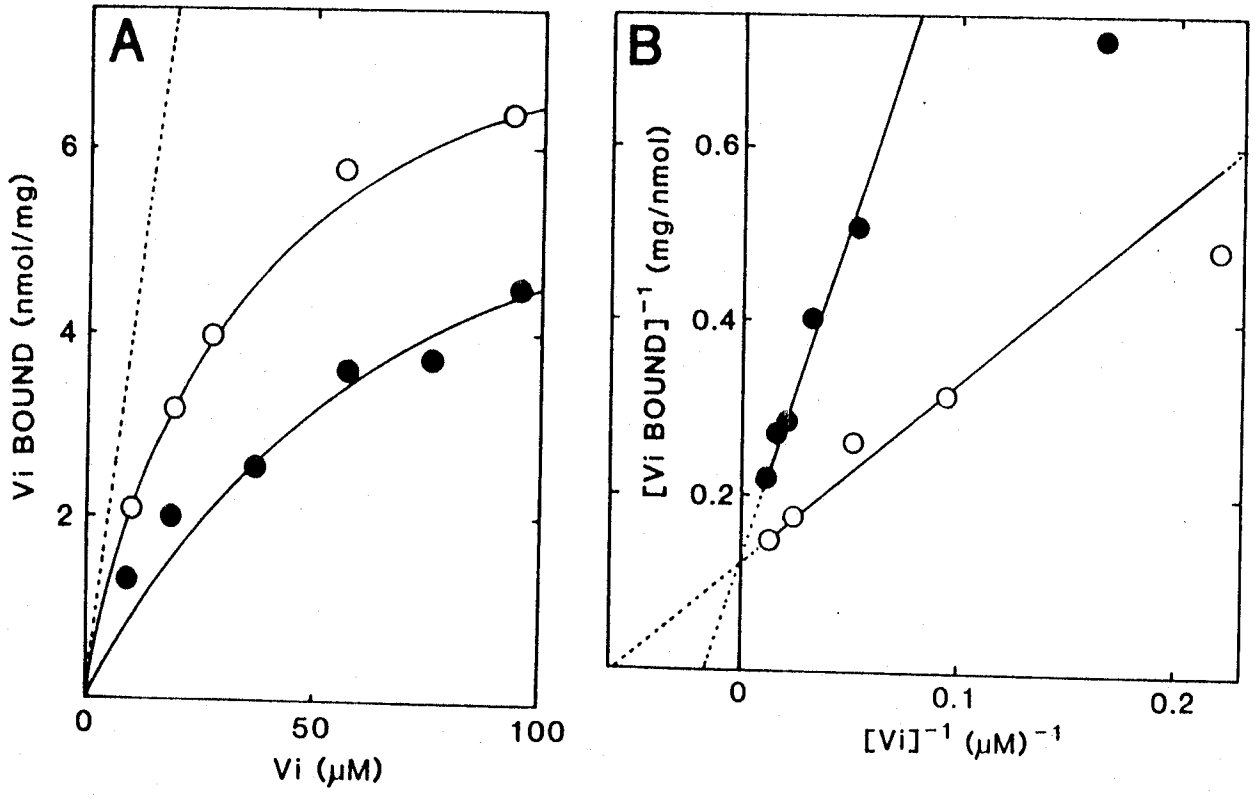

Fig. 7 Competitive inhibition of vanadate binding to solubilized SR by inorganic phosphate.-----Panel A: SR vesicles (2.5 mg/ml) were preincubated with (●) or without (○) of 0.5 mM sodium phosphate in the medium of 0.1 M KCl, 100 mM TES (pH 7.2), 1 mM $MgCl_2$, 1 mM EGTA and 10% Me_2SO. SR was solubilized by 30 mg/ml $C_{12}E_9$ immediately before addition of 0-100 μM vanadate. The amount of vanadate bound to solubilized SR was determined as described in Fig. 6. Panel B: Double reciprocal plot of vanadate binding in the presence (●) or absence (○) of 0.5 mM phosphate. The data came from panel A.

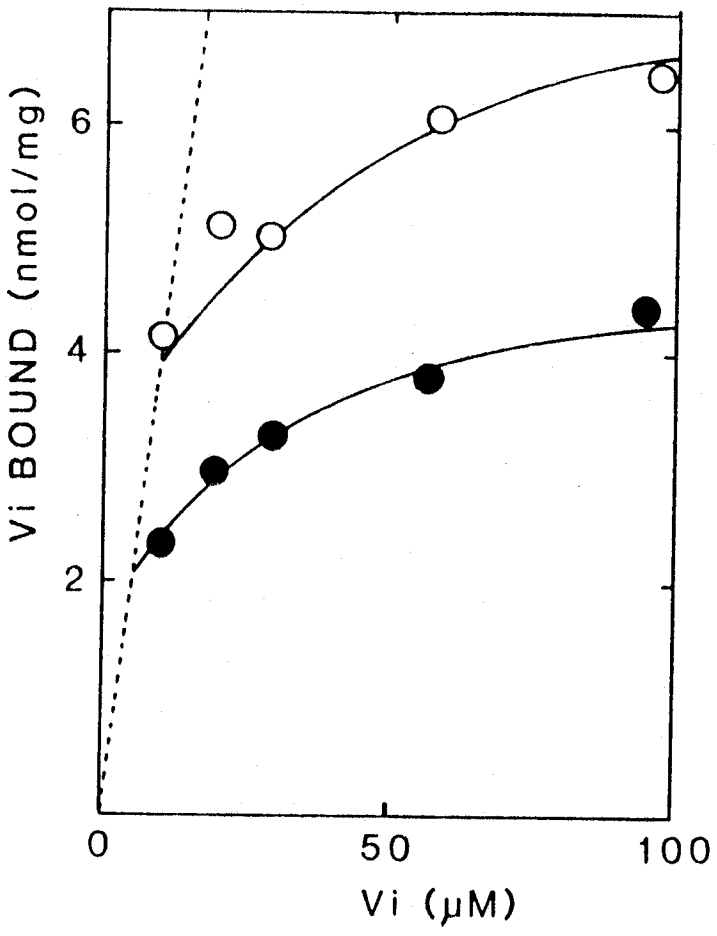

Fig. 8 Vanadate binding to reconstitued SR vesicles------SR vesicles (2.5mg/ml) were solubilized by 50 mg/ml $C_{12}E_9$ in the presence of 0.1M KCl, 100 mM TES (pH 7.2), 1 mM $MgCl_2$ and 0.1 mM $CaCl_2$. $C_{12}E_9$ was removed by 1 h incubation with Bio-beads SM-2 and reconstitued vesicles (RSR) were collected by centrifugation. Vanadate binding to RSR (●) and intact SR (○) were measured by centrifugation method as described in Fig. 1. The data for intact SR came from Fig. 5.

DISCUSSION

As shown in Fig. 1, the vanadate binding to partially purified ATPase exhibited a biphasic concentration dependency curve, as was observed with intact SR vesicles. This observation eliminates the possibility that any kind of SR protein other than Ca^{2+}-ATPase may be involved in the vanadate-binding reaction. Numerous studies of the effect of vanadate as an analogue of phosphate on SR ATPase have been published in the past several years (29,32-40), but there are few reports concerned with the number of vanadate-binding sites. With our SR preparations, the maximum amount of vanadate binding ranged from 5.2 to 7.2 nmol/mg protein, which corresponds to approximately one mol of vanadate-binding site per mol of 115,000-dalton Ca^{2+}-ATPase, assuming that the enzyme accounts for 60-80% of the total SR proteins. This value is consistent with our previous observation (22) as well as others' (32,33), but is inconsistent with that of Andersen and Moller (39), who measured ^{48}vanadate binding to purified enzyme using a filtration method; they suggested that only a half mol of vanadate was bound per mol of the purified ATPase under optimal conditions. The reason for this discrepancy remains to be established. In the present study, we have provided new evidence for the existence of two distinct kinds of vanadate-binding sites which have greatly different affinities for vanadate. Several reports have described vanadate binding to SR measured as a function of vanadate concentration (22,32,33). In the measurements of vanadate binding, Varga *et al.* (32), as well as we (22), determined the amount of vanadate bound to SR from the

decrease in the vanadate concentration of the supernatant after centrifugation of the reaction mixture. The accuracy of these measurements depends on the SR protein concentration in the reaction mixture. It is particularly difficult to measure high-affinity vanadate binding to SR vesicles at relatively high concentrations of protein (> 2.5 mg/ml). In addition, the accuracy of measurement is markedly reduced as the vanadate concentration becomes higher, because of the significant increase in the background of free vanadate. Medda and Hasselbach (33) measured vanadate binding to isolated SR vesicles from the decrease in the level of EP formed by ATP after incubating SR with vanadate. In these experiments, the plot of bound vanadate against the logarithm of added vanadate concentration appeared to be monophasic. However, replotting of the data against the logarithm of the free vanadate concentration or against the added concentration on a linear scale, gave a biphasic curve which indicates the existence of high- and low-affinity vanadate-binding sites.

The present study yielded direct evidence for the existence of 0.5 mol of both low- and high-affinity vanadate-binding sites per mol of Ca^{2+}-ATPase in intact SR membrane (Fig. 2). This "half-of-the-sites" behavior of Ca^{2+}-ATPase has been observed for the phosphorylation of the enzyme by ATP (16-18,41,42). Recently, Suzuki et al. (43) observed that 1 mol of low-affinity ATP-binding site and 1 mol of high-affinity ATP-binding site exist per 1 mol of phosphorylatable site of the enzyme.

There are two possible explanations for the "half-of-the-sites" behavior in the vanadate binding to SR. The first is that

a single polypeptide chain of Ca^{2+}-ATPase contains either one of the two classes of vanadate-binding site, and that two equal populations of the ATPase having different affinities for vanadate exist in the SR membrane. The second is that two distinct classes of vanadate-binding sites exist in a single polypeptide chain of partially denatured Ca^{2+}-ATPase. However, the latter explanation is unlikely, because in the detergent-solubilized condition, 1 mol of vanadate was bound to a single site of the ATPase with a dissociation constant of 13 μM (Fig. 7). This result implies that Ca^{2+}-ATPase probably has only one type of vanadate-binding site when Ca^{2+}-ATPase exists in a monomeric form. Based on these considerations, the "half-of-the-sites" behavior of vanadate-binding sites can be explained as follows. A single polypeptide of Ca^{2+}-ATPase has one kind of vanadate-binding site. In the intact SR membrane, Ca^{2+}-ATPase exists as a dimer, in which interaction occurs between the two vanadate-binding sites. This interaction causes the difference between these sites, making it seem that there are two species of vanadate-binding sites. In fact, observation of the two-dimensional crystal structure shows that Ca^{2+}-ATPases come close in the SR membrane to form a dimer when SR vesicles are incubated with vanadate under Ca^{2+}-free conditions (6). The formation of a dimeric structure in the two-dimensional crystal may cause the "half-of-the-sites" behavior of vanadate- binding sites.

REFERENCES

1. Yamamoto,T., Takisawa,H., & Tonomura,Y. (1979) Curr.Top.Bioenerg. 9, 179-236

2. Inesi,G., Kurzmack,M., & Lewis,D., (1988) Methods Enzymol. 157, 154-190

3. MacLennan,D.H., Brandl,C.J., Korczak,B., & Green,N.M. (1985) Nature 316, 696-700

4. Brandl,C.J., Green,N.M., Korczak,B., & MacLennan,D.H. (1986) Cell 44, 597-607

5. Le Maire,M., Møller,J.V., & Tardieu,A. (1981) J.Mol.Biol. 150, 273-296

6. Dux,L., Taylor,K.A., Ting-Beall,H.P., & Martonosi,A. (1985) J.Biol.Chem. 260, 11730-11743

7. Wang,C.T., Saito,A., & Fleischer,S. (1979) J.Biol.Chem. 254, 9209-9219

8. Andersen,J.P., Fellmann,P., Møller,J.V., & Devaux,P.F. (1981) Biochemistry 20, 4928-4936

9. Scales,D., & Inesi,G. (1976) Biophys.J. 16, 735-751

10. Birmachu,D., & Thomas,D.D. (1990) Biochemistry 29, 3904-3914

11. Napolitano,C.A., Cooke,P., Segalman,K., & Herbette,L. (1983) Biophys.J. 42, 119-125

12. Hymel,L., Maurer,A., Berenski,C., Jung,C.Y., & Fleischer,S. (1984) J.Biol.Chem. 259, 4890-4895

13. Franzini-Armstrong,C., & Ferguson,D.G. (1985) Biophys.J. 48, 607-615

14. Vanderkooi,J., Ierokomas,A., Nakamura,H., & Martonosi,A.

(1977) Biochemistry 16, 1262-1267

15. Fagan,M.H., & Dewey,T.G. (1986) J.Biol.Chem. 261, 3654-3660
16. Froehlich,J.P., & Taylor,E.W. (1975) J.Biol.Chem. 250, 2013-2021
17. Verjovski-Almeida,S., Kurzmack,M., & Inesi,G. (1978) Biochemistry 17, 5006-5013
18. Ferreira,S.T., & Verjovski-Almeida,S. (1988) J.Biol.Chem. 263, 9973-9980
19. Lewis,S.M., & Thomas,D.D. (1986) Biochemistry 25, 4615-4621
20. Andersen,J.P., & Vilsen,B. (1985) FEBS lett. 189, 13-17
21. Yamasaki,K., & Yamamoto,T. (1989) J.Biochem. 106, 1114-1120
22. Yamasaki,K., Sano,N., Ohe,M., & Yamamoto,T. (1990) J.Biochem. 108, 918-925
23. Yamada,S., Yamamoto,T., & Tonomura,Y. (1970) J.Biochem. 61, 789-794
24. Meissner,G., Conner,G.E., & Fleischer,S. (1973) Biochim.Biophys.Acta 298, 246-269
25. Goodno,C.C. (1979) Proc.Natl.Acad.Sci.U.S. 76, 2620-2624
26. Takisawa,H., & Tonomura,Y. (1979) J.Biochem. 86, 425-441
27. Laemmli,U.K. (1970) Nature 227, 680-685
28. Cantley,L.C., Cantley,L.G., & Josephson,L. (1978) J.Biol.Chem. 253, 7361-7368
29. O'Neal,S.C., Rhoads,R.B., & Racker,E. (1979) Biochim.Biophys.Res.Commun. 89, 845-850
30. Møller,J.V. Lind, K.E., & Andersen,J.P. (1980) J.Biol.Chem. 255, 1912-1920
31. Swoboda,G., & Hasselbach,W. (1988) Eur.J.Biochem. 172,325-332

32. Varga,S., Csermely,P., & Martonosi,A. (1985) Eur.J.Biochem. 148, 119-126

33. Medda,P., & Hasselbach,W. (1983) Eur.J.Biochem. 137, 7-14

34. Dupont,Y., & Bennet,N. (1982) FEBS Lett. 139, 237-240

35. Dux,L., & Martonosi,A. (1983) J.Biol.Chem. 258, 2599-2603

36. Inesi,G., Lewis,D., & Murphy,A.J. (1984) J.Biol.Chem. 259, 996-1003

37. Ortiz,A., García-Carmona,F., García-Cánovas,F., & Gómez-Fernández,J.C. (1984) Biochem.J. 221, 213-222

38. Highsmith,S., Barker,D., & Scales,D.J. (1985) Biochim. Biophys.Acta 817, 123-133

39. Andersen,J.P., & Møller,J.V. (1985) Biochim.Biophys.Acta 815, 9-15

40. Markus,S., Priel,Z., & Chipman,D.M. (1989) Biochemistry 28, 793-799

41. Ikemoto,N. (1982) Annu.Rev.Physiol. 44, 297-317

42. Dupont,Y., Pougeois,R., Ronjat,M., & Verjovski-Almeida,S. (1985) J.Biol.Chem. 260, 7241-7249

43. Suzuki,H., Kubota,T., Kubo,K., & Kanazawa,T. (1990) Biochemistry 29, 7040-7045

Part II

Effects of Vanadate Binding to High- and Low-Affinity Sites on the Phosphorylation of Sarcoplasmic Reticulum Ca^{2+}-ATPase by Phosphate

SUMMARY

In our previous report, we showed that 1 mol of Sarcoplasmic reticulum Ca^{2+}-ATPase has 0.5 mol of high-affinity vanadate binding sites as well as 0.5 mol of low-affinity vanadate binding sites (Yamasaki,K., & Yamamoto,T. (1991) J.Biochem. 110, 915-921). In the present paper, we studied the effects of vanadate binding to the high- and low- affinity sites on the phosphorylation of the enzyme by phosphate were studied. The Ca^{2+}-ATPase of sarcoplasmic reticulum was phosphorylated by inorganic phosphate (Pi) to form phosphoenzyme (E_2P). When vanadate was added, the steady state level of E_2P decreased due to inhibition of E_2P formation. The time course of E_2P decay after addition of vanadate exhibited a biphasic character. The size of E_2P decay in the fast-phase increased from 40 to 70% of initial amount of E_2P, when concentration of added vanadate increased from 20-50 μM. Pi competitively interrupted E_2P decay in the fast-phase. The dissociation constant of vanadate was estimated as 17 μM from concentration dependence of the fast-phase decay of E_2P, which was close to the dissociation constant of low-affinity vanadate binding site. From the competition with vanadate in the inhibition of the fast-phase decay of E_2P, the dissociation constant of phosphate was estimated as 7.4 mM which was very close to the Km value for E_2P formation measured under the same condition. These observations suggested that the low-affinity vanadate binding site correlated to the phosphorylation site of Ca^{2+}-ATPase. The fast-phase E_2P decay was rapidly reversed when vanadate concentration was decreased.

The rate of E_2P decay in the slow-phase corresponded well to the rate of vanadate binding to the high-affinity sites. When Ca^{2+}-ATPase was preincubated with 5 μM vanadate, the amount of E_2P decreased as a function of the incubation time. After 10min it decreased to 5% of control. Under this concentration, vanadate binding to the low-affinity site was negligibly small, so these inhibitions of E_2P formation must be caused by vanadate binding to the high-affinity site. The inhibition of E_2P formation required Mg^{2+}, but this inhibition was restored at the extremely slow rate after removal of Mg^{2+}. Phosphate also interrupted the inhibition of E_2P formation by vanadate binding to the high-affinity site. The apparent dissociation constant in the Pi-binding under this condition was estimated to be less than 0.8 mM. These results raise the possibility that a high-affinity phosphate binding site other than the phosphorylation site may exist in the Ca^{2+}-ATPase of SR.

INTRODUCTION

Vanadate is known as an inhibitor of 'P-type' transport ATPases (1,2). The inhibition occurs when vanadate binds to phosphorylation site of these ATPases in replace of phosphate at concentrations below 1 μM. The Ca^{2+}-ATPase of sarcoplasmic reticulum is also inhibited by vanadate (3-6). Vanadate can bind to SR Ca^{2+}-ATPase only in the absence of Ca^{2+} (6,7) where Ca^{2+}-ATPase exists in the E_2 form which the enzyme can be phosphorylated by inorganic phosphate but not by ATP (8). So enzyme-vanadate complex (E_2Vi)is assumed to be analogue of phosphoenzyme, E_2P. Numerous studies of the effect of vanadate on SR Ca^{2+}-ATPase have been published, but there are several reports concerned with the number of vanadate binding sites (3-7,9,10). With our SR preparation, the maximum amount of vanadate binding ranged from 5.2 to 7.2 nmol/mg, which corresponds to approximately 1 mole of vanadate per mole of 115,000 Daltons Ca^{2+}-ATPase (11). Similar number was also obtained by other investigators (12-14). On the other hands, under the optimum conditions, the amount of EP formation was generally reported to be 3-4 nmol/mg, which correspond to 0.5 mole of phosphorylation site per mole of Ca^{2+}-ATPase. This difference of the maximum capacities of vanadate binding and EP formation has been remained unsolved.

Recently, we suggested that Ca^{2+}-ATPase possessed two distinct kinds of vanadate binding sites which have greatly different affinity for vanadate(11). The high-affinity vanadate binding sites had a dissociation constant below 0.1 μM and the low-

affinity sites one of 20-40 μM. The maximum amount of vanadate bound to each of the high- and low-affinity site was estimated to be 2.6-3.6 nmol/mg. These maximum amount of vanadate corresponded approximately 0.5 mol of vanadate per mole of ATPase and agreed with the number of the phosphorylation site, and these vanadate binding sites existed on different Ca^{2+}-ATPase molecules. In the present study, we examined in detail the mechanism in which E_2P formation was inhibited by vanadate binding to the high- and low-affinity sites. Vanadate binding to either of the high- and low-affinity sites resulted in the complete inhibition of E_2P formation. These results suggests that interaction between the high- and low-affinity vanadate binding sites may involve in the inhibition of E_2P formation.

EXPERIMENTAL PROCEDURES

Materials------Sarcoplasmic reticulum (SR) was isolated from rabbit dorsal and hind limb white muscles by a method described previously (15). SR vesicles suspended in 60 mM KCl, 20% glycerol and 10 mM Tris-maleate (pH 7.0) were divided into small portions, rapidly frozen using liquid nitrogen and stored at -80° C. Monovanadate was prepared from V_2O_5 according to Goodno (16). 4-(2-Pyridylazo)resorcinol was obtained from Dojin.

Phosphorylation Assay------Phosphorylation of SR by inorganic phosphate was performed in the medium containing 2.5 mg/ml SR, 0.1 M KCl, 20 mM TES (pH 7.2), 10 mM $MgCl_2$, 1 mM EGTA, 10% Me_2SO and 2-10 mM [^{32}P]phosphate. After incubation, the phosphorylation was quenched with 5% trichloroacetic acid containing 10 mM nonradioactive phosphate. The amount of phosphoenzyme (EP) formed was determined as described elsewhere (17).

Measurement of vanadate binding to SR------Vanadate binding to SR vesicles was carried out at 20° C in assay medium containing 2.5 mg/ml SR protein, 0.1 M KCl, 20 mM TES (pH 7.2), 10 mM $MgCl_2$, 1 mM EGTA, 10% Me_2SO and 10 μM vanadate. After incubation, the SR mixture (0.2 ml) was passed through a Dowex 2x8 (100-200 mesh) short column (about 0.2 ml) to remove free vanadate. The eluted SR vesicles were solubilized by 1% SDS for the determination of free vanadate concentration. The concentration of vanadate was measured by the method of Goodno using the metallochromic dye 4-(2-pyridylazo)resorcinol as an indicator (16).

Biphasic decay of E_2P by addition of vanadate----- It was already observed that when Pi was added to the medium containing SR vesicles , EGTA and Mg^{2+}, Ca^{2+}-ATPase of SR was rapidly phosphorylated and formed phosphoenzyme (E_2P.) The equilibrium of E_2P was attained within 0.1 sec under the normal condition (18-20). Vanadate is considered to bind to E_2 state of the Ca^{2+}-ATPase as an analogue of phosphate (6,7), and inhibit E_2P formation (5). In the preceding paper we found that vanadate was bound to the high- and low-affinity sites of the Ca^{2+}-ATPase under the conditions for E_2P formation (11). Therefore, it is interesting to investigate kinetically the mechanism of inhibition of the E_2P formation by vanadate. In Fig. 1, time-course of E_2P decay were followed after addition of 20 μM vanadate to the medium containing 2.5 mg/ml SR vesicles, 2 mM [^{32}P]Pi, 0.1 M KCl, 20 mM TES (pH 7.2), 10 mM $MgCl_2$, 1 mM EGTA and 10% Me_2SO at various temperature. It was found that at all the temperature tested, decay of E_2P level showed biphasic time-course; E_2P decay in the fast phase was completed within 20 sec after the addition of vanadate, which was followed by a linear slow decay of E_2P. By extrapolating the slow-phase to time zero, the fraction of the fast-phase of E_2P decay was estimated to be more than 40% of the initial E_2P level under these conditions. The initial level of E_2P varied from 0.6 to 1.2 nmol/mg depending on the experimental temperature ranging from 10 to 20° C. But the ratio of the fast-phase fraction to the initial amount of E_2P was independent to the temperature. When excess amount of

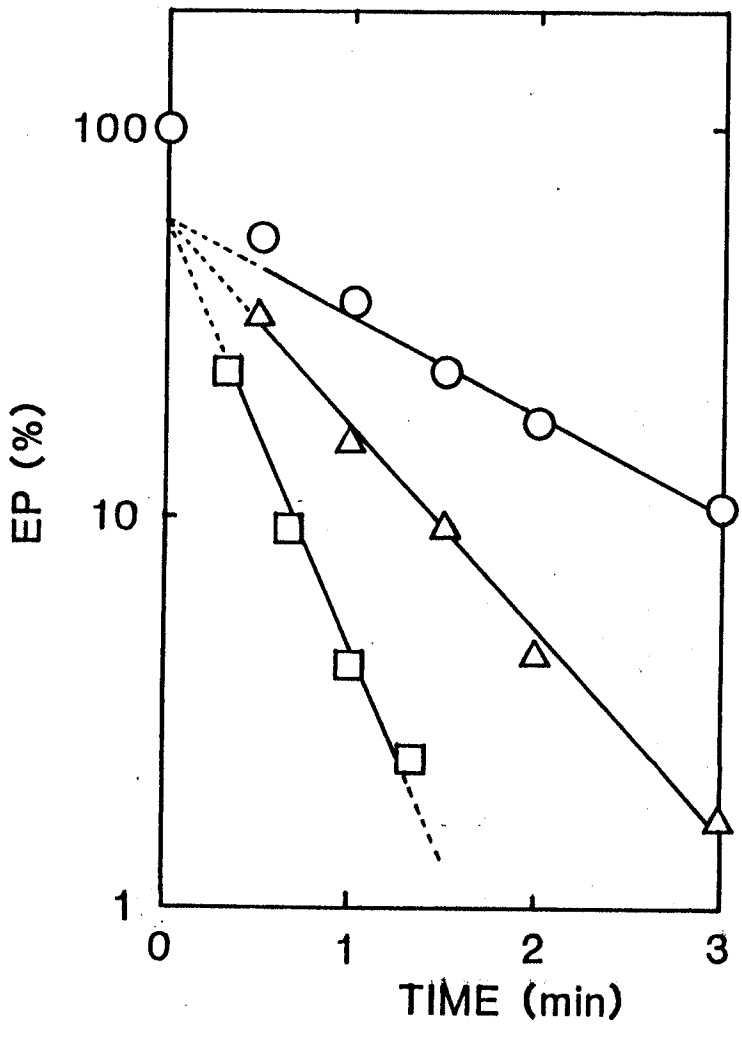

Fig. 1 Time course of phosphoenzyme decay after addition of vanadate-----SR vesicles (2.5mg/ml) was phosphorylated by 2 mM [^{32}P] Pi in a medium of 0.1M KCl, 20mM TES (pH 7.2), 10 mM $MgCl_2$, 1 mM EGTA and 10% Me_2SO at 10 (○), 15 (△) and 20° C (□). Vanadate was added to medium at concentration of 20 μM. After incubation with vanadate for indicated time, reaction was quenched by 5% TCA and the amount of E_2P was determined as described in "EXPERIMENTAL PROCEDURE." The amount of E_2P was expressed as percent of that formed in the absence of vanadate.

non-radioactive phosphate was added to the medium, the amount of $E_2{}^{32}P$ was decreased at a rate much higher than that of E_2P decay after addition of vanadate. Therefore, we considered that the slow-phase of E_2P decay was not due to the dephosphorylation of phosphoenzyme, but due to inactivation of Ca^{2+}-ATPase.

Time course of E_2P decay after addition of various concentrations of vanadate were measured in the presence of 2 or 10 mM Pi (Fig. 2.) To show the biphasic character of E_2P decay more clearly, following experiments were performed at 10° C. In the presence of 2 mM Pi, size of E_2P decay in the fast-phase was increased from 40 to 70% of initial amount of E_2P, when concentration of added vanadate increased from 20 to 50 μM. On the other hand, rate of E_2P decay in slow-phase also seemed to vary depending on the vanadate concentration. When concentration of added vanadate increased from 20 to 50 μM, the rate of E_2P decay in the slow-phase increased in almost twice in the presence of 2 mM Pi. Both of E_2P decay in the fast- and slow-phases were reversed by increasing concentration of phosphate. The size of E_2P decay in the fast-phase after addition of 20 μM vanadate decreased from 40 to 20% of initial amount of E_2P when phosphate concentration increased from 2 to 10 mM. The rate of slow-phase decay also decreased to one third.

Analysis of fast-phase E_2P decay----- Biphasic character of E_2P decay suggests that vanadate inhibits the E_2P formation at least in the two distinct manner. Our preceding data showed that two distinct classes of vanadate binding sites exist in the Ca^{2+}-ATPase (11). The high-affinity vanadate binding site have a

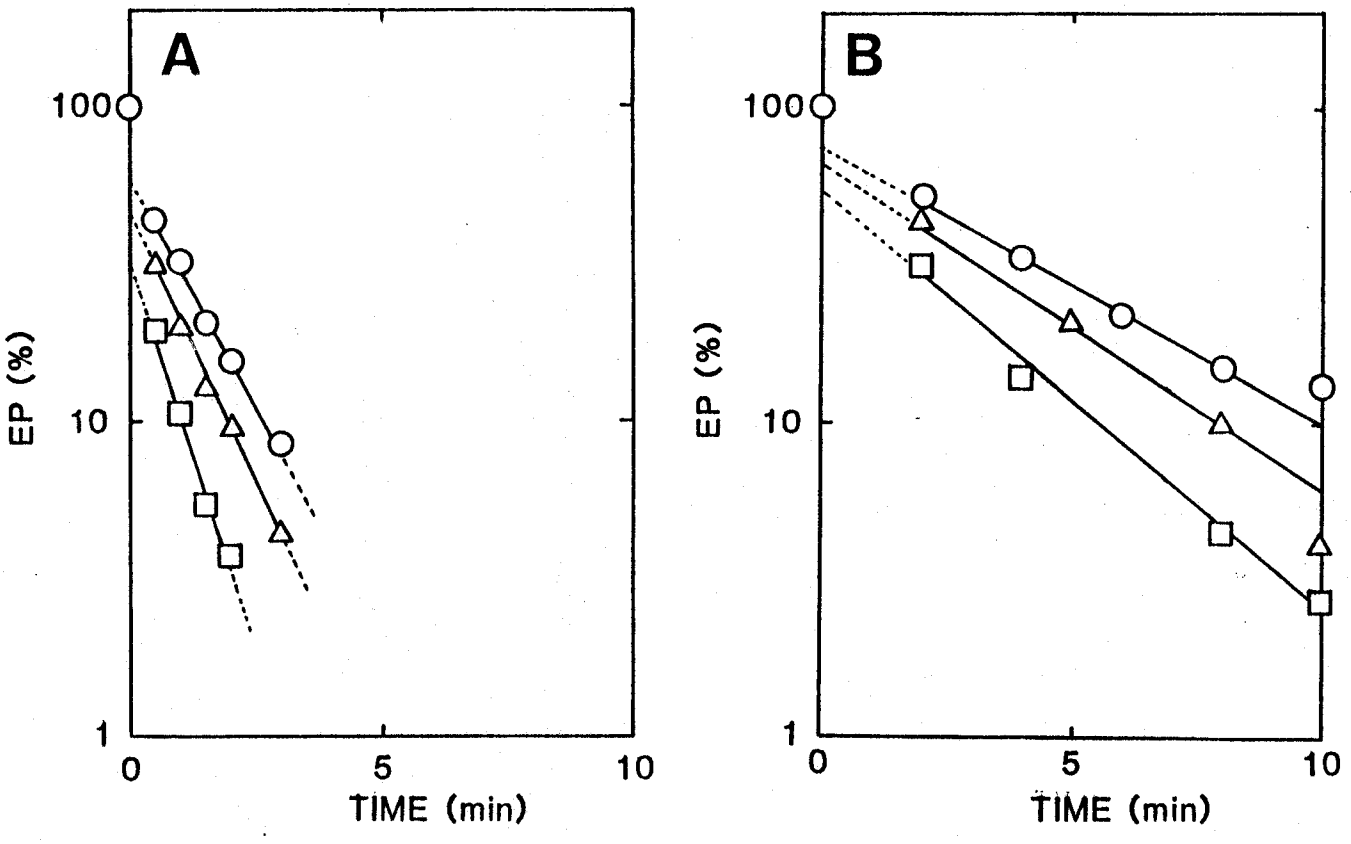

Fig. 2 Time course of E_2P decay after addition of different concentration of vanadate----- SR vesicles (2.5mg/ml) was phosphorylated by 2 (panel A) or 10 mM [^{32}P]Pi (panel B) at 10° C in the same medium as described in Fig. 1. Vanadate was added in the concentrations of 20 (○), 30 (△) and 50 μM (□). Other procedures are same as described in Fig. 1

dissociation constant below 0.1 μM, and low-affinity sites one of 20-40 μM. The maximum amount of vanadate bound to each of the high- and low-affinity sites was estimated to be 2.6-3.6 nmol/mg SR protein, which corresponds to approximately 0.5 mol of vanadate binding sites per 1 mol of Ca^{2+}-ATPase. Therefore it is assumed that each binding of vanadate to different class of vanadate binding site may involve in the biphasic E_2P decay. To examine this possibility, we tried to compare the kinetical properties of vanadate binding and E_2P decay in the fast- and slow-phase.

Fig. 3 shows double-reciprocal plot of the size of E_2P decay in the fast-phase against vanadate concentration. From this plot. apparent dissociation constants of vanadate binding to the sites were estimated to be 21 and 40 μM in the presence of 2 and 10 mM Pi, respectively. So it was assumed that this site had a dissociation constant of about 17 μM in the absence of Pi. This value of dissociation constant is close to that of low-affinity vanadate binding site. As shown in Fig. 3, the size of E_2P decay in the fast-phase seemed to be competitively decreased by phosphate. If the fast-phase E_2P decay was assumed to be induced by low-affinity vanadate binding, this decrease in the vanadate effect by phosphate agreed with our previous observation that low-affinity vanadate binding was competitively inhibited by phosphate. From the competitive inhibition of E_2P decay in the fast-phase (Fig. 3), the dissociation constant of phosphate was estimated as 7.4 mM. This value was close to the Km value for E_2P formation measured under the same condition (4-10mM.) Therefore, it is suggested that the low-affinity vanadate binding site is

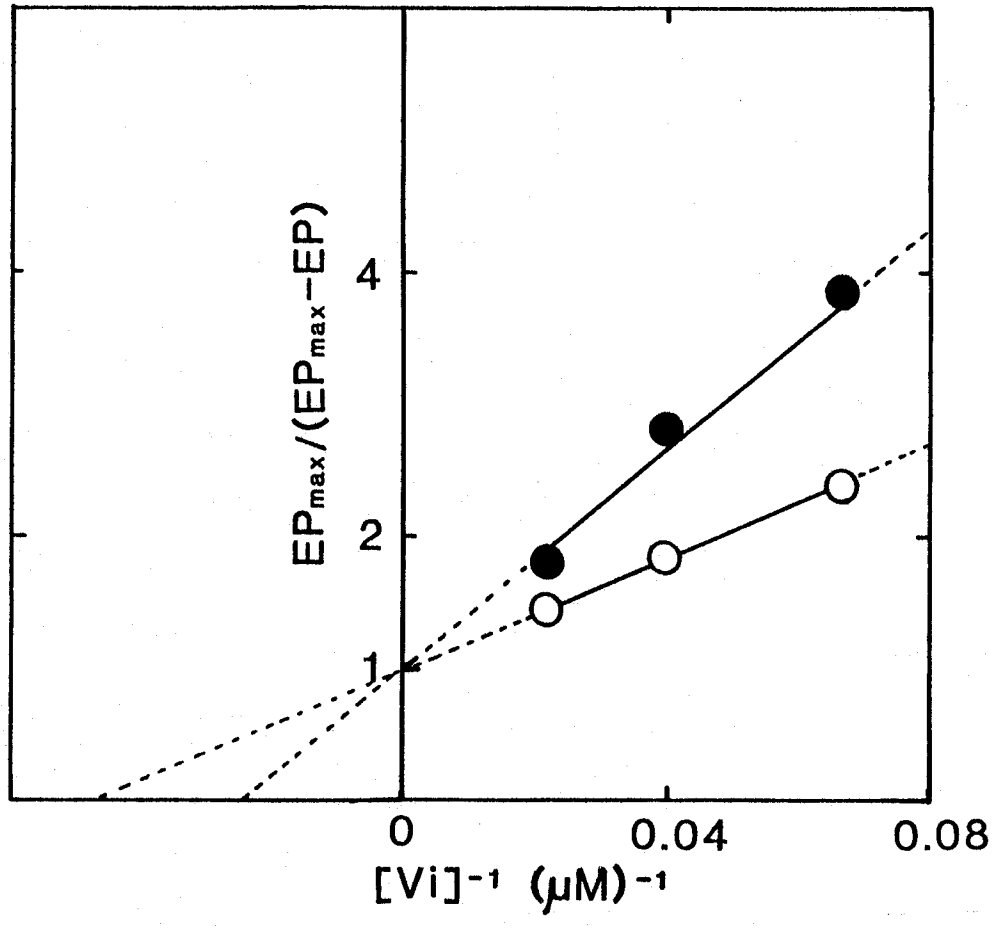

Fig. 3 Competition between vanadate and phosphate in the fast phase of E_2P-decay----- The size of the fast E_2P decay was obtained from the data of Fig. 2 by extrapolating its time-course in the slow phase to time 0, and represented as a ratio to the initial level of E_2P. Double-reciprocal plot of the size of fast-phase decay in the presence of 2 (○) and 10 mM Pi (●) was performed against vanadate concentration

close by co-related to the phosphorylation site of Ca^{2+}-ATPase. As shown in the Fig. 3, the maximum level of fast-phase decay of E_2P was estimated to be equal to the initial amount of E_2P. This means that saturation of the low-affinity site with vanadate results in a completely inhibition of E_2P formation. Therefore it can be concluded that low-affinity vanadate binding site is the phosphorylation site.

Fig. 4 shows recovery of fast-phase decay by decreasing of vanadate concentration. Ca^{2+}-ATPase was phosphorylated by 2 mM Pi, then 50 μM vanadate was added to induce E_2P decay. At 1 min after addition of vanadate, its concentration was reduced to 20 μM by dilution. Then the amount of E_2P immediately recovered to the same level as was seen when E_2P decay was induced by addition of 20 μM vanadate. This recovery was completed within 20 sec after dilution of vanadate. This rapid recovery of E_2P suggests that the effect of vanadate on the E_2P decay in the fast-phase was completely reversible. To explain these observations, we proposed a reaction scheme for the fast-phase decay of E_2P as follow;

$$E_2Vi \underset{}{\overset{K_{VL}}{\rightleftharpoons}} E_2 \overset{K_{PL}}{\rightleftharpoons} E_2Pi \underset{k-1}{\overset{k+1}{\rightleftharpoons}} E_2P$$

Scheme 1

Where Vi and Pi denote orthovanadate and inorganic phosphate, respectively. According to this scheme, in the absence of vanadate, the equilibrium is maintained among three components E_2, $E_2 \cdot Pi$ and E_2P. Vanadate shifts the equilibrium towards the

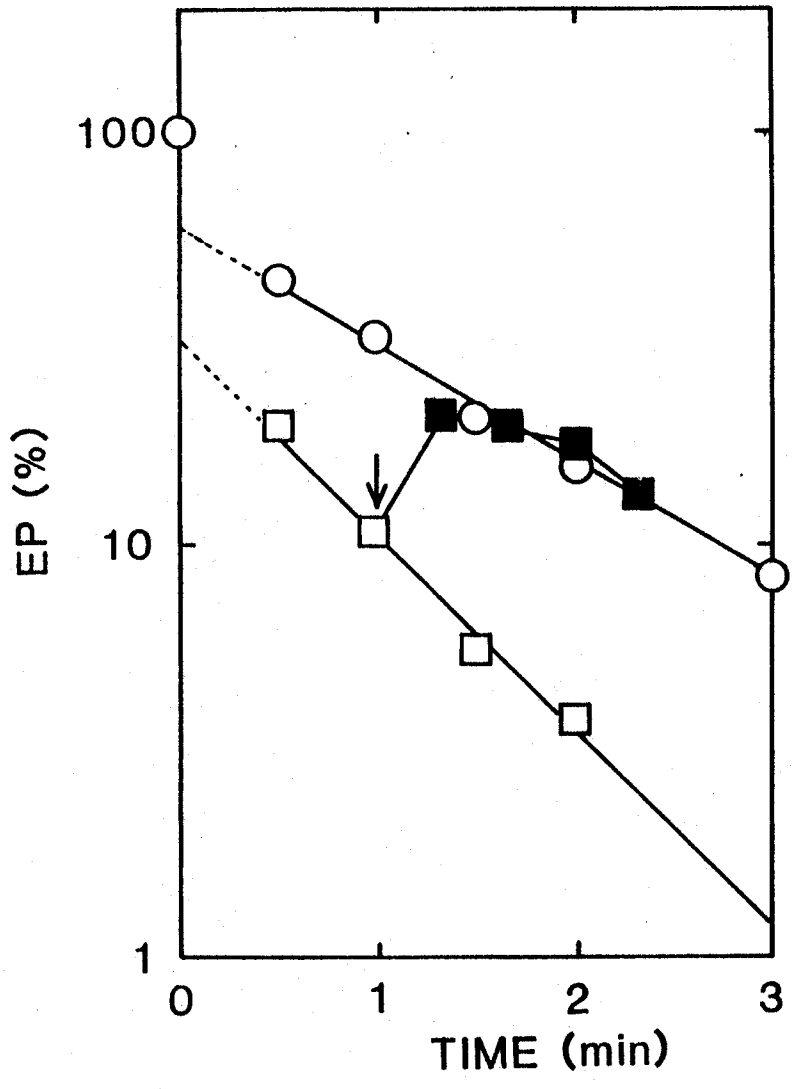

Fig. 4 Reversible effect of vanadate on the of fast phase inhibition of E_2P----- SR vesicles (2.5mg/ml) were phosphorylated by 2 mM [^{32}P]Pi in the presence of 0.1 M KCl, 20 mM TES (pH 7.2), 10 mM $MgCl_2$, 1 mM EGTA and 10% Me_2SO at 10° C. Vanadate was added at a concentration of 50 μM. After 1 min incubation reaction medium was diluted by 1.5 volume of the same medium omitting SR and vanadate (pointed by arrow.) At the indicated time reaction was quenched by 5% TCA (closed symbols.) In the control, open symbols show time course of E_2P decay in the presence of 20 (○) and 50 μM vanadate (□). These data were obtained from Fig. 2A.

left and hence the amount of E_2P is decreased.

Analysis of slow-phase E_2P decay----- As described in the previous section, it was indicated that the fast-phase E_2P decay was related with the low-affinity vanadate binding to the Ca^{2+}-ATPase. In this section, we examined whether slow-phase E_2P decay was affected by vanadate binding to the high-affinity site. In the preceding paper(11), it was observed that the rate of vanadate binding to high-affinity site was reduce when SR was preincubated with phosphate. Fig. 5 shows time-courses of vanadate binding to SR in the presence of various concentrations of Pi. The medium was contained 2.5 mg/ml SR vesicles, 0.1 M KCl, 20 mM TES (pH 7.2), 10 mM $MgCl_2$, 1 mM EGTA and 10 % Me_2SO, and vanadate was added at the concentration of 10 μM Under this condition, almost all vanadate was bound to the high-affinity site of Ca^{2+}-ATPase. When vanadate was added to the medium in the absence of Pi, the amount of vanadate binding increased slowly and reached maximum level within 3 min after addition of vanadate. The rate of vanadate binding to the high-affinity site become lower as Pi concentration in the medium was higher. In the presence of 10 mM Pi, the rate of vanadate binding was reduced to 7% of the control. But the maximum level of vanadate binding was same irrespective of the presence or absence of Pi. If the E_2P decay of slow-phase is caused by these slow vanadate binding to the high-affinity site, it is expected that the time-course of vanadate binding to high-affinity site will coincide with that of slow-phase E_2P decay. Fig. 6 shows time courses of E_2P decay of the slow-phase and vanadate binding to the high-affinity site

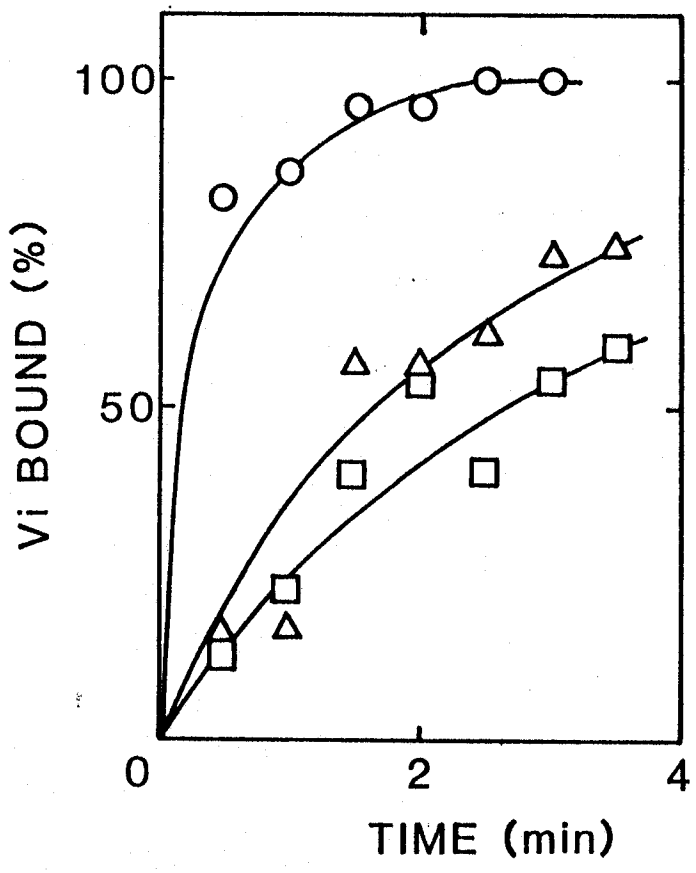

Fig. 5 Time course of vanadate binding to high-affinity site----- SR vesicles (2.5mg/ml) were incubated in the medium containing 0.1 M KCl, 20 mM TES (pH 7.2), 10mM $MgCl_2$, 1 mM EGTA and 10% Me_2SO in the presence of 0 (○), 5 (△), and 10 mM Pi (□). Vanadate was added at the concentration 10 μM. After incubation with vanadate for indicated time, the amount of bound vanadate was measured by the Dowex column method as described in "EXPERIMENTAL PROCEDURE." Nonspecific vanadate binding was determined in the medium containing 3 mM $CaCl_2$. The amount of vanadate binding was represented as percent of the maximum vanadate binding. The maximum vanadate binding was determined as the amount of vanadate binding when vanadate was added to the medium before Pi.

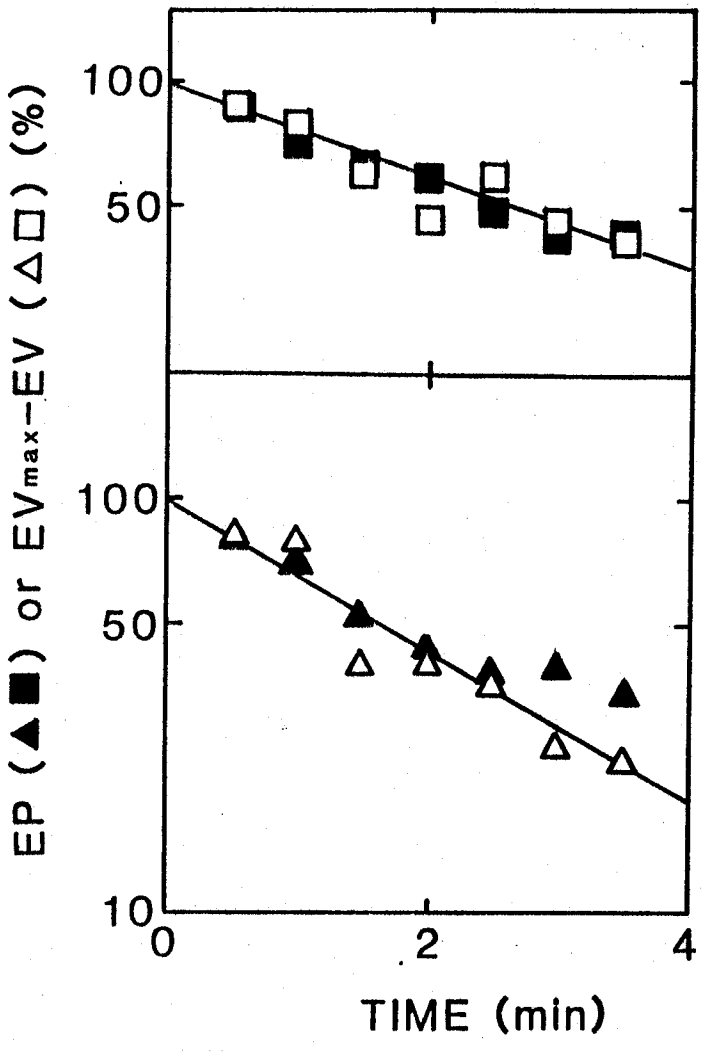

Fig. 6 Time courses of slow-phase E_2P decay and vanadate binding to the high-affinity site----- Open symbols indicate the amount of high-affinity vanadate binding sites which remain unoccupied with vanadate. Data was obtained from Fig. 5. Closed symbols indicate the time course of slow-phase E_2P decay by adding 10 μM vanadate in the presence of 10 (□,■) and 5 mM Pi(△,▲).

after addition of 10 μM vanadate to the reaction medium containing 10 (upper panel) and 5 mM (lower panel) Pi. To adjust the direction of vertical axis, the amount of vanadate binding was represented by difference between the amount of vanadate binding at maximum level and the amount of vanadate binding at indicated time. Both in the presence of 5 and 10 mM Pi, time-courses of vanadate binding to the high-affinity site fit to that of E_2P decay in the slow-phase. These observations suggested that the slow-phase E_2P decay might be caused by the vanadate binding to the high-affinity site.

Inhibition of E_2P formation by preincubation with vanadate-----
In the preceding section, E_2P decay was observed after addition of vanadate to the reaction mixture containing Pi. In this section the effect of high-affinity vanadate binding on the E_2P formation was examined after preincubation of SR with low concentration of vanadate. As shown in Fig. 7, the E_2P level decreased as a function of time interval of incubation in which 0.2 mg/ml SR vesicles was included with 0.1 M KCl, 20 mM TES (pH 7.2), 10 mM $MgCl_2$, 1 mM EGTA and 10% Me_2SO in the presence of various concentrations of vanadate. After 10 min, inhibition of E_2P formation by vanadate reached the maximum. The maximum inhibition of E_2P formation varied from 80 to 95% with increasing vanadate concentration from 1 to 5 μM. Since the effect of vanadate binding to the low-affinity site was negligible under these condition, inhibition of E_2P formation was considered to be due to vanadate binding to the high-affinity binding site. When SR vesicles were incubated with vanadate in the absence of Mg^{2+},

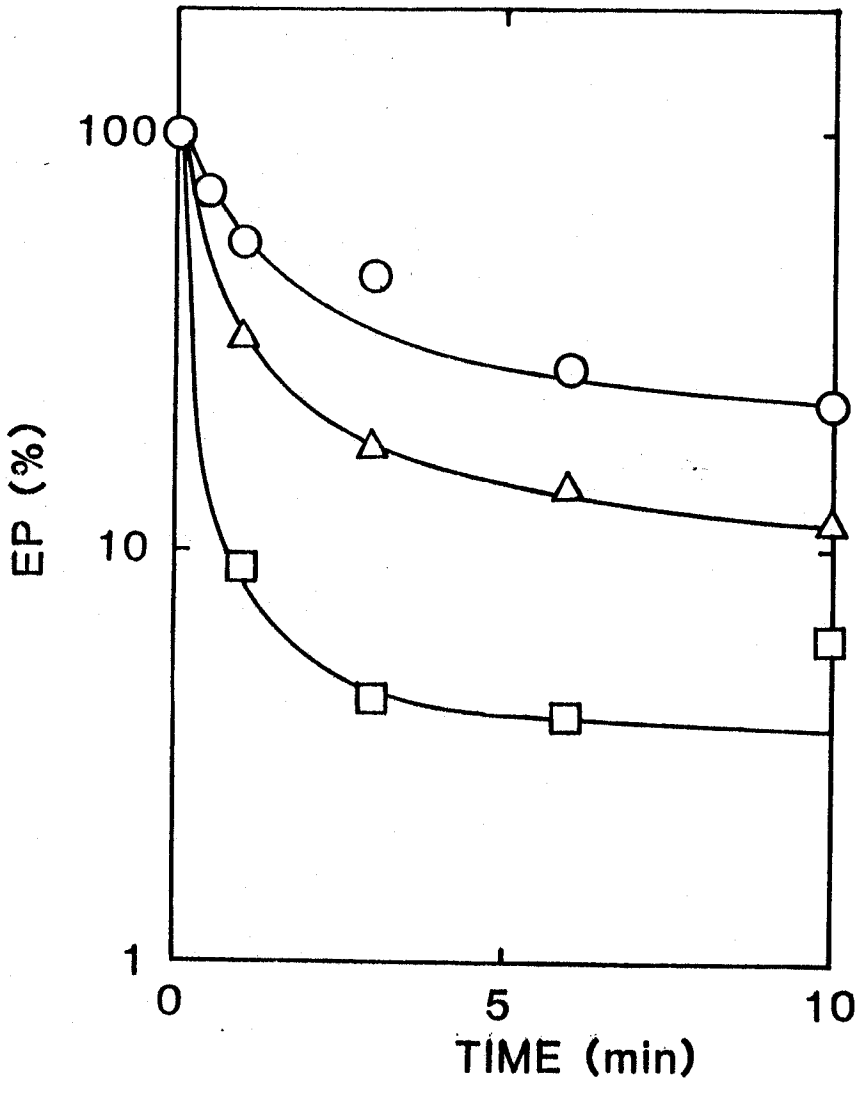

Fig. 7 Inhibition of E_2P formation by vanadate binding to high-affinity sites----- SR vesicles (0.2mg/ml) were incubated with 1 (□), 2 (△) and 5 μM vanadate (○) in the presence 0.1 M KCl, 20 mM TES (pH 7.2), 10 mM $MgCl_2$, 1 mM EGTA and 10% Me_2SO at 20° C. At the indicated time, E_2P was formed by adding 10 mM [^{32}P]Pi. After incubation for 10 sec, reaction was terminated by 5% TCA. The amount of E_2P was expressed as a percent of initial one.

inhibition of E_2P formation by vanadate was not observed (Fig. 8), while strong inhibition was observed in the presence of Mg^{2+}, indicating that vanadate binding to the high-affinity site absolutely requires Mg^{2+} ion to inhibit E_2P formation. On the contrary the inhibitory effect of vanadate was removed by addition of EDTA to chelate Mg^{2+} of the medium, the activity of E_2P formation scarcely restored at least up to 2 min after addition of EDTA. To explain these observations, we proposed a mechanism for the inhibition of E_2P formation by vanadate binding to high-affinity site as follow.

$$^{*}E_2Vi \overset{k}{\rightleftharpoons} E_2Vi \overset{K_{VH}}{\rightleftharpoons} E_2 \overset{K_{PH}}{\rightleftharpoons} E_2Pi$$

Scheme 2

It should be noted that the vanadate binding site differs from that of scheme 1 that E_2P never forms phosphate. Where $^{*}E_2$ denotes an inactive form of Ca^{2+}-ATPase. The formation of $^{*}E_2$ form Ca^{2+}-ATPase is cause of inhibition of E_2P formation. We assumed that the rate of transition from E_2Vi to $^{*}E_2Vi$ was slow and that the reverse step was more slow. This mechanism can easily explain the observations that inhibition of E_2P formation by vanadate reached equilibrium after 10 min incubation (Fig. 7) and that vanadate inhibition was eliminated with a definite lag phase after addition of ATP and $Ca^{2;}$ (9). According with scheme 2, the rate of inhibition (k_{app}) is given by eq 1.

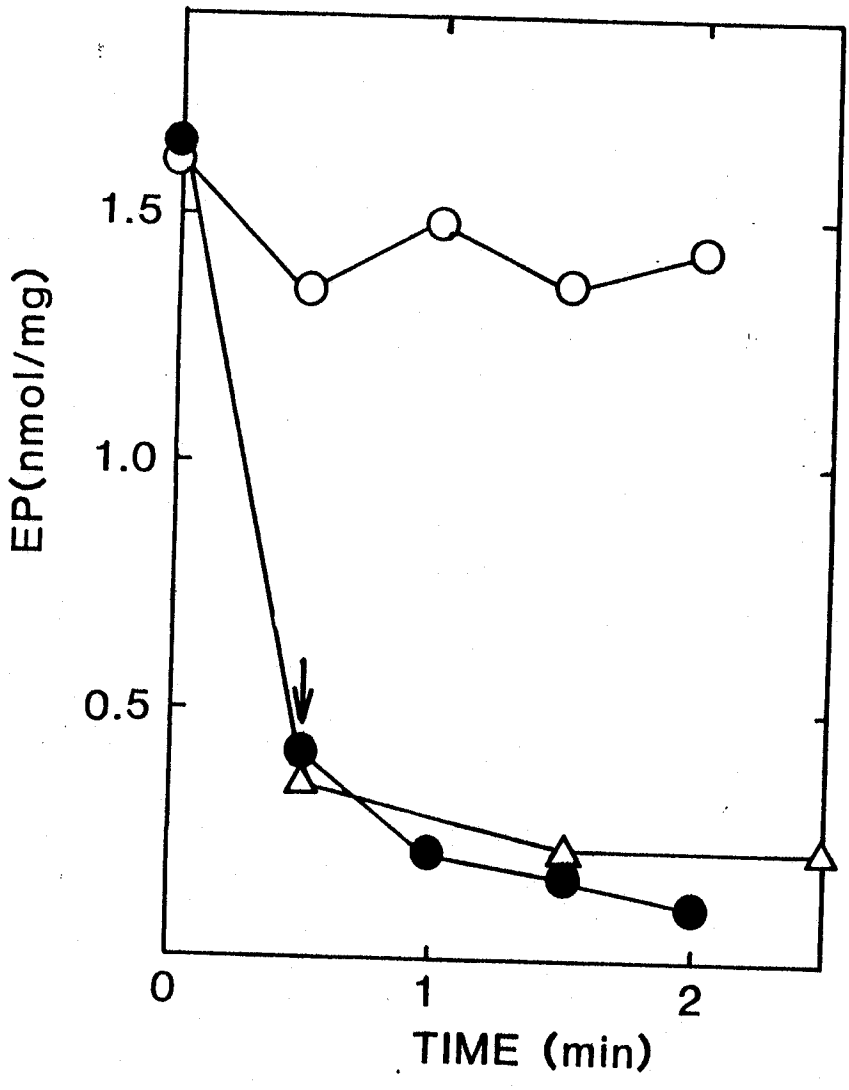

Fig. 8 Reversibility of the inhibition of E_2P formation by vanadate binding to high-affinity site----- SR vesicles were incubated with 20 μM vanadate in the presence (●) or absence (○) of 10mM $MgCl_2$ at 20° C. (Triangles):After 30 sec incubation in the presence of 10mM $MgCl_2$, 12 mM EDTA was added in the medium (pointed by arrow.) At indicated time, E_2P level was measured by adding 10 mM [^{32}P]Pi (●) or 10 mM [^{32}P]Pi and 10 mM $MgCl_2$. (○,△)

$$k_{app}=k[E_2Vi]/[E]_0 \quad (1)$$

Where $[E]_0$ denote total amount of Ca^{2+}-ATPase. The value of k_{app} decreases as a function of phosphate concentration according to the eq. 2.

$$k_{max}/(k_{max}-k_{app})=(K_{PH}[Vi]+K_{VH}K_{PH})/K_{VH}[Pi]+1 \quad (2)$$

Where the value of k_{app} in the absence of phosphate is defined as k_{max}. Fig. 9 shows time courses of E_2P decay after addition of 10 μM vanadate to the reaction medium, where SR was phosphorylated by Pi at various concentrations. According to the eq. 2, the first order rate constant of slow-phase E_2P decay was plotted against Pi concentration (Fig. 9 inset). These plot gave a straight line with a an apparent dissociation constant (K_p) of 0.8 mM. Where, K_p represents the Pi-concentration which gives the half maximum protection from the inhibition by vanadate at a given concentration. K_P was expressed as follow.

$$K_P=K_{PH}[Vi]/K_{VH}+K_{PH} \quad (3)$$

According to eq 3, the value of K_{PH} was estimate as less than 0.8 mM. This value was more than 10 times smaller than Km value for E_2P formation (4-10 mM). Therefore, these assumption lead us the conclusion that there exists a Pi binding site which is different from the phosphorylation site.

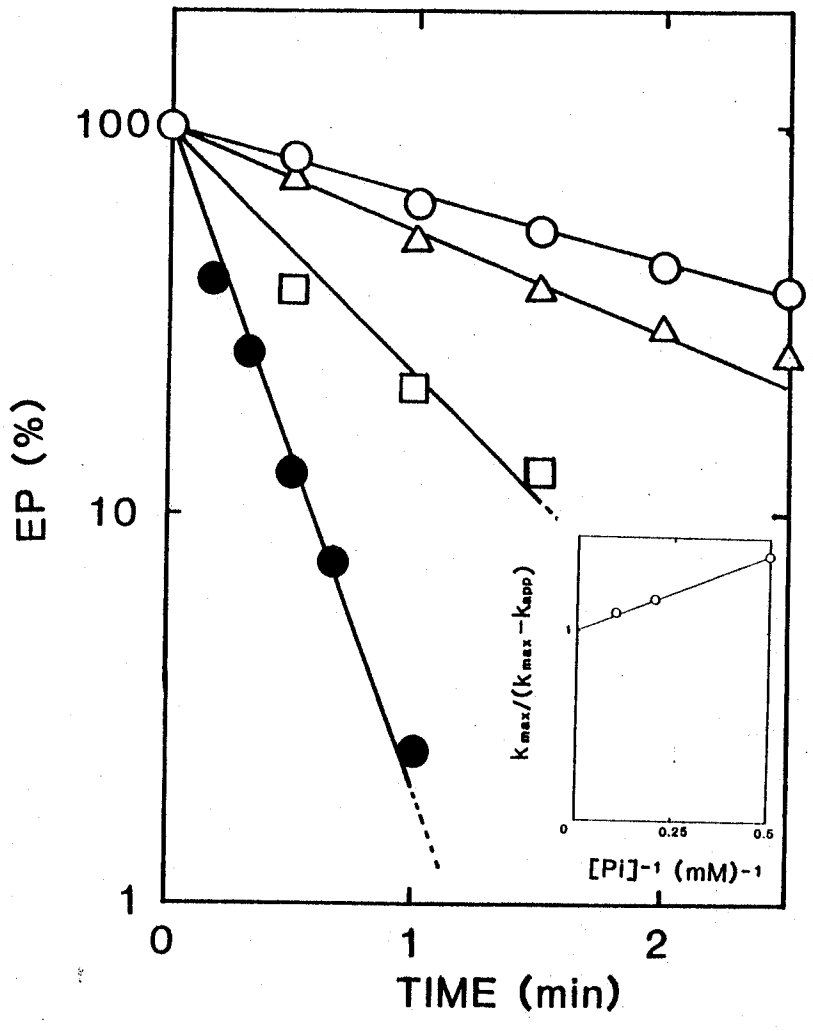

Fig. 9 Phosphate concentration dependency of slow-phase inhibition rate----- Open symbols show time course of E_2P decay by the addition of 10 μM vanadate, that were measured as described in Fig. 2 in the presence of 2 (□), 5 (△) and 10 mM Pi (○). Closed symbols show time course of inhibition of E_2P formation by 10 μM vanadate in the absence of Pi. At indicated time, inhibition was terminated by adding 12 mM EDTA, and E_2P level was measured as in Fig. 8. Inset shows double-reciprocal plot of the decay rate against Pi concentration. From this plot, the value of apparent Kd was 0.8mM.

DISCUSSION

Vanadate is known as an analogue of phosphate and it inhibits the activities of ATPases such as Na^+-K^+-ATPase (1), plasma membrane ATPase (21) and myosin ATPase (16) at concentrations below 1 μM. Several authors have previously shown that Ca^{2+}-ATPase of SR was also inhibited by vanadate (3-6). The vanadate-induced inactivation of Ca^{2+}-ATPase is considered to be caused by binding of vanadate to E_2 state of Ca^{2+}-ATPase as an analogue of phosphate (6,7). Vanadate binding to Ca^{2+}-ATPase results in formation of enzyme-vanadate complex (E_2Vi) which is assumed to be analogous to E_2P (3,7,12). So, the study of E_2Vi formation has been thought to serves as a tool for the investigation of phosphorylation and dephosphorylation steps of E_2P. However, there is a large difference in the binding capacity of Ca^{2+}-ATPase between phosphate and vanadate. The maximum vanadate binding capacity of 6-8 nmol/mg appears to be twice greater than maximum E_2P level which dose not exceed 3-4 nmol/mg. In the previous reports there have been no convincing explanation for this difference. Recently, we reported that two classes of vanadate binding sites having a great different affinities exist in the Ca^{2+}-ATPase, and that both of these sites had the same maximum binding capacity of 2.6-3.6 nmol/mg, which correspond to 0.5 mol/mol ATPase (11). Since these values of vanadate binding capacity are almost equal to the maximum amount of E_2P, so it was assumed that either one of the high- or low-affinity vanadate binding site corresponded to phosphorylation site of Ca^{2+}-ATPase. The study of E_2P decay after addition of

vanadate exhibited a biphasic time course (Fig 1 and 2). The fast- and slow-phase of E_2P decay were considered to be caused by vanadate binding to the low- and high-affinity sites, respectively. The fast-phase E_2P decay was competitively prevented by phosphate at low affinity site (Fig. 3). Furthermore, saturation of the low-affinity site with vanadate resulted in a complete inhibition of E_2P formation (Fig. 3). These observations lead us a conclusion that the low-affinity vanadate binding site is the catalytic site where E_2P is formed from Pi. Since the amount of low-affinity vanadate binding site was 0.5 mol per 1 mol of Ca^{2+}-ATPase, this conclusion supports the "half-of-the-site" theory indicating that only one subunit of dimer can exist in a phosphorylated form (22-24).

On the other hand, the slow-phase decay of E_2P level was assumed to be induced by the vanadate binding to the high-affinity site of the ATPase (Fig. 6). Similar observations of this slow reaction of vanadate with Ca^{2+}-ATPase have been reported by many investigators on the basis of kinetic measurement such as changes in fluorescence of FITC bound to the ATPase (5) and that of intrinsic tryptophan (7), inhibition of E_2P formation from ATP (12), re-activation of ATPase on removal of vanadate (9). Therefore, it is more likely that these slow reactions reflect the conformational changes induced by vanadate binding to the high-affinity site (as shown in scheme 2), rather than vanadate binding to the low affinity site or the phosphorylation site.

The time course of vanadate binding to high-affinity site agreed with that of E_2P decay in slow-phase(Fig. 6). Furthermore,

the preincubation of SR with concentrations of vanadate inhibited E_2P formation. These observations suggest that vanadate binding to high-affinity site as well as to low-affinity site can induce a complete inhibition of E_2P formation. However, the high-affinity vanadate binding site is located on a different Ca^{2+}-ATPase molecule from that which possessing low-affinity vanadate binding site (11). So it is suggested that the mechanism by which E_2P formation is inhibited by vanadate binding to high affinity site may be different from that of inhibition of E_2P formation by vanadate binding to low-affinity site. One of the possible explanation for this difference is that Ca^{2+}-ATPase molecules exist in SR membrane in dimeric form (25) and that the dimeric interaction may be involved in the E_2P formation. From the experiment shown in Fig. 9, it is possible that Ca^{2+}-ATPase has a high-affinity phosphate binding site which is different from the phosphorylation site. The high-affinity vanadate binding may inhibit E_2P formation by interrupting the phosphate binding to the high affinity site. It is unknown how the molecular interaction involves in the E_2P formation. It may bring a conformational change of Ca^{2+}-ATPase, which makes Ca^{2+}-ATPase reactive to phosphate. The phosphate binding to the non-catalytic site has not yet been directly observed yet. Because the value of the dissociation constant in the Pi binding was too high ($\sim 10^{-4}$ M), so high back ground will disturb the precise measurements of the specific phosphate binding.

REFERENCES

1. Cantley,L.C., Cantley,L.G., & Josephson,L. (1978) J.Biol.Chem. 253, 7361-7368
2. Macara,I.G. (1980) Trends Biochem.Sci. 5, 92-94
3. O'Neal,S.G., Rhoads,D.B. & Racker,E. (1979) Biochem.Biophys. Res.Commun. 89, 845-850
4. Wang,T., Tsai,L.I., Slaro,R.J., Grassi deGende, A.O. & Schwartz,A. (1979) Biochem.Biophys.Res.Commun. 91, 356-361
5. Pick,U. (1982) J.Biol.Chem. 257, 6111-6119
6. Pick,U, & Karlish,S.J.D. (1982) J.Biol.Chem. 257, 6120-6126
7. Dupont,Y. & Bennett,N. (1982) FEBS Lett. 130, 237-240
8. deMeis,L (1981) in "The Sarcoplasmic Reticulum. pp.44-54 John Wiley & Sons, New York
9. Ortiz,A., García-Carmona,F., García-Cánovas,F. & Gómez-Fernández,J.C. (1985) Biochem.J. 221, 213-222
10. Markus,S., Priel,Z., & Chipman,D.M. (1989) Biocemistry 28, 793-799
11. Yamasaki,K. & Yamamoto,T. (1991) J.Biocem. 110, 915-921
12. Medda,P. & Hasselbach,W. (1983) Eur.J.Biochem. 137, 7-14
13. Varga,S., Csermely,P., & Martonosi,A. (1985) Eur.J.Biochem 148, 119-126
14. Andersen,J.P., & Møllar,J.V. (1985) Biochim.Biophys.Acta. 815, 9-15
15. Yamada,S., Yamamoto,T., & Tonomura,Y. (1970) J.Biochem. 61, 789-794
16. Goodno,C.C. (1979) Proc.Natl.Acad.Sci.US 76, 2620-2624
17. Takisawa,H. & Tonomura,Y. (1979) J.Biochem. 86, 425-441

18. Boyer,P.D., deMeis,L., Carvalho,M.G.C., & Hackney,D.D. (1977) Biochemistry 16, 136-140

19. Chaloub,R.M., Guimaraes-Motta,H., Verjovski-Almaeida,S., deMeis,L. & Inesi,G. (1979) J.Biol.Chem. 254, 9464-9468

20. Guimaraes-Motta,H., & deMeis,L. (1980) Arch.Biochem.Biophys. 203, 395-403

21. Carafoli,E. & Zurini,M (1982) Biochim.Biophys.Acta, 683, 279-301

22. Froehlich,J.P., & Taylor,E.W. (1975) J.Biol.Chem. 250, 2013-2021

23. Verjovski-Almeida,S., Kurzmack,M., & Inesi,G. (1978) Biochemistry 17, 5006-5013

24. Ferreira,S.T., & Verjovski-Almeida,S. (1988) J.Biol.Chem. 263, 9973-9980

25. Dux,L., Taylar,K.A., Ting-Beall,H.P., & Martonosi,A. (1985) J.Biol.Chem. 260 11730-11743

Part III

Effects of Adenyl-5'-Imidodiphosphate and Vanadate Ion on the Intermolecular Cross-Linking of Ca^{2+}-ATPase in the Sarcoplasmic Reticulum Membrane with N,N'-(1,4-Phenylene) Bismaleimide

SUMMARY

The functional significance of the molecular interaction of Ca^{2+}-ATPase in the sarcoplasmic reticulum (SR) membrane was examined using intermolecular cross-linking of Ca^{2+}-ATPase with N,N'-(1,4-phenylene) bismaleimide (PBM). When SR vesicles were allowed to react with 1 mM PBM at pH 7 and 23° C for various intervals and subjected to SDS-PAGE, the amount of the major band of monomeric ATPase decreased with a half life of about 20 min. Higher orders of oligomers were concurrently formed without accumulation of any particular species of oligomer.

When SR vesicles were allowed to react with 1 mM PBM in the presence of 1 mM adenyl-5'-imidodiphosphate (AMP-PNP), the rate of oligomerization was markedly reduced and the amount of dimeric Ca^{2+}-ATPase increased with time. After 1 h, more than 40% of the Ca^{2+}-ATPase had accumulated in the dimeric form. When 1 mol of fluorescein isothiocyanate (FITC) was bound per mol of ATPase, the effects of AMP-PNP on the cross-linking with PBM were completely abolished.

When SR vesicles were treated with PBM in the presence of 0.1 mM vanadate in Ca^{2+} free medium, the oligomerization of the Ca^{2+}-ATPase by PBM was strongly inhibited. The vanadate effect on the cross-link formation was completely removed by the presence of Ca^{2+} and AMP-PNP in the reaction medium.

When SR vesicles were pretreated with PBM in the presence of AMP-PNP and digested with trypsin for a short time, the dimeric ATPase was degraded to a peptide with an apparent molecular mass of about 170 kDa. Further digestion resulted in

degradation to a 130k Da peptide. As they were phosphorylated by [γ-^{32}P]ATP in the presence of Ca^{2+}, these peptides contained the subfragment A. In addition, the SDS-PAGE pattern of the dimeric ATPase after the prolonged digestion lacked subfragment A_1, suggesting that ATPase molecules were cross-linked by PBM through an SH group in the A_1 region of this enzyme.

INTRODUCTION

Active transport of Ca^{2+} across the SR membrane is tightly coupled with ATP hydrolysis by membrane-bound Ca^{2+}-ATPase. A number of investigations have suggested that ATPase molecules exist in the intact SR membrane in an oligomeric form (1-3), and it has been postulated that the protein-protein interaction in the SR membrane might be involved in the catalytic function of the Ca^{2+} transport. Several attempts have been made to elucidate this mechanism. For example, Dux et al. (4) showed by electron microscopy that the Ca^{2+}-ATPase forms two distinct types of crystals within the SR membrane, depending on the E_1 and E_2 conformations of the enzyme. Andersen et al. (5) suggested from analysis of HPLC profiles of solubilized ATPase that the equilibrium between monomeric and oligomeric ATPase was controlled by the presence of Ca^{2+} and nucleotide.

To obtain direct evidence for this possibility, and to determine the neighboring site on the ATPase molecules in the SR membrane, we have explored the conditions for cross-linking the ATPase molecules by the use of N,N'-(1,4-phenylene)bismaleimide (PBM). We observed that the cross-linking reaction with PBM between Ca^{2+}-ATPase molecules in the intact SR membrane was greatly affected by the binding of AMP-PNP or vanadate to the ATPase. Analysis of tryptic digests of the ATPase cross-linked by PBM in the presence of AMP-PNP suggested that a cross-link was formed with PBM between the A_1 subfragments of the associated protein.

EXPERIMENTAL PROCEDURES

Materials-- Sarcoplasmic reticulum (SR) was isolated from rabbit dorsal and hind limb white muscles by a method described previously (6). The isolated SR vesicles suspended in 60 mM KCl, 20% glycerol and 10 mM Tris-maleate (pH 6.5) were divided into small portions, rapidly frozen by aqueous nitrogen and stored at -80° C. [γ-^{32}P]ATP was synthesized according to Johnson and Walseth (7). AMP-PNP was obtained from Sigma Co. PBM was purchased from Wako Pure Chemicals Ltd. Monovanadate was prepared from V_2O_5 according to Goodno (8). All other reagents were of analytical grade.

Treatment of SR with PBM--The reaction was started by adding a small portion of PBM dissolved in DMSO to the incubation medium, which contained 2.5 mg/ml of SR protein, 0.1 M KCl, 20% glycerol, and 10 mM Tris-maleate at pH 7.0 and 23° C. Unless otherwise specified, final concentrations of PBM and DMSO were 1 mM and 10%, respectively. The reaction was terminated by addition of 14 mM -mercaptoethanol. As indicated in the figure legends, the reaction mixture had been centrifuged or passed through a short column of Sephadex G-50 to remove free PBM prior to starting the reaction.

Gel Electrophoresis-- SDS-PAGE was performed by the method of Laemmli (9) or of Weber and Osborne (10). Before electrophoresis, samples were dissolved in sample buffer containing 1% SDS, 1% β-mercaptoethanol, 20% glycerol, 10 mM Tris-HCl (pH 8.8) and 0.1% bromophenol blue. The samples were then loaded on a polyacrylamide slab gel of 1 mm thickness and

subjected to electrophoresis. The gel was stained for protein with Coomassie brilliant blue. In some experiments, densitometric traces of the lanes were obtained by scanning at 570 nm. The area under each protein peak was determined by cutting it out and weighing it.

Measurements of ATPase Activity and EP Formation--The reaction of the steady state ATPase activity was started by adding 1 mM ATP to 0.8 ml fractions obtained by HPLC. After 40 min incuvation at 23° C, it was terminated by the addition of 5% TCA. The amount of Pi liberated was determined by a method of Martin and Doty (11). The activity of EP formation was measured under the condition described above except that 50 μM [γ-^{32}P]ATP was used instead of 1 mM nonradioactive ATP and that the reaction was stopped at 15 s after addition of ATP. The amount of EP formed was determined as described elsewhere (12).

Autoradiography-- Ca^{2+}-ATPase was phosphorylated by [γ-^{32}P]ATP as described in the legend for Fig. 8. SR protein was precipitated with 5% TCA solution and the pellet was collected by centrifugation. The pellet was dissolved in 1% LDS and used for SDS-PAGE by the method of Weber and Osborne (10). The gel was stained with Coomassie brilliant blue and then dried. Radioactivity was detected using Kodak Diagonistic film X-OMA AR. Autoradiography was carried out at -80° C.

1. Effects of Nucleotide Binding to Ca^{2+}-ATPase on the Cross-Link Formation with PBM-- We examined the conditions for the intermolecular cross-linking of the ATPase by using PBM, and found that nucleotide binding to the ATPase strongly affected the cross-linking reaction. As shown in Figs. 1 and 2, SR vesicles (2.5 mg/ml protein) were allowed to react with 1 mM PBM for the indicated times in the medium containing 60 mM KCl, 20% glycerol, and 10 mM Tris-maleate at pH 7.0 and 23° C. After quenching the incubation by adding an excess of β-mercaptoethanol, a small portion of the mixture was taken for electrophoresis in 5% polyacrylamide gel in the presence of SDS (Fig. 1A). When the PBM reaction had not been done, the gel electrophoresis pattern showed a major band of a Ca^{2+}-ATPase monomer with a molecular mass of about 110 kDa, and several minor bands with molecular mass lower than 50 kDa. Some faint protein bands with molecular masses higher than 200 kDa were also seen in the PAGE pattern of the control sample, but their content was negligibly small compared to that of the monomeric ATPase. When the reaction time of SR with PBM increased, the amount of the monomeric ATPase decreased sharply, and new protein bands with molecular masses higher than 200 kDa were formed (Figs. 1A,2A). This observation suggests that Ca^{2+}-ATPase molecules are packed so closely in the SR membrane that they interact successively with each other to form various species of oligomers. The reaction of SR vesicles with PBM also resulted in the formation of another protein band with an apparent molecular mass of about 125 kDa. This appears to

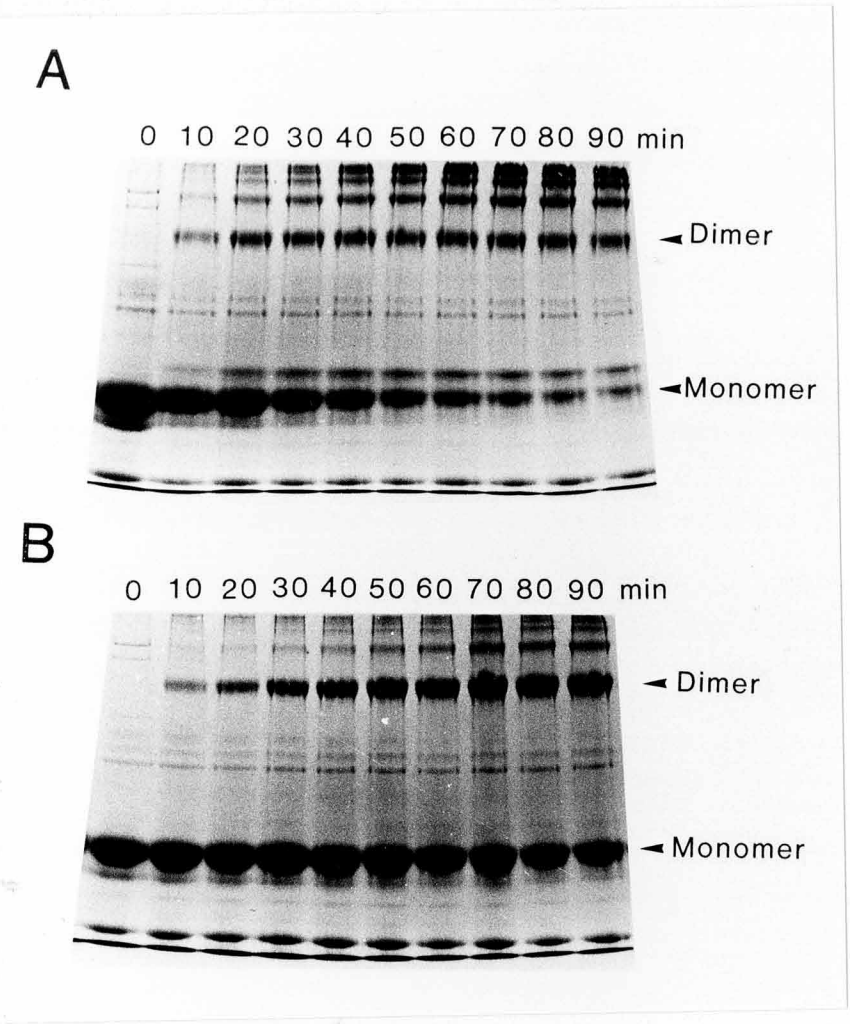

Fig.1 SDS-gel electrophoresis of SR proteins cross-linked with PBM: SR vesicles (2.5 mg/ml protein) were allowed to react with 1 mM PBM in a solution of 20% glycerol, 10 mM Tris-maleate (pH 7.0) and 10% DMSO in the absence (A) or presence (B) of 1 mM AMP-PNP at 23° C. The reaction was quenched with 14 mM β-mercaptoethanol at the indicated times. SR vesicles were solubilized with 1% SDS and taken for electrophoresis on 5% polyacrylamide gel according to the method of Laemmli (9).

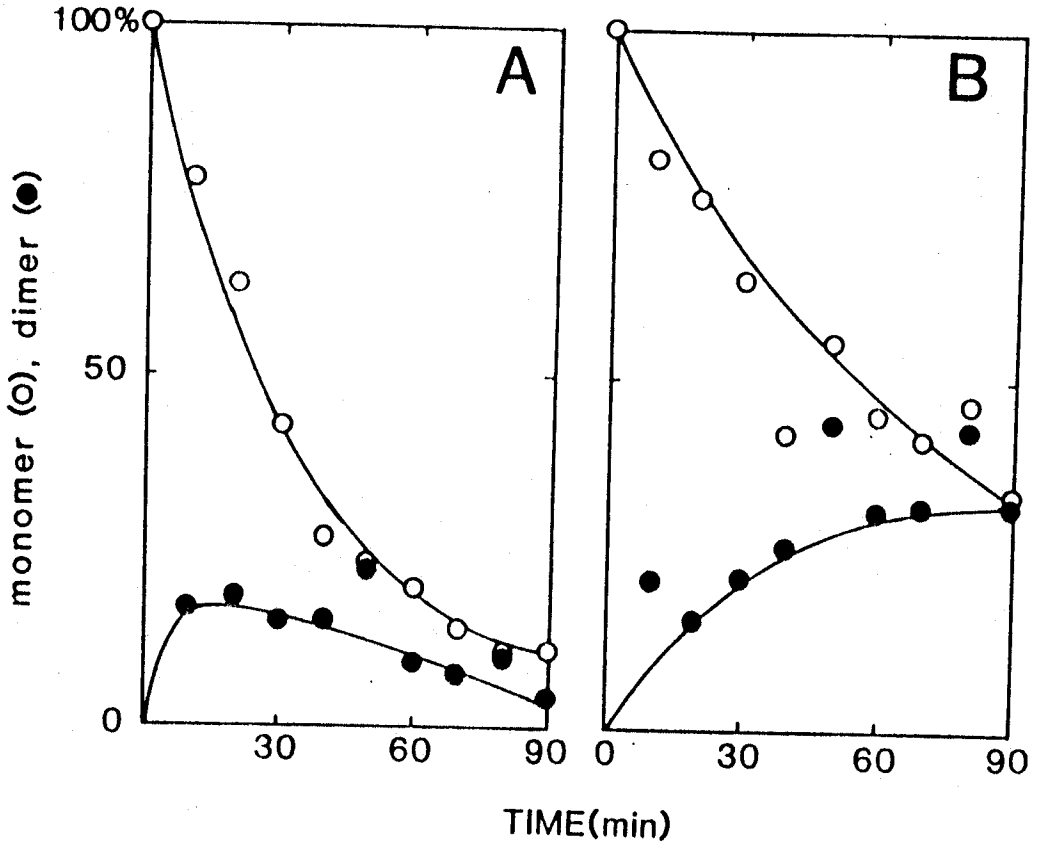

Fig.2 Time courses of changes in the amount of monomeric and dimeric Ca^{2+}-ATPase after addition of PBM to SR: Treatment of SR vesicles with PBM in the absence (A) or presence (B) of AMP-PNP and the SDS-PAGE of these samples were performed under the conditions given in Fig. 1. After staining the gel with Coomassie Blue, the amounts of monomeric (○) and dimeric (●) Ca^{2+}-ATPase were determined by measuring the density of the protein bands with a densitometer, and expressed as percent of the initial amount of the Ca^{2+}-ATPase monomer.

result from an intramolecular cross-linking of the Ca^{2+}-ATPase due to the PBM modification (13).

When SR was allowed to react with PBM in the presence of 1 mM AMP-PNP, the oligomerization pattern of the Ca^{2+}-ATPase revealed by SDS-PAGE was quite different from that observed in the absence of the nucleotide. As shown in Figs. 1B and 2B, the rate of the decrease in the amount of monomeric ATPase after addition of PBM was remarkably reduced by the presence of 1 mM AMP-PNP. Furthermore, the amount of dimeric ATPase increased with time after the addition of PBM, and a maximum of about 40% of the ATPase became cross-linked to form the dimer after the 1 h incubation (Fig. 2B). This is in contrast to the time course of dimer formation in the absence of AMP-PNP in which the dimeric ATPase level increased to about 20% of the monomeric ATPase in 10 min after the addition of PBM, and gradually decreased to a level lower than 10% 1 h later (Fig. 2A).

We also tried to separate the cross-linked ATPase without denaturing in SDS by using molecular sieve HPLC in the presence of $C_{12}E_9$. Fig. 3 shows the elution pattern of the SR protein solubilized in $C_{12}E_9$ after treatment of SR with PBM for 1 h in the presence of AMP-PNP. A new peak of SR protein emerged at the position between the void volume and the monomeric ATPase peak. SDS-PAGE analysis indicated the new protein peak to be the dimeric ATPase. The amount of dimeric ATPase was markedly reduced when SR was preincubated with PBM in the absence of AMP-PNP. Interestingly, dimeric ATPase, as well as the monomeric one, retains the phosphorylation activity. This activity was almost the same as that of intact SR. Furthermore, these PBM-modified ATPase

fractions also showed ATP hydrolytic activity, although it was much lower than that of intact SR (data not shown).

The amount of dimeric ATPase formed by PBM increased depending on the AMP-PNP concentration with a half effective concentration below 50 μM. Accumulation of the dimeric ATPase was also seen in the presence of 10 mM ADP instead of AMP-PNP. These results indicate that saturation of the high affinity nucleotide binding site on the Ca^{2+}-ATPase with AMP-PNP may affect the intermolecular cross-linking with PBM. To test this possibility, we investigated the effect of pretreatment of Ca^{2+}-ATPase with FITC on the cross-link reaction of the Ca^{2+}-ATPase by PBM. As shown in Fig. 4, when about 6 nmol of FITC was bound to 1 mg of SR protein, the amount of monomeric ATPase that remained after 1 h incubation with PBM in the presence of AMP-PNP decreased to the control level, measured after the PBM treatment of SR without nucleotide. Under these conditions, ATPase activity was completely inhibited. These results indicate that FITC inhibited the AMP-PNP binding to the high affinity site of the ATPase to eliminate the nucleotide effect on the PBM modification of SR.

2. Effect of Vanadate on the Cross-Linking of ATPase by PBM

Vanadate is presumed to bind with high affinity to the phosphorylation site of the Ca^{2+}-ATPase as an analogue of Pi, and to inhibit the ATPase activity by the formation of a stable E_2-vanadate complex (14,15). Vanadate is also known to promote the second dimensional crystallization of the Ca^{2+}-ATPase on the SR membrane (16-19). The crystal has dimer chains as structural units. Therefore, it is of interest to examine the effect of vanadate on the cross-linking of the ATPase molecules by PBM. As

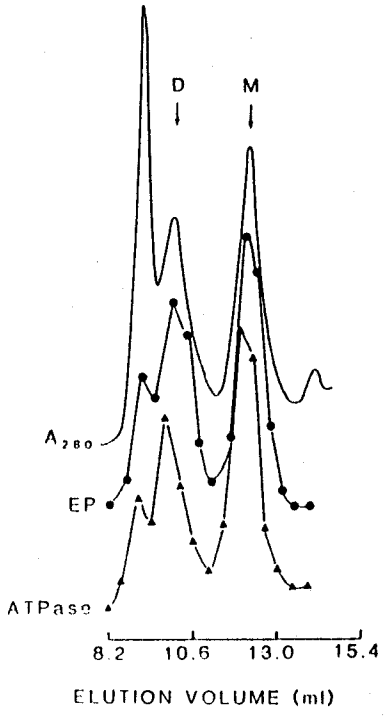

Fig.3 Association of EP formation and ATPase activity with the dimeric and monomeric ATPase fractions separated on HPLC: SR vesicles (2.5 mg/ml protein) were allowed to react with 1 mM PBM in the presence of AMP-PNP for 60 min under the conditions described in Fig. 1. The PBM-treated SR membrane was solubilized with 50 mg/ml $C_{12}E_9$ in a solution containing 20% glycerol, 10 mM TES (pH. 7.3), 0.1 M KCl, 5 mM $CaCl_2$, and 5 mM $MgCl_2$. ATPase was fractionated by HPLC using a TSK-G3000SW column which was equilibrated with the solution described above, except that the 50 mg/ml $C_{12}E_9$ was replaced with 10 mg/ml of detergent. The elution was monitored for protein concentration at 280 nm (solid line). The dimeric (D) and monomeric (M) peeks are indicated by arrows. Each 0.4 ml eluted was collected and the activities of EP formation (●) and ATP hydrolysis (▲) were measured.

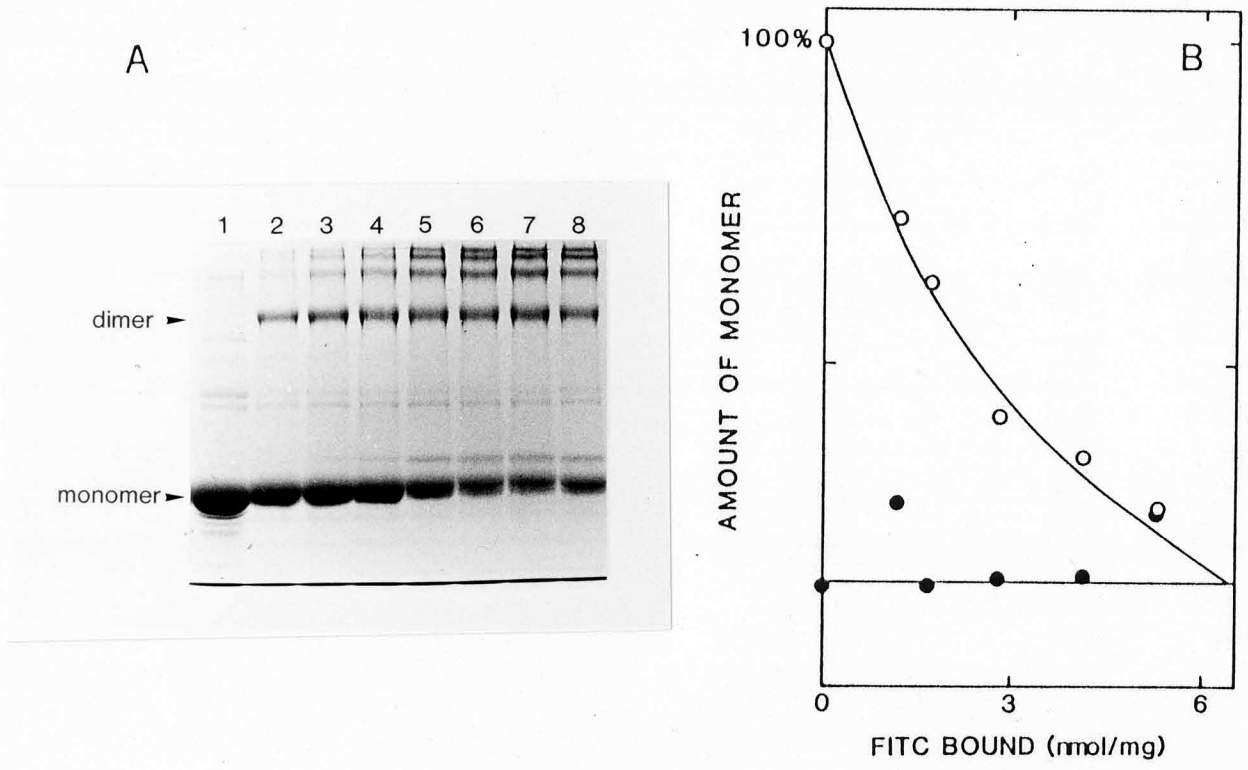

Fig. 4 Effect of pretreatment of SR with FITC on the cross-link of Ca^{2+}-ATPase with PBM: (A) SR (2.5 mg/ml) was preincubated with 0 (lanes 2 and 8), 2 (lane 3), 6 (lane 4), 10 (lane 5), 20 (lane 6) and 30 (lane 7) μM FITC for 2 h at 25° C in a solution of 0.1 M KCl, 20 mM Tris-HCl (pH 8.0), 5 mM $MgCl_2$ and 0.1 mM $CaCl_2$. After removal of free FITC by Sephadex G-50 chromatography, the labeled SR vesicles were allowed to react with 1 mM PBM (lane 1, without PBM) for 60 min at 23° C in the presence (lane 2-7) or absence (lane 8) of 1 mM AMP-PNP under the conditions given in Fig. 1. Aliquots of the cross-linked SR were taken for SDS-PAGE as in Fig. 1. (B) The amount of monomeric ATPase was determined from the PAGE pattern (A) described in Fig. 2, and plotted as the percentage of total ATPase against the amount of FITC bound to SR protein. Open and closed circles indicate the PBM modification in the presence and absence of AMP-PNP, respectively.

revealed by the gel-electrophoresis pattern, the cross-link formation of Ca^{2+}-ATPase with PBM was strongly prevented when 1 mM vanadate was present in the reaction medium (Fig. 5). On the other hand, the vanadate inhibition could be completely avoided when Ca^{2+} and AMP-PNP were simultaneously added to the reaction medium. A little protection from the vanadate inhibition was seen when 1 mM AMP-PNP alone was added to the reaction mixture. The marked protection after addition of 1 mM $CaCl_2$ (see lane 5, Fig. 5) seems to be caused by reduction of the vanadate concentration in the reaction medium by the formation of Ca-vanadate complex. Fig. 6 shows the time courses of the decrease in the amount of monomeric ATPase after addition of 1 mM PBM in the presence of various concentrations of vanadate. When vanadate was present in the reaction medium at concentration higher than 100 μM, the monomeric ATPase level decreased only slowly, and 70% of the ATPase remained as the monomer after 1 h incubation with PBM. However, the initial level of the monomeric ATPase decreased to almost 0 within 1 h when vanadate was present at concentrations below 10 μM. When SR was incubated with various concentrations of vanadate under conditions similar to those for PBM modification. the amount of vanadate bound to SR protein increased with an increase in the vanadate concentration. About 6 nmol of vanadate was bound to 1 mg SR protein under the optimal conditions, while no vanadate was bound to SR protein when 1 mM Ca^{2+} and AMP-PNP were present in the reaction medium (data not shown).

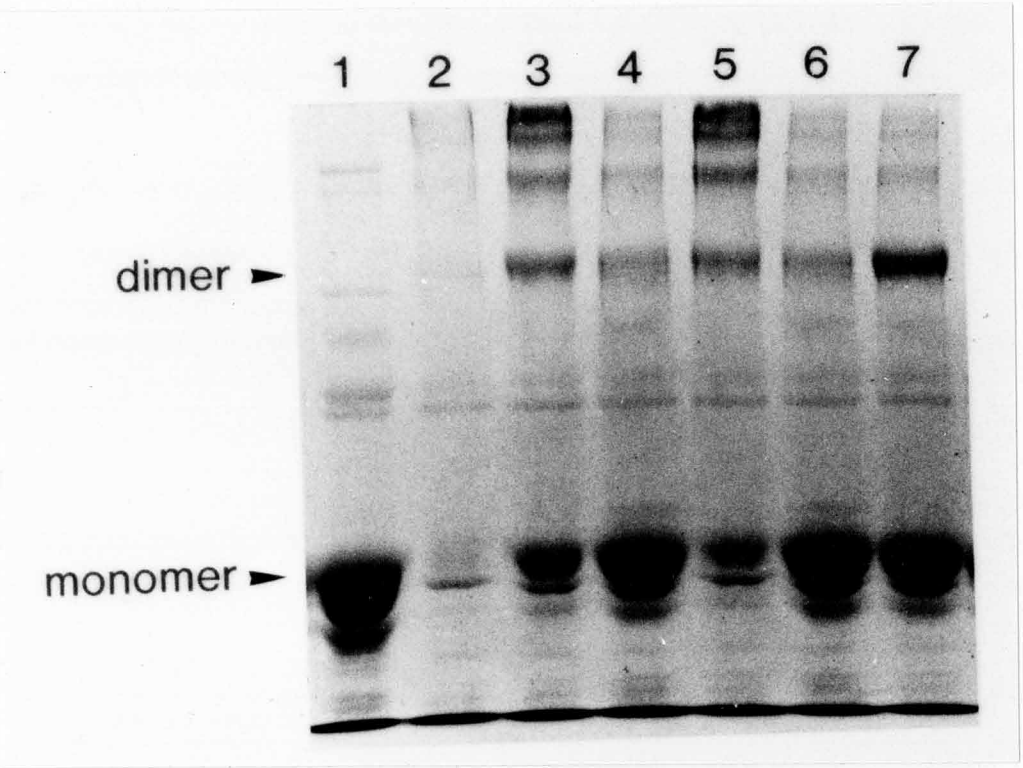

Fig. 5 Effect of vanadate on the cross-linking pattern of Ca^{2+}-ATPase with PBM: SR vesicles (2.5 mg/ml protein) were incubated in a solution of 0.1 M KCl, 5 mM $MgCl_2$, 20 mM TES (pH 7.3), and 10% DMSO at 23° C for 60 min. Further additions of reagents were as follows: lane 1, no addition; lane 2, 1 mM PBM; lane 3, 1 mM PBM + 1 mM AMP-PNP; lane 4, 1 mM PBM + 1 mM vanadate; lane 5, 1 mM PBM + 1 mM vanadate + 1 mM $CaCl_2$; lane 6, 1 mM PBM + 1 mM vanadate + 1 mM AMP-PNP; lane 7, 1 mM PBM + 1 mM vanadate + 1 mM AMP-PNP + 1 mM $CaCl_2$.

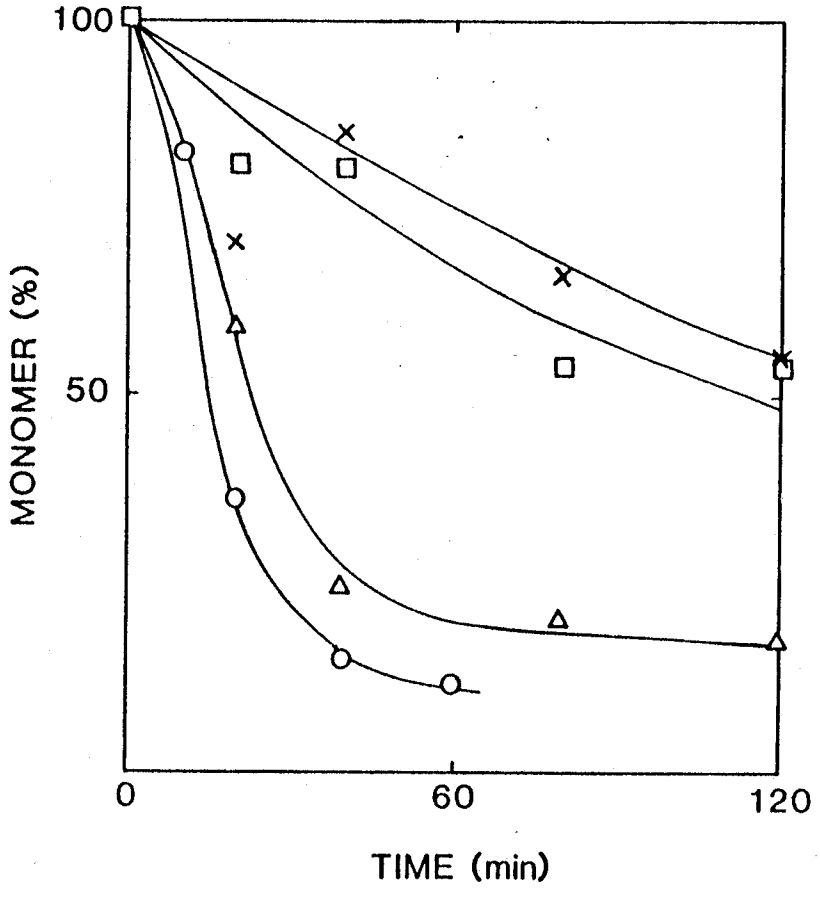

Fig. 6 Time course of decrease in monomeric ATPase in the reaction of SR with PBM at various concentrations of vanadate: SR vesicles (2.5 mg/ml protein) were allowed to react with 1 mM PBM in the presence of 0 (○), 10 (△), 100 (□) μM and 1mM (×) vanadate in 0.1 M KCl, 5 mM $MgCl_2$, 0.5 mM EGTA, 20 mM TES (pH 7.3) and 10% DMSO for 0-120min at 23° C. The reactions were quenched with 14 mM β-mercaptoethanol. Small aliquots were taken for SDS-PAGE as given in Fig. 5. The amount of monomer was determined as described in Fig. 2 and Experimental procedures.

3. Location of the Cross-Linking Site on Ca^{2+}-ATPase

To identify the positions on the ATPase molecules at which PBM can react to form the intermolecular cross-link between them, SR vesicles were allowed to react with trypsin after the PBM treatment in the presence of AMP-PNP.

The PBM-treated SR vesicles were digested with trypsin for various lengths of time at the weight ratio of trypsin to SR protein of 1:200. The SR sample was solubilized in 1% SDS and tryptic subfragments of the Ca^{2+}-ATPase were separated by electrophoresis in 5% gel. As shown in Fig. 7, the amount of the 220 kDa band of the dimeric ATPase decreased immediately after initiation of the digestion, and a new band with a molecular weight of about 170 kDa transiently appeared. The 170 kDa intermediate of the tryptic fragment is assumed to consist of the ATPase monomer and the tryptic subfragment A or B, with molecular masses of 55 kDa and 45 kDa, respectively. Further digestion of the PBM-modified SR with trypsin resulted in degradation of the 170 kDa protein band into major and minor protein bands with very similar molecular masses of about 130 kDa (Fig. 7).

Electrophoresis was carried out in 10% gel with the same sample used for Fig. 7. The major band of the monomeric ATPase, which had been kept for 1 h without being cross-linked by PBM, was cleaved quickly into A and B subfragments by tryptic digestion. A similar digestion pattern was obtained with the unmodified SR under the same conditions described above (data not shown). These results indicate that tryptic digestion pattern of SR-ATPase was not affected by the modification of SR with PBM. Therefore, the two protein bands with molecular weights of around 130 kDa were

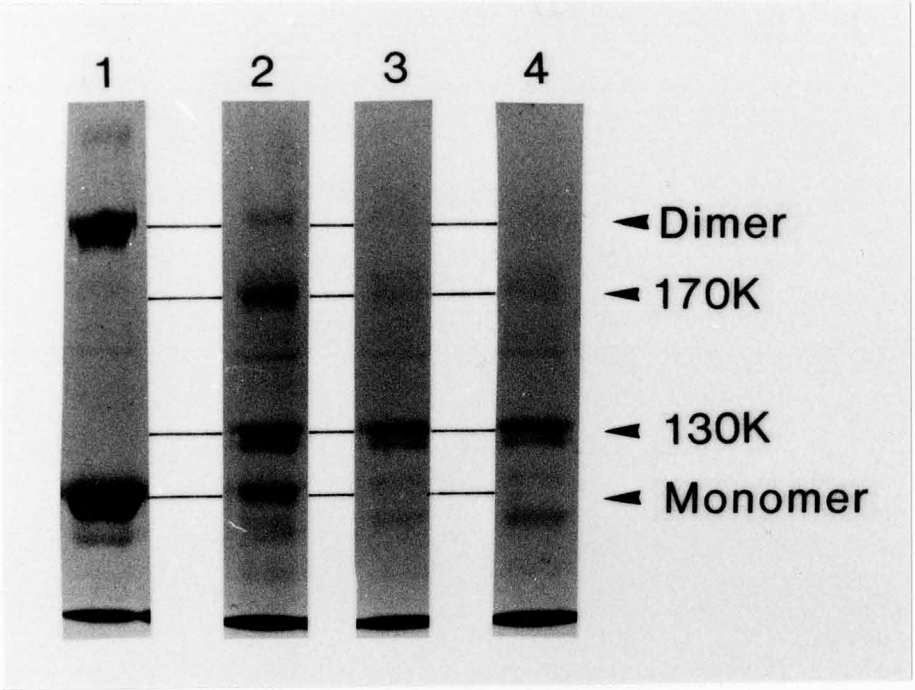

Fig. 7 Trypsin digestion of cross-linked SR protein: SR vesicles (2.5 mg/ml protein) were allowed to react with 1 mM PBM for 60 min in the presence of 1 mM AMP-PNP under the conditions described in Fig. 1. After quenching of the reaction with 14 mM β-mercaptoethanol, trypsin at 1/200 of SR protein by weight and 1 mM $CaCl_2$ were added to the reaction medium, and the mixture was incubated for 0 (lane 1), 2 (lane 2), 10 (lane 3), and 30 (lane 4) min. Digestion was terminated by adding trypsin inhibitor at a concentration in five-fold excess of trypsin. Tryptic subfragments of the Ca^{2+}-ATPase were separated on SDS-PAGE as described in Fig. 1.

produced from the dimeric ATPase via a 170 kDa fragment by cleavage with trypsin at the T_1 site of Ca^{2+}-ATPase.

In Fig. 8, the cross-linked Ca^{2+}-ATPase was phosphorylated by [γ-^{32}P]-ATP at 0, 1, and 20 min after tryptic digestion. The tryptic fragments were separated on SDS-PAGE according to Weber and Osborn (10), and the radioactivity was detected by autoradiography. As seen in the autoradiogram, the dimeric ATPase formed by PBM has an EP formation activity which is as high as that of monomeric ATPase. Furthermore, the tryptic fragments of both 170 kDa and 130 kDa were also phosphorylated, suggesting that these tryptic intermediates contain the subfragment A of Ca^{2+}-ATPase.

In order to distinguish between the proteolytic fragments dissociated from monomeric and dimeric ATPases, they had to be separately isolated and analyzed for the tryptic digests on SDS-PAGE. For this purpose, PBM-treated SR vesicles were solubilized with $C_{12}E_9$ after digestion with trypsin for 90 min and passed through a Sephacryl S-400 column in the presence of the detergent. The monomeric and dimeric ATPase fractions could thus be separated with high purity. These fractions were precipitated with TCA to condense the protein and then subjected to SDS-PAGE (Fig. 9). The SDS-PAGE showed that the prolonged digestion of SR with trypsin resulted in dissociation of the A_1 and A_2 fragments from the monomeric ATPase (Fig. 9B, lane 6), whereas only the A_2 fragment was produced from the cross-linked ATPase (Fig. 9, lanes 3,4,5). These results indicate that when SR was treated with PBM in the presence of AMP-PNP, ATPase molecules were cross-linked with the adjacent

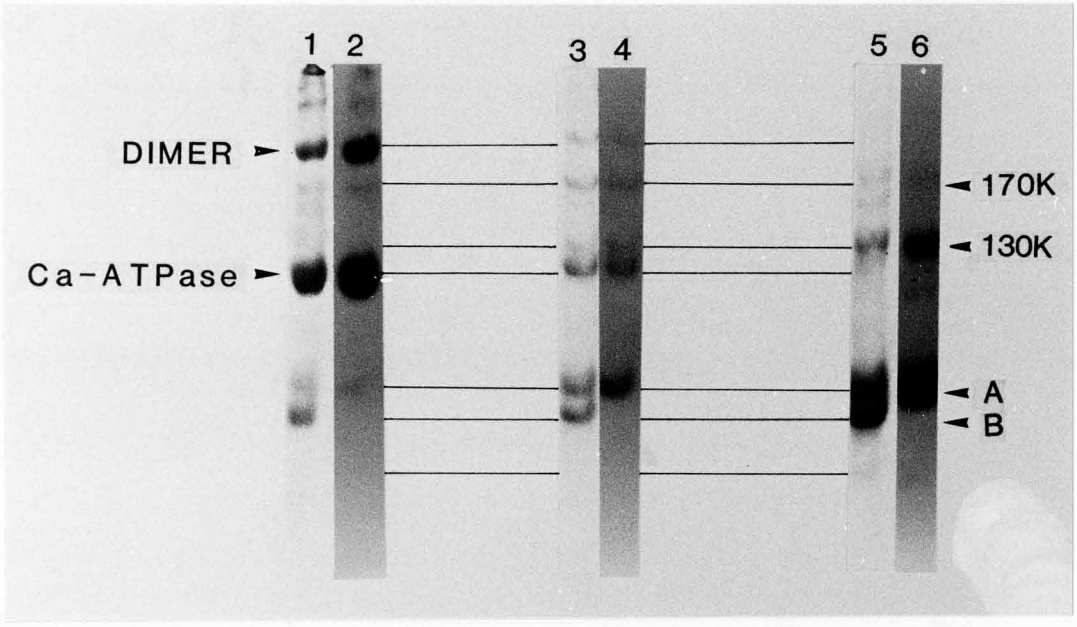

Fig. 8 Autoradiogram of the phosphorylated sub-fragments after tryptic digestion of the cross-linked SR: SR vesicles (2.5 mg/ml protein) were allowed to react with 1 mM PBM for 60 min at 23° C in the presence of 1 mM AMP-PNP in the presence of 80 mM KCl, 20 mM Tris-maleate (pH 7.0), 10 mM $MgCl_2$, 0.1 mM $CaCl_2$ and 10% DMSO, followed by tryptic digestion for 0 (lane 1,2), 1 (lane 3,4), and 20 (lane 5,6) min at 23°C. The Ca^{2+}-ATPase was phosphorylated with 50 μM [γ-^{32}P]ATP for 10 sec at 0° C and quenched with 5% TCA. The samples were centrifuged and the pellets were resuspended in 1% LDS and subjected to 5% polyacrylamide gel electrophoresis by the method of Weber and Osborn (10). The gel was stained with Coomassie blue (left side lanes), dried, and then subjected to autoradiography (right side lanes).

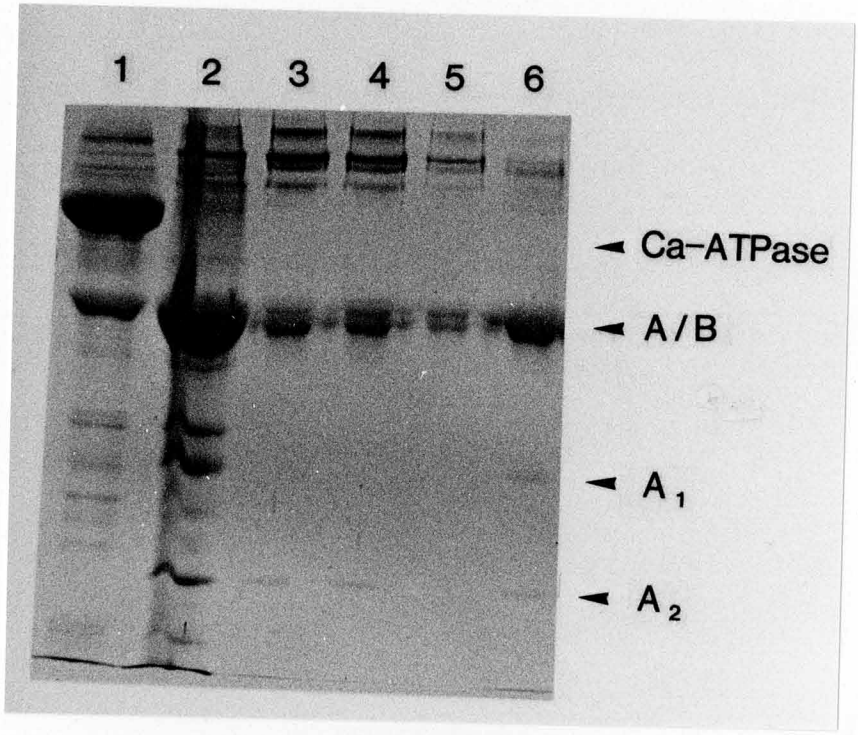

Fig. 9 Tryptic degradation of the Ca^{2+}-ATPase dimer into smaller fragments: SR vesicles were cross-linked in the presence of AMP-PNP for 60 min, followed by 1/200 trypsin digestion for 90 min as described in Fig. 7. The sample was solubilized in $C_{12}E_9$ and fractionated on a Sephacryl S-400 column which had been equilibrated with the elution buffer described for Fig. 2. Dimeric and monomeric ATPase fractions of 5 ml each were collected and condensed by TCA precipitation. SDS-PAGE of these samples was performed as given in Fig. 1. Lane 1, intact SR; lane 2, digested SR; lanes 3-5, dimeric ATPase fractions; lane 6, monomeric ATPase fraction.

molecule through PBM at the A_1 region of the ATPase.

To determine whether or not the tryptic fragment B is contained in either of the two 130 kDa bands, the following experiments were performed. SR was labeled with IAEDANS under the conditions described by Suzuki et al. (20) to modify Cys-642 of the Ca^{2+}-ATPase. This modification did not affect the subsequent treatment with PBM and the ATPase protein was oligomerized by PBM in essentially the same pattern as the IAEDANS-modified and unmodified SR vesicles. After the treatment with PBM, IAEDANS-modified SR was allowed to react with trypsin for 2 min at 20° C, and the tryptic digests were separated on electrophoresis in 5% gel. As a result, the fluorescence of IAEDANS was associated with the tryptic fragments of 170 kDa and the minor band of 130 kDa protein, but not with the major band of 130 kDa protein (data not shown). These results indicate that the major band of 130 kDa may be a complex of A-A fragments, while that the minor band of 130 kDa protein may be a complex of either A-B or B-B, or a mixture of them.

DISCUSSION

Many kinds of cross-linking reagents have been used to study the geometric arrangement of the Ca^{2+}-ATPase in the intact SR membrane (21-23), but there have been few reports on cross-linking experiments to investigate alterations of the molecular interaction during the catalytic cycle. In this study, we used a bifunctional reagent, PBM, to study the protein-protein interaction and identify the particular SH groups involved in the cross-linking between the Ca^{2+}-ATPase molecules.

As shown in Figs. 1A and 2A, under ligand-free conditions the amount of monomeric ATPase decreased due to the intermolecular cross-linking by PBM with a half-life time of about 20 min. SDS-PAGE revealed that various species of the oligomeric ATPase could be successively formed with incubation, but no particular form of the oligomer accumulated under these conditions. These observations suggest that Ca^{2+}-ATPase exists in the SR membrane in a very closely packed arrangement, as has also been indicated by many other observations (24,25).

The SDS-PAGE pattern of the Ca^{2+}-ATPase after modification of the SR vesicles with PBM in the presence of AMP-PNP was quite different from that obtained without addition of the nucleotide (Figs. 1B, 2B). In the presence of nucleotide, monomeric Ca^{2+}-ATPase was slowly oligomerized by PBM with a half life of about 1 h. Furthermore, dimeric ATPase accumulated predominantly on incubation with PBM. These results indicate that the nucleotide preferentially prevented the PBM reaction in the step between the ATPase dimer and the higher order of oligomer over that in the step

of dimer formation. Since the effect of AMP-PNP on the cross-linking reaction was observed at relatively low concentrations, and since this nucleotide effect was not observed when about one mol of FITC was attached per mol of ATPase, the binding of substrate to the catalytic site of the Ca^{2+}-ATPase may have altered the cross-linking pattern of the Ca^{2+}-ATPase by PBM.

Two possible mechanisms can be considered to explain the nucleotide effect upon PBM modification: 1) the binding of AMP-PNP to the Ca^{2+}-ATPase may stimulate the dimer association between the ATPase molecules through a conformation change of the enzyme, and/or 2) the binding of AMP-PNP to the Ca^{2+}-ATPase may lead to blockage of the SH group which is presumed to be involved in further cross-linking of dimeric ATPase to form a higher order oligomer. The FITC titration curve of Fig. 4 shows some divergence from a linear relationship between bound FITC and inhibition of the nucleotide effect upon cross-linking. The effect of the nucleotide on the cross-linking reaction was reduced to about 30% when half of the nucleotide binding sites were occupied by FITC. One of the possible explanations for the non-linear relationship between FITC binding and the nucleotide effect is that, in the cross-linking with PBM, both of the enzyme molecules must be saturated with nucleotide at the catalytic site to exert their effect on the PBM modification. These considerations lead us to conclude that the nucleotide induces a conformational change of the ATPase which form a stable dimer and prevents further oligomerization.

As shown in Fig. 5, cross-linking between the Ca^{2+}-ATPase molecules with PBM was specifically inhibited by vanadate.

Titration of SH groups of the ATPase with DTNB suggested that vanadate ion did not inhibit the PBM modification of SH groups other than that involved in the intermolecular cross-linking (data not shown). This finding agrees well with those showing that intermolecular cross-linking of the ATPase by PBM was completely inhibited when about one mol of vanadate became bound per mol of ATPase, and that the cross-linking reaction was fully restored in parallel with liberation of the ion from the ATPase upon the simultaneous addition of Ca^{2+} and AMP-PNP to the reaction medium (Fig. 6). Vanadate ion has been thought to inhibit the P-type ion motive ATPase by forming a stable complex of E_2V as an analogue of E_2P. Therefore, it seems likely that vanadate ion may have prevented the PBM-induced cross-linkage of the ATPase by changing the enzyme state from E_1 to E_2.

Based on electron microscopy, Dux et al. (4) suggested that vanadate induced the formation of two-dimensional crystals, which consist of dimer chains as structural units, of the Ca^{2+}-ATPase in the SR membrane. Under such a condition, the rate of cross-linking between the dimeric ATPase should be much lower than that between the monomeric ATPase. We found that vanadate greatly lowered the rate of PBM-induced cross-linking of the ATPase (Fig. 6).

Comparison of our observation with that of Dux et al. led us to conclude that the vanadate ion changes the arrangement of the ATPase molecules in the SR membrane which might inhibit the PBM-induced intermolecular cross-linkage by distancing the SH groups involved in the cross-link formation with PBM. Another explanation for the vanadate inhibition of the cross-linking of

the ATPase is that vanadate ion blocks the SH group which is involved in the cross-linkage with PBM, because vanadate ion is assumed to bind as an analogue of phosphate to the phosphorylation site on the A_1 region of the ATPase peptide chain (24). Furthermore, the A_1 region is presumed to be exposed to the cytoplasmic surface of the SR membrane; eight or more SH groups are located on this region. Therefore, PBM may easily became attached to one of them,thus forming the cross-link between the ATPase molecules. This interpretation agrees well with the results from our analysis of tryptic digests of the dimeric ATPase, which suggest a majority of the enzyme molecules were cross-linked with PBM at the A_1 fragment. Thus, the vanadate ion seems to block the SH group in the A_1 region which is involved in the cross-linkage of the ATPase.

Further investigation is required to elucidate the mechanism by which the nucleotide and vanadate ion affect the cross-linking between the ATPase molecules by PBM. Identification of the cross-linking site on the ATPase is now being attempted using ^{14}C-labeled PBM.

REFERENCES

1. Wang,C.T.,Saito,A. & Fleischer,S. (1979) J.Biol. Chem. 254, 9209-9219
2. Andersen,J.P.,Fellman,P.,Møller,J.V. & Devaux,P.F. (1981) Biochemistry 20, 4928-4936
3. Scales,D. & Inesi,G. (1976) Biophys.J. 16, 735-751
4. Dux,L.,K.A.Taylor,H.P.Ting-Beall, & A.Martonosi (1985) J.Biol.Chem. 260, 11730-11743
5. Andersen,J.P. & Vilsen,B, (1985) FEBS letter. 189, 13-17
6. Yamada,S.,Yamamoto,T. & Tomomura,Y. (1970) J.Biochem. 61, 789-794
7. Johnson,R.A. & Walseth,T.F. (1979) Adv.Cyclic Nucleotide Res. 10, 137-167
8. Goodno,C.C. (1979) Proc.Natl.Acad.Sci.USA 76,2620-2624
9. Laemmli,U.K. (1970) Nature 227, 680-685
10. Weber,K. & Osborn,M. (1969) J.Biol.Chem. 244, 4406-4412
11. Martin,J.B & Doty,D.M (1949) Anal.Chem. 21,965-967
12. Takisawa,H. & Tonomura,Y. (1979) J.Biochem. 86,425-441
13. Ross,D,C, & McIntosh,D.B. (1987) J.Biol.Chem. 262, 2042-2049
14. Pick,U. (1982) J.Biol.Chem. 257, 6111-6119
15. Pick,U. & Karlish,S.J.D. (1982) J.Biol.Chem. 257, 6120-6126
16. Dux,L. & Martonosi,A. (1981) J.Biol.Chem. 258, 2599-2603
17. Dux,L. & Martonosi,A. (1981) J.Biol.Chem. 258,

10111-10115

18. Dux,L. & Martonosi,A. (1981) J.Biol.Chem. 258, 11896-11902

19. Dux,L. & Martonosi,A. (1981) J.Biol.Chem. 258, 11903-11907

20. Suzuki,H.,Obara,M.,Kuwayama,H. & Kanazawa,T. (1987) J.Biol.Chem. 262, 15448-15456

21. Kurobe,Y.,Nelson,R.W. & Ikemoto,N. (1983) J.Biol. Chem. 258, 4381-4389

22. Squier,T.C.,Hughes,S.E. & Thomas,D.D. (1988) J.Biol.Chem. 263, 9162-9170

23. Baskin,R.J.,Hanna,S. (1979) Boichem.Biophys.Acta 576, 61-70

24. Scale,D & Inesi,G. (1976) Biophys.J. 16 735-751

25. Wang,C.T.,Saito,A., & Flischer,S. (1979) J.Biol.Chem. 254, 9209-9219

26. MacLennan,D.D.,Brandl,C.J.,Korczak,B., & Green,N.H. (1985) Nature 316, 696-670

Part IV

Determination of the Primary Structure of Intermolecular Cross-Linking Sites on the Ca^{2+}-ATPase of Sarcoplasmic Reticulum Using ^{14}C-Labeled N,N'-(1,4-Phenylene) Bismaleimide or N-Ethylmaleimide

SUMMARY

To determine the intermolecular cross-linking site on the primary structure of sarcoplasmic reticulum (SR) Ca-ATPase, the conditions for the specific binding of ^{14}C-labeled 1,4-phenylene bis maleimide (PBM) or ^{14}C-labeled N-ethylmaleimide (NEM) to the ATPase were explored. SR vesicles were preincubated with nonradioactive PBM in the presence of 1 mM vanadate for 1 h, then washed by centrifugation to remove free PBM and vanadate. When the pretreated SR vesicles were allowed to react with 1 mM ^{14}C-PBM in the presence of 1 mM AMPPNP, the amount of ^{14}C-PBM incorporated into the ATPase increased with time in parallel to the formation of dimeric ATPase and reached the maximum labeling density of 1 mol ^{14}C-PBM per mol of dimeric ATPase at 40 min after the start of the reaction. When the pretreated SR vesicles were allowed to react with 2 mM ^{14}C-NEM in the absence of AMPPNP, a maximum of about 2 mol of NEM was bound per mol of the ATPase monomer. The labeling density of ^{14}C-NEM decreased from 2 to 1 mol per mol of the ATPase when the SR vesicles were made to react with ^{14}C-NEM in the presence of AMPPNP. From the analysis of the amino acid composition of the two major ^{14}C-NEM labeled peptides isolated from thermolytic digest of the enzyme after the reaction of SR with ^{14}C-NEM in the absence of AMPPNP, we deduced that ^{14}C-NEM was incorporated into Cys_{377} and Cys_{614}. On the other hand, the labeling of SR in the presence of AMPPNP resulted in inhibition of the ^{14}C-NEM binding to Cys_{614} leaving Cys_{377} unaltered. Based on these findings, we propose that at least two distinct SH groups of Cys_{377} and Cys_{614} on the primary structure

of the ATPase are involved in the intermolecular cross-linking with PBM; that of Cys_{377} is involved in the formation of dimeric ATPase, while that of Cys_{614}, which is sensitive to AMPPNP, is involved in further oligomerization of the dimeric ATPase.

INTRODUCTION

Ca-ATPase of the sarcoplasmic reticulum (SR) is able to actively transport Ca^{2+} across the membrane at the expense of ATP hydrolysis (1). The molecular basis for the Ca-pump in SR has been extensively investigated since the primary structure of this enzyme was entirely determined by analyzing cDNA (2,3). Recently, some amino acid residues involved in the partial reaction of the pump cycle have been identified using site-directed mutagenesis (4-7). Although a number of the amino acid residues including cysteine and lysine have been characterized by means of chemical modification (8-14), there have been few reports concerning the amino acid residues involved in the cross-linking with a bifunctional reagent among the ATPase molecules in the SR membrane (15).

Our previous paper (16) reported that PBM cross-linked the Ca-ATPase molecules in the SR membrane to form a high molecular weight oligomer under the ligand-free condition, but preferentially formed a dimeric ATPase in the presence of an ATP analogue, AMPPNP. We also observed that the cross-linking between the ATPase molecules could be avoided by adding vanadate to the reaction medium under the Ca-free condition(16). These results raise the possibility that the interaction between the ATPase molecules might be regulated in the SR membrane during the course of the catalytic cycle. In the present study, we explored the conditions for selective binding of ^{14}C-labeled PBM or NEM to the cross-linking site(s) on the ATPase by pretreating the SR vesicles with nonradioactive PBM in the presence of vanadate.

Our results indicated that under the conditions of ligand-free, PBM may be incorporated into both Cys_{377} and Cys_{614} residues to form oligomers of higher orders, while that in the presence of the nucleotide analogue, PBM may be incorporated only into Cys_{377} to form the dimeric ATPase.

EXPERIMENTAL PROCEDURE

Materials--- Sarcoplasmic reticulum (SR) was isolated from rabbit dorsal and hind limb white muscles by a method described previously (17). SR vesicles suspended in 60 mM KCl, 20% glycerol, and 10 mM Tris-maleate (pH 6.5) were divided into small portions, rapidly frozen using liquid nitrogen and stored at -80° C. Monovanadate was prepared from V_2O_5 according to Goodno (18). ^{14}C-PBM was synthesized from 1,4-phenylenediamine and [2,3-^{14}C] maleic anhydride by the method described by Wells and Yount (19). The synthesized ^{14}C-PBM was thoroughly washed with water to remove unreacted ^{14}C-labeled compounds, phenylenemaleimide, or any other side reaction products according to Nishimura et al (20), then evaporated to dryness. Recovery of the ^{14}C-PBM was about 50%. The purity of the synthesized PBM was about 90% as determined by comparison of the cross-linking activity with the commercial reagent under the same conditions by using the same samples. [2,3-^{14}C]maleic anhydride and N-[ethyl-1-^{14}C]maleimide were purchased from Amersham, AMPPNP from Sigma, unlabeled PBM from Wako Pure Chemicals. Thermolysin was from Daiwa Kasei and ODS-120 T reversed phase column from Toyo Sohda.

Pretreatment of SR with PBM---The reaction was started by addition of a small portion of PBM dissolved in DMSO to the standard medium, which contained 2.5 mg/ml SR protein, 0.1 M KCl, 2-5 mM $MgCl_2$, 0.5-1.0 mM EGTA, and 10 mM Tris-maleate at pH 7 and 23° C. Unless otherwise specified, the final concentration of PBM and DMSO were 1 mM and 10% , respectively. The reaction was

terminated by the addition of 14 mM β-mercaptoethanol. As indicated in the figure legends, the reaction mixture had been centrifuged or passed through a short column of Sephadex G-50 to remove free PBM prior to labeling of the SH group with ^{14}C-PBM or NEM.

Gel electrophoresis--- SDS-PAGE was performed by the method of Laemmli (21). Samples were dissolved in a solution containing 1% SDS, 1% β-mercaptoethanol, 0.1% bromophenol blue, and 10 mM Tris-HCl at pH 8.8 and subjected to electrophoresis on 7.5% poly acrylamide gel. The gel was stained with Coomassie Brilliant Blue, and scanned for the absorbance.

Measurements of ^{14}C-PBM or -NEM binding to SR protein---SR vesicles (2.5 mg/ml protein) were allowed to react with 1 mM ^{14}C-PBM in 2 ml of the standard medium as described above at 23° C. At the indicated times, 0.4 ml aliquots of reaction mixture were taken into 1.8 ml of the quenching solution which contained 25 mM β-mercaptoethanol and 10 mM unlabeled PBM solubilized in acetone. SR was washed twice by centrifugation in the same solution. The washed SR was then solubilized with 2% Triton X-100, and the radioactivity was measured in 5 ml of scintillation mixture using liquid scintillation counter. ^{14}C-NEM binding was measured under conditions similar to those described above except that ^{14}C-NEM was used instead of ^{14}C-PBM. SR membrane was washed by 5% TCA. In some experiments, ^{14}C-PBM or -NEM labeled SR was washed twice by the centrifugation in the standard medium containing 14 mM mercaptoethanol, then radioactivity was measured as described above.

Thermolytic digestion of ^{14}C-NEM labeled SR---After labeling of

SR with ^{14}C-NEM or -PBM, SR vesicles were partially purified by DOC extraction to remove extrinsic proteins according to Meissner and Fleischer (22). The thermolysis of SR was carried out essentially according to Saito-Nakatsuka et al. (9). SR protein, 10 mg/ml, was allowed to react with 0.1 mg/ml thermolysin in the presence of 0.2 M NH_4HCO_3 and 1 mM $CaCl_2$ at 46° C for 1 h. The digestion was terminated by the addition of EDTA to give 10 mM. After addition of 2.7% formic acid, the mixture was centrifuged at 1000xg for 3 min and the supernatant was collected.

Purification of ^{14}C-NEM labeled peptides---The supernatant described above was evaporated to dryness and dissolved in 10% CH_3CN containing 0.1% TFA. Separation of ^{14}C-NEM labeled peptides was performed by using an HPLC system (Toyo Sohda 803D) with an ODS-120T reversed phase column. The mixture was applied to the column and eluted with a 10-50% gradient of CH_3CN in 0.1% TFA. The absorption of the eluted peptide was monitored at 215 nm. The radioactive fraction was collected, evaporated and redissolved in 10% CH_3CN containing 0.1% TFA. The sample was again applied and eluted by HPLC according to the same procedure as described above except that a 25 to 35% CH_3CN gradient was used.

Amino acid analysis of purified ^{14}C-NEM labeled peptides---The final purified peptides were hydrolyzed in 5.7 N HCl for 24 h at 105° C under high vacuum. Amino acid compositions of the samples were determined using a Hitachi amino acid analyzer (L-8500).

1. Effect of vanadate on cross-linking between Ca-ATPase molecules with PBM----In the preceding paper(16), we reported that incubation of SR vesicles with PBM under a ligand free condition resulted in the formation of high molecular weight oligomers of ATPase, while incubation in the presence of AMPPNP preferentially induced the formation of dimeric ATPase. Furthermore, the cross-linking reaction with PBM between the ATPase molecules was inhibited by the binding of vanadate to the ATPase. These results suggest that at least two distinct cross-linking sites may exist in the ATPase; one involves the formation of dimeric ATPase (tentatively referred to as SH_a), and the other site (SH_b) involves further oligomerization of the ATPase. Based on the SDS-PAGE analysis of the tryptic digest of the dimeric ATPase which was cross-linked by PBM in the presence of AMPPNP, we also suggested that SH_a is located in the region of "fragment A_1" in each of the neighboring ATPases (16). In the present study, we tried to determine the cross-linking sites, SH_a and SH_b, in the primary structure of the ATPase by using ^{14}C-labeled PBM or ^{14}C-labeled NEM. However, as previously suggested, PBM reacts with many SH groups of the ATPase other than that involved in the intermolecular cross-linking. Therefore, before labeling the ATPase with a ^{14}C-labeled reagent, the nonspecific SH groups had to be masked with cold PBM. In the experiments shown in Figs. 1 and 2, we examined in detail the effect of vanadate upon the time course of cross-linking of the ATPase after the addition of PBM to SR in the presence of 2-5 mM $MgCl_2$, 1 mM EGTA, 10%

DMSO, 0.1 M KCl, and 20 mM TES at pH 7.2 (Figs. 1,2). Analysis of SDS-PAGE of the SR proteins after the cross-linking reaction revealed that the major band of monomeric ATPase decreased on addition of PBM with a half life time of about 10 min. On the other hand, the rate of decrease in the monomeric ATPase was greatly reduced by the addition of 1 mM vanadate, and more than 70% of the monomeric ATPase remained after 80 min of incubation. As shown in Fig. 2, the initial rate of cross-linking of ATPase with PBM was decreased to 50% by the addition of 10 μM vanadate and was almost completely inhibited by 100 μM vanadate.

For the Fig. 3 data, we measured vanadate binding to SR under the same conditions as used for Fig. 2. The amount of vanadate bound to SR increased as the concentration increased and saturation reached at about 100 μM vanadate. The half saturation concentration of vanadate was about 10 μM. The dependence of vanadate binding on its concentration was very similar to that of the inhibition of the PBM-induced cross-linking of the ATPase (Fig. 2). When 1 mM $CaCl_2$ and 1 mM AMPPNP were simultaneously added to the reaction medium, vanadate binding to SR was no longer observed (16). These results support our previous suggestion that the intermolecular cross-linking of Ca-ATPase with PBM is almost completely inhibited by the binding of 1 mol vanadate per mol ATPase to form an E_2.vanadate complex. It appeared from the data of Fig. 3, that further increase in the vanadate concentration above 200 μM resulted in the binding of 1 mol vanadate to another site with an affinity of about 160 to 200 μM. These results fit well with the observations reported by Varga et al.(23) and Medda and Hasselbach (24). However, the

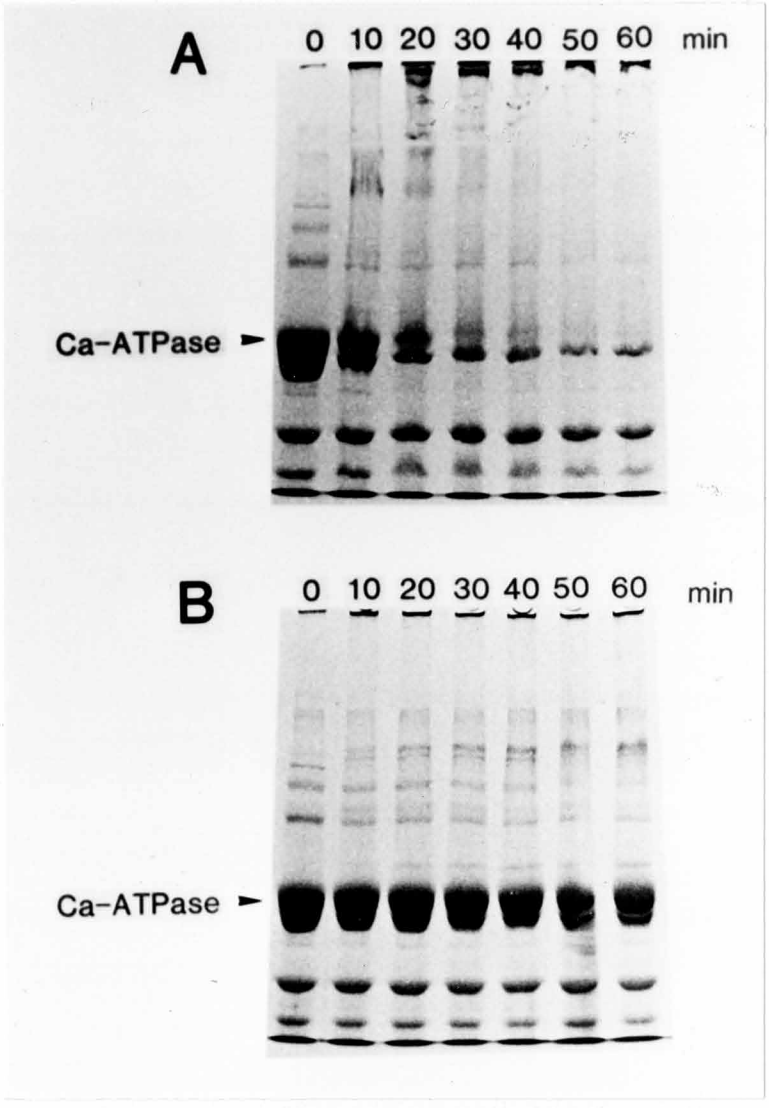

Fig. 1. SDS-gel electrophoresis of SR proteins cross-linked with PBM in the absence and presence of vanadate.

SR vesicles (2.5 mg/ml protein) were allowed to react at 23° C with 1 mM PBM in a solution of 0.5 mM EGTA, 0.1 M KCl, 10% DMSO, and 20 mM TES (pH 7.2) in the absence (A) and presence (B) of 1 mM vanadate. The reaction was quenched with 14 mM β-mercaptoethanol at the indicated times. SR vesicles were solubilized with 1% SDS and prepared for electrophoresis as described in "EXPERIMENTAL PROCEDURES".

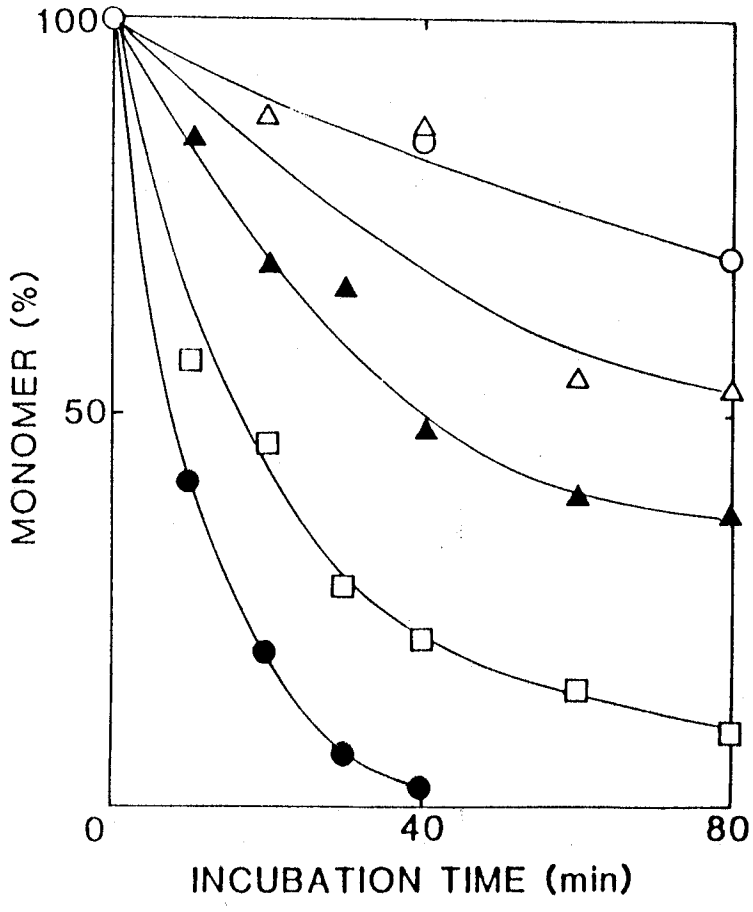

Fig. 2. Time courses of decrease in the amount of monomeric ATPase in the reaction of SR with PBM at various concentrations of vanadate.

SR vesicles were allowed to react with 1 mM PBM in the presence of 0 (●), 10 (□), 20 (▲), 100 μM (△) and 1mM (○) vanadate under the conditions described in Fig. 1. After quenching the reaction at the indicated times with β-mercaptoethanol, small aliquots were taken for SDS-PAGE as given in Fig. 1. After staining the gel with Coomassie Blue, the amount of ATPase monomer was determined by measuring the density of the protein band with a densitometer and expressed as the percent of the initial amount of ATPase.

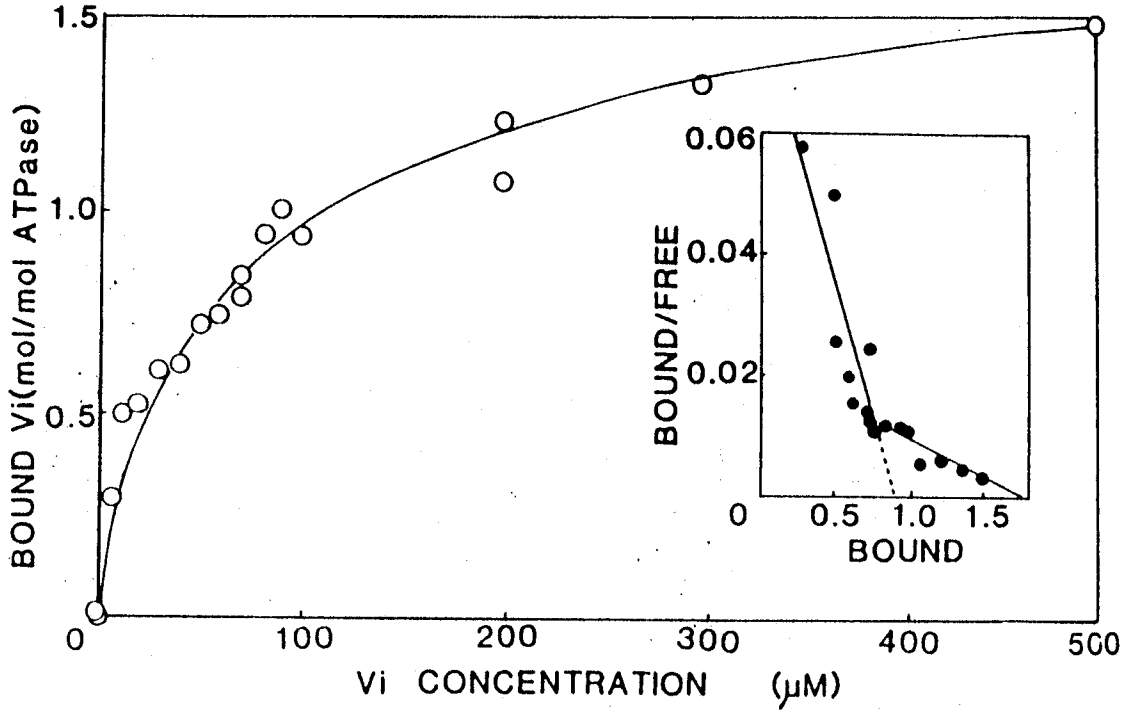

Fig. 3. Dependence of vanadate binding to SR vesicles on the concentration of vanadate.

SR vesicles (2.5 mg/ml protein) were incubated with 0-0.5 mM vanadate in a solution consisting of 0.45 mM EGTA, 4.5 mM $MgCl_2$, 90 mM KCl, 10% DMSO, and 18 mM TES (pH 7.2) at 23° C for 30 min, followed by centrifugation at 520 k x g for 10 min. The free concentration of vanadate was determined according to Goodno (18). The amount of vanadate bound to SR was determined from the decrease in the free vanadate concentration in the supernatant, and the values were represented as mol/mol ATPase by assuming that the ATPase accounts for 70% of the total SR protein and that its molecular weight is 115k. The inset is a Scatchard plot of the data in this figure.

position and functional role of the low affinity vanadate binding site remained to be established.

As shown in Fig.4, 10 to 15 mol SH groups per mol ATPase were titrated with DTNB under the condition used. The amount of SH groups decreased with an increase in the incubation time of SR vesicles with PBM, and almost all the SH groups of the SR protein seemed to be modified with PBM in 1 h irrespective of the presence or absence of vanadate. However, in the early phase of SR incubation with PBM in the absence of vanadate, the amount of SH group titrated with DTNB was 1-2 mol greater than that obtained after the incubation in the presence of vanadate.

2. Binding of ^{14}C-PBM and ^{14}C-NEM to Ca-ATPase after treatment of SR with PBM in the presence of vanadate------ As expected from the data shown in Figs. 3 and 4, PBM reacted with all the SH groups of the ATPase except for that involved in the intermolecular cross-linking when SR vesicles were allowed to react with PBM in the presence of vanadate. For close examinations, we tried to label the specific SH groups of the ATPase with ^{14}C-PBM or ^{14}C-NEM after incubation of the SR vesicles with PBM in the presence of vanadate.

As shown in Fig. 5, when SR vesicles were preincubated without PBM, a large amount of ^{14}C-PBM was rapidly incorporated into SR protein in 20 min of the reaction. The extent of ^{14}C-PBM binding to SR protein decreased sharply from 15 to 5 mol per mol ATPase during the first 20 min of the preincubation, and 40 min later, it decreased to 1-2 mol/mol ATPase. This result supports the possibility that ^{14}C-PBM might be selectively incorporated into the SH groups which participate in the cross-linkage between

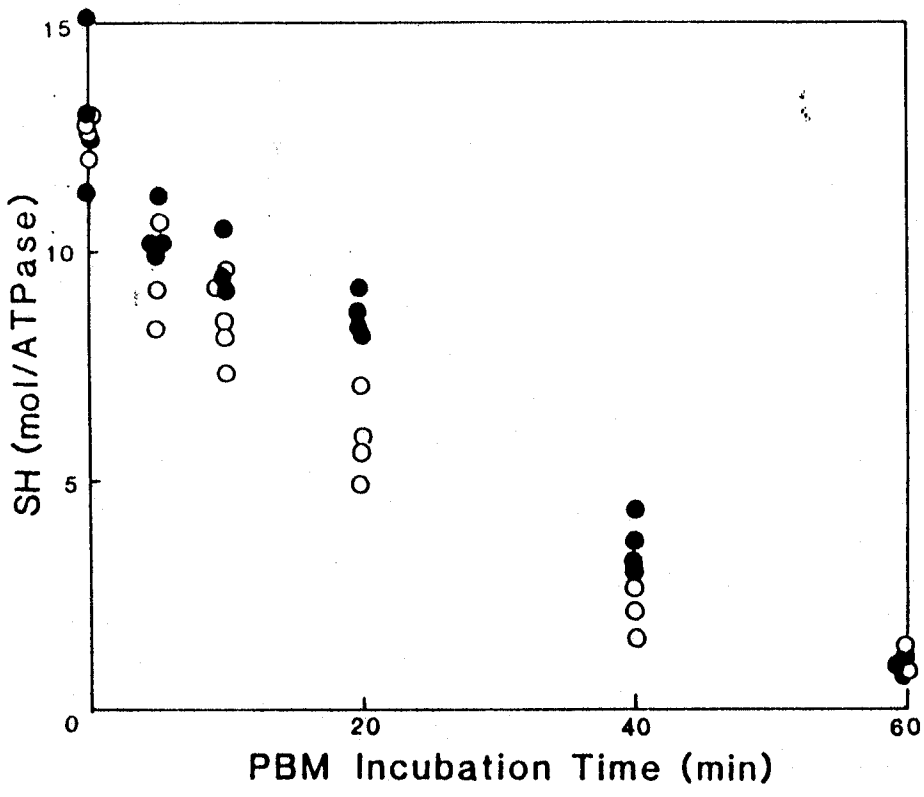

Fig. 4. SH titration of SR-ATPase by DTNB after incubation of SR vesicles with PBM in the absence and presence of vanadate.

SR vesicles (2.5 mg/ml protein) were allowed to react with 1 mM PBM in the absence (○) and presence (●) of 1 mM vanadate in 1 mM EGTA, 5 mM $MgCl_2$, 60 mM KCl, 10% DMSO, and 10 mM Tris-maleate (pH 7.0). The reaction was quenched with 14 mM β-mercaptoethanol at the indicated times, followed by three times centrifugations in 5% TCA. The SR membranes were solubilized in the solution containing 2% SDS, 10 mM Tris-HCl (pH 8.0), and 2 mM DTNB. The amount of SH group titrated was determined by measuring absorbance at 412 nm using an extinction coefficient of $1.36 \times 10^4 M^{-1}.cm^{-1}$, and the value was represented as mol/mol ATPase as in Fig. 3.

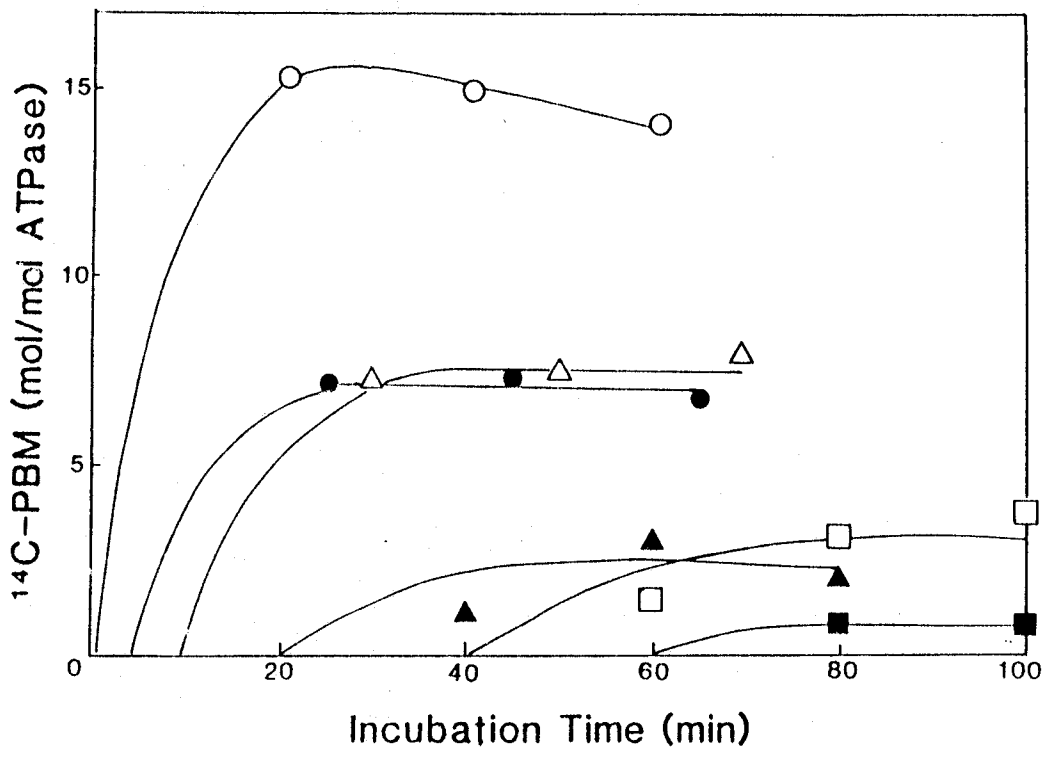

Fig. 5. Time courses of ^{14}C-PBM incorporation to SR protein after the incubation of SR vesicles with PBM in the presence of vanadate.

SR vesicles (2.5 mg/ml protein) were incubated under the conditions described in Fig. 4 with 1 mM PBM in the presence of 1 mM vanadate for 2 (○), 5 (○), 10 (△), 20 (△), 40 (□), and 60 (■) min at 23° C. The reaction was quenched by 14 mM β-mercaptoethanol, followed by centrifugation twice with washing solution of 60 mM KCl, 20% glycerol, and 10 mM Tris-maleate (pH 7.0). The washed SR vesicles were resuspended in the same solution and allowed to react with 1 mM ^{14}C-PBM in the presence of 1 mM AMPPNP. At the indicated times, the reaction was quenched with β-mercaptoethanol. The amount of ^{14}C-PBM incorporated by the ATPase was measured as described in "EXPERIMENTAL PROCEDURES", and expressed as mol/mol ATPase.

the ATPase molecules.

In the experiments shown in Fig. 6, SR vesicles were preincubated for 1 h with 1 mM of cold PBM in the presence of vanadate. The reaction was stopped by the addition of β-mercaptoethanol, then the SR vesicles were centrifuged to remove free PBM as well as vanadate. The washed SR vesicles were made to react with 1 mM ^{14}C-PBM in the presence of 1 mM AMPPNP for various lengths of time. After terminating the reaction by adding β-mercaptoethanol, the vesicles were washed again by centrifugation. The labeled SR was solubilized with 50 mg/ml $C_{12}E_9$, and the Ca-ATPase was separated on HPLC in the presence of detergent at 10 mg/ml. From the absorbance at 280 nm, the ATPase protein emerged at three distinct elution volumes, representing the higher orders of oligomers, dimers and monomers of ATPase. This elution pattern of the SR proteins was essentially the same as that obtained in the previous study (16), where molecular sizes of the lager oligomer, dimer, and monomer of the ATPase were estimated on the basis of SDS-PAGE. The amount of dimeric ATPase increased as a function of the incubation time after the addition of ^{14}C-PBM to SR, and reached the maximal level at 40 min. The amount of ^{14}C-PBM incorporated into the dimeric ATPase also increased with time in parallel with the formation of this fraction. These results suggest that ^{14}C-PBM can be selectively incorporated into the SH groups which participate in the intermolecular cross-linking. Figure 6 also indicated that ^{14}C-PBM can react to some extent with SH groups of the monomeric ATPase without the accompanying oligomerization even after prolonged incubation of SR vesicles with PBM in the presence of

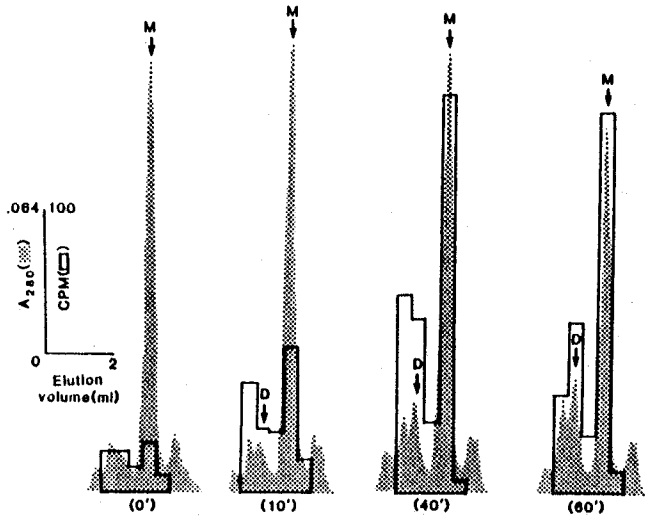

Fig. 6. Correlation between the formation of oligomeric ATPase and the incorporation of ^{14}C-PBM into the enzyme after the pretreatment of SR with PBM in the presence of vanadate.

SR vesicles were pretreated with PBM for 1 h in the presence of vanadate as in Fig. 5. After washing the SR membranes by centrifugation at 520 k xg for 10 min, they were made to react with 1 mM ^{14}C-PBM in the presence of 1 mM AMPPNP. The reaction was terminated with 14 mM β-mercaptoethanol at the indicated times, followed by centrifugation to remove free ^{14}C-PBM. The washed SR membranes were solubilized with 50 mg/ml $C_{12}E_9$ in a solution containing 5 mM $CaCl_2$, 20% glycerol, 0.1 M KCl, and 10 mM TES (pH 7.2). Monomeric and oligomeric ATPases were separated by HPLC using a TSK-G3000 sw column which as equilibrated with the solution described above with the exception that 10 mg/ml $C_{12}E_9$ was used instead of 50 mg/ml. The elution was monitored for protein concentration at 280 nm (shaded area). The dimeric (D) and monomeric (M) ATPase peaks are indicated by arrows. The radioactivity of ^{14}C-PBM associated with these fractions was measured as described in "EXPERIMENTAL PROCEDURES"(□).

vanadate. The amounts of ^{14}C-PBM incorporated into fractions of the monomeric and dimeric ATPases were estimated from the data of Fig. 6 and are summarized in Table I as the molar ratio of PBM to the Ca-ATPase assuming that the ATPase accounts for 75% of the total SR protein and that the molecular weight of the monomeric ATPase is 115,000. The number of PBM covalently attached to the ATPase increased as a function of incubation time and reached the maximum value of 3 mol per mol of the dimeric ATPase. On the other hand, PBM was maximally incorporated as a univalent reagent into the monomeric ATPase fraction with a molar ratio of 1:1. These observations are interpreted as evidence for the involvement of 1 mol PBM in the formation of the dimeric ATPase by the cross-linking between the ATPase monomers.

In the preceding section, we presumed that Ca-ATPase may contain at least two different kinds of SH groups which are involved in the intermolecular cross-linking; they were tentatively referred as SH_a and SH_b. SH_a is assumed to participate in the formation of dimeric ATPase with PBM in the presence of AMPPNP, and SH_b in the formation of oligomers larger than a dimer with PBM under a ligand-free condition. We demonstrated that almost all the SH groups on the ATPase except for SH_a and SH_b reacted readily to PBM when vanadate was added to the reaction medium to a final concentration of as much as 100 μM (16). This enabled us to label only SH_a and SH_b with the radioactive SH reagents after adequate preincubation of SR with PBM in the presence of vanadate. To test this possibility, we examined whether or not ^{14}C-labeled NEM, similarly to ^{14}C-PBM can react with the SH-groups that remained after the preincubation of

Table I. Incorporation of ^{14}C-PBM into the monomeric and dimeric ATPase

	Incubation Time (min)			
Bound PBM (mol/mol)	0	10	40	60
Monomeric ATPase	0.06	0.45	0.88	1.05
Dimeric ATPase		1.90	3.30	2.61

Data was obtained from the experiment shown in Fig. 6, and presented as mol PBM per mol of monomeric or dimeric ATPase, by assuming that Ca-ATPase accounts for 70% of the total SR protein and that its molecular weight is 115,000.

SR with PBM in the presence of vanadate. For the Fig.7 data, SR vesicles were incubated for 1 h with 1 mM PBM in the absence or presence of 1 mM vanadate, then washed by centrifugation to remove free PBM and vanadate. The washed SR vesicles were allowed to react with various concentrations of ^{14}C-NEM for 2 h in the presence or absence of 1 mM AMPPNP. Under the conditions tested, a significant amount of NEM was incorporated into SR protein even after prolonged incubation with PBM in the absence of vanadate. On the other hand, further increase in the amount of ^{14}C-NEM bound to SR protein was observed when SR was treated by PBM in the presence of vanadate prior to the NEM modification. Thus the amount of NEM incorporated into SR protein increased with the NEM-concentration with an apparent Kd of 0.1 to 0.2 mM and reached a maximum amount of 3 mol NEM per mol of the ATPase above 2 mM NEM (closed circle), while 1 mol NEM was bound to the ATPase in the control SR which was preincubated with PBM in the absence of vanadate (closed triangle). These results suggest that maximally 2 mol of SH groups in the ATPase protein was protected by vanadate against the PBM modification. It was also observed in this figure that the amount of NEM incorporation into the SR which had been treated by PBM with vanadate was decreased by the addition of 1 mM AMPPNP from 2 to 1 mol per mol of the ATPase (open circle), while that the incorporation of NEM into the SR treated by PBM without vanadate was unaffected by the nucleotide(open triangle). These observations may be taken as support for our previous suggestion that the intermolecular cross-bridges are formed with PBM through the nucleotide sensitive and insensitive SH-groups in adjacent molecules of the ATPase, and that vanadate

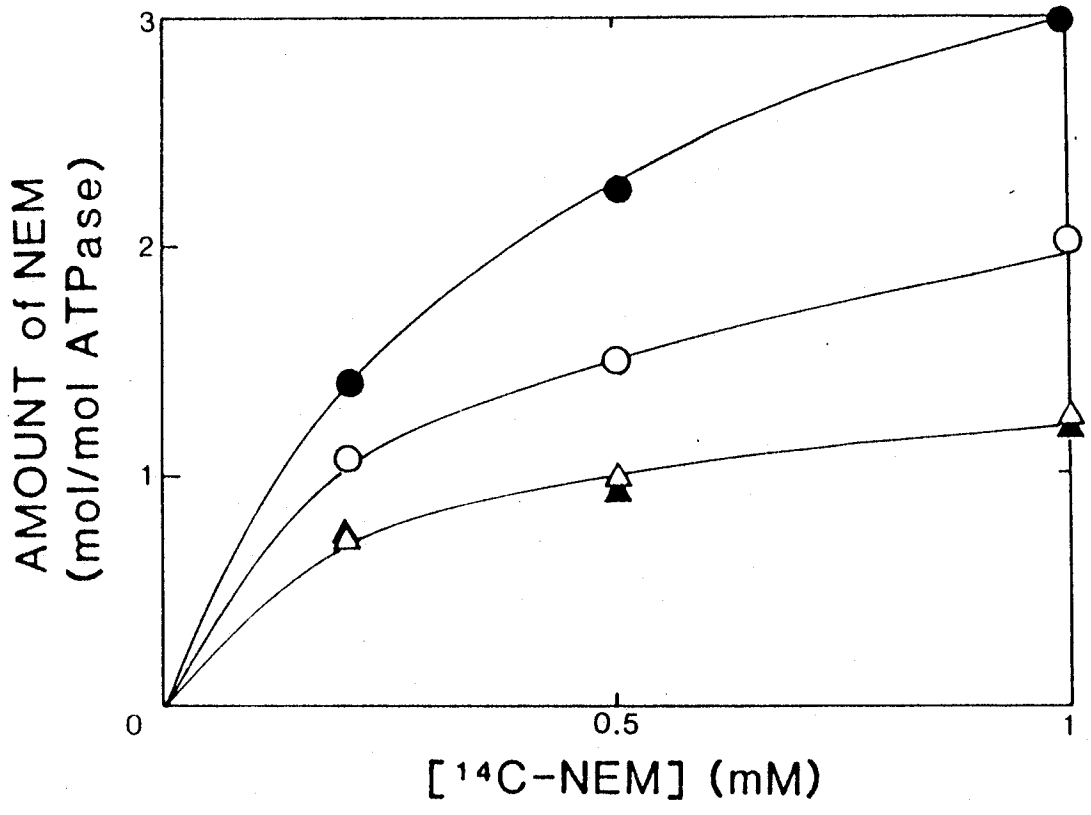

Fig. 7. Effect of AMPPNP upon the ^{14}C-NEM binding to the ATPase after the preincubation of SR with PBM in the absence and presence of vanadate.

SR vesicles were incubated with PBM in the absence (△, ▲) and presence (○, ●) of 1 mM vanadate and allowed to react with various concentrations of ^{14}C-NEM in the absence (▲, ●) and presence (△, ○) of 1 mM AMPPNP. The amount of ^{14}C-NEM bound to SR was measured as in "EXPERIMENTAL PROCEDURES" and expressed as mol/mol ATPase.

specifically inhibits the reaction of these SH-groups with PBM.

3. Identification of the intermolecular cross-linking site on the single polypeptide of the Ca-ATPase------ Ca-ATPase was labeled by having SR vesicles react with ^{14}C-NEM for 1 h in the absence or presence of AMPPNP after pretreatment with cold PBM in the presence of vanadate. The ^{14}C-NEM incorporation into the control SR treated by PBM without vanadate was very slow at a rate compared with that into the SR treated by PBM with vanadate (data not shown). In the following experiments, the incubation of SR vesicles with ^{14}C-NEM was carried out for 1 h instead of 2 h to reduce the amount of NEM bound to the control SR. Under these conditions, about 1.4 and 0.6 mol ^{14}C-NEM were incorporated into 1 mol ATPase in the absence and presence of AMPPNP, respectively. When SR vesicles were pretreated with PBM in the absence of vanadate, the amount of ^{14}C-NEM incorporated into the ATPase was negligible. Each of the labeled SR membranes was solubilized in DOC by the method of Meissner and Fleischer (22) to remove extrinsic SR proteins. The partially purified Ca-ATPase was then digested with 0.1 mg/ml thermolysin for 1 h at 46° C as described by Saito-Nakatsukasa et al. (19), and the thermolytic digest was obtained in the supernatant by centrifugation of the SR suspension after addition of formic acid up to 2.7%. As estimated from the radioactivity, about 50% of the original amount of ^{14}C-NEM-labeled ATPase was recovered in the supernatant after precipitation of SR membrane by formic acid. This relatively low recovery of the ^{14}C-NEM labeled peptides may have been caused by incomplete digestion of the SR membrane with thermolysin under

thermolysin under our conditions.

In Fig. 8A, the thermolytic digest of the Ca-ATPase, which was labeled by allowing SR vesicles to react with ^{14}C-NEM in the absence of AMPPNP, was applied to an ODS-120T column and eluted with 10-50% CH_3CN gradient. Three major radioactive peaks, which are tentatively denoted as Peak 13, Peak 17, and Peak 19, emerged at CH_3CN concentrations of about 37, 44, and 48%, respectively. Essentially the same elution profile of radioactivity was observed for the thermolytic digest of Ca-ATPase which was labeled by allowing SR vesicles to react with ^{14}C-NEM in the presence of AMPPNP, except that Peak 13 had almost completely disappeared (Fig. 8B). This indicates that Peak 13 contains a peptide of the Ca-ATPase on which a nucleotide sensitive SH group (SH_b) is located. The peptides from Peaks 13, 17, and 19 were collected separately and they were further purified by the reversed phase HPLC with 25-35% CH_3CN gradient. This step was repeatedly performed for the samples obtained from each peak fraction until the single peptide associated with ^{14}C-NEM was obtained (Data not shown). The final purified peptides were then subjected to amino acid analysis and the results were summarized in Table II. The molar ratio of amino acids were obtained from the average of three to five measurements for each purified peptide. The amino acid compositions of the purified peptide which were obtained from peak 17 and peak 19 in Fig. 8 were very close except for the Asp residue. This indicates that the thermolytic digestion of Ca-ATPase was incomplete under the conditions used, and various lengths of peptides which carried the same SH group (SH_a) might be equally produced by the

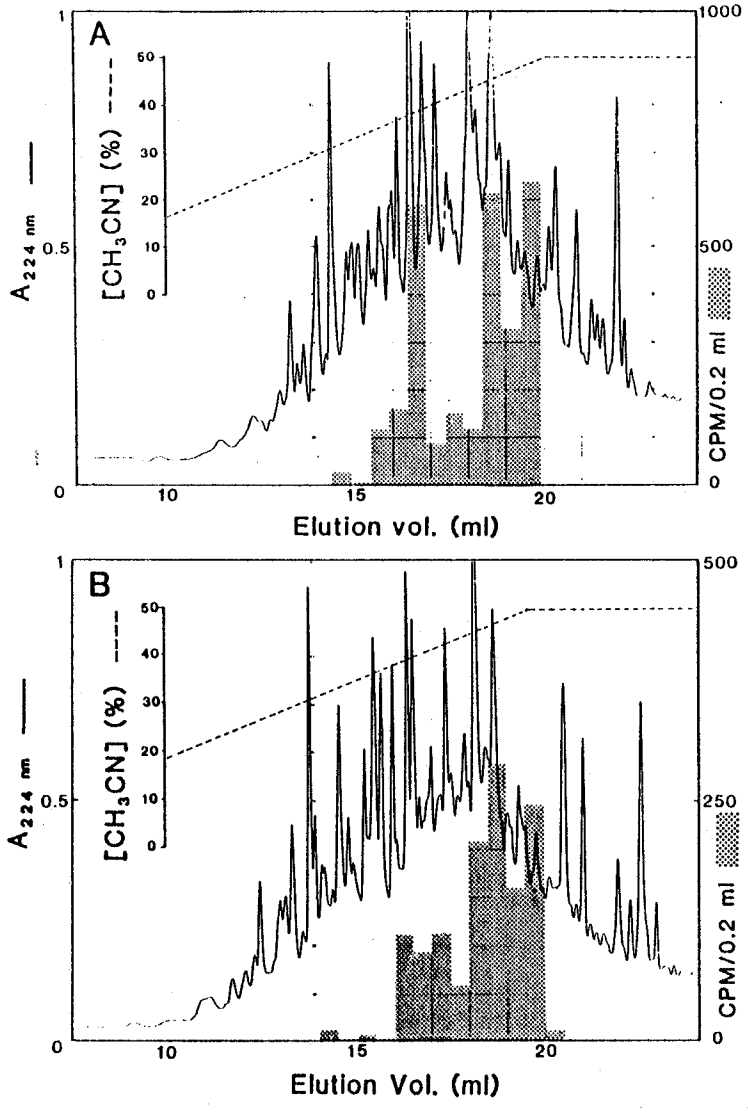

Fig. 8. Elution profiles of thermolytic digests of the ^{14}C-NEM labeled ATPase on reversed phase HPLC.

SR vesicles were incubated with PBM for 1 h in the presence of vanadate as in FIg. 4, followed by labeling with ^{14}C-NEM as given in the absence (A) or presence (B) of 1 mM AMPPNP. The SR membranes were extracted by DOC and digested with thermolysine as in "EXPERIMENTAL PROCEDURES" . The digests were applied to a ODS-120 T column and eluted with a CH_3CN gradient in 0.1% TFH. The absorption of the eluted peptides was monitored at 214 nm and the radioactivity of ^{14}C-NEM in the fraction is represented by the shaded area.

Table II. Amino acid composition of ^{14}C-NEM-labeled peptides purified from the thermolytic digest of Ca-ATPase

Amino acids	^{14}C-NEM-Peptides Peak 13	Peak 17	Peak 19
D/N	0.99 + 0.097 (1)	1.47 + 0.076 (2or1)	0.81 + 0.006 (1)
T	0.48 + 0.012 (0)	0.48 + 0.047 (0)	0.26 + 0.001 (0)
S	1.10 + 0.104 (1)	0.79 + 0.096 (1)	0.87 + 0.035 (1)
E/Q	1.22 + 0.180 (1)	0.90 + 0.034 (1)	1.14 + 0.020 (1)
G	1.74 + 0.153 (2)	0.88 + 0.086 (1)	1.51 + 0.028 (1)
A	1.12 + 0.113 (1)	0.49 + 0.072 (0)	0.49 + 0.024 (0)
V	0.83 + 0.146 (1)	0.31 + 0.080 (0)	0.33 + 0.053 (0)
C	0.17 + 0.140 (0)	0.06 + 0.064 (0)	0.01 + 0.013 (0)
M	0.03 + 0.136 (0)	0.01 + 0.015 (0)	0.01 + 0.008 (0)
I	0.52 + 0.081 (1)	0.19 + 0.042 (0)	0.28 + 0.034 (0)
L	1.17 + 0.083 (1)	0.75 + 0.064 (1)	0.50 + 0.028 (1)
Y	0.03 + 0.016 (0)	0.11 + 0.061 (0)	0.10 + 0.015 (0)
F	0.80 + 0.073 (1)	0.52 + 0.045 (1)	0.41 + 0.034 (1)*
K	0.55 + 0.027 (1)	0.47 + 0.018 (0)	0.36 + 0.011 (0)
H	0.30 + 0.051 (0)	0.28 + 0.053 (0)	0.13 + 0.015 (0)
R	0.65 + 0.090 (1)	0.35 + 0.073 (0)	0.37 + 0.052 (0)

^{14}C-NEM-labeled peptides were purified by repeated chromatography of the thermolytic digest of the ATPase as described in "EXPERIMENTAL PROCEDURES" and hydrolyzed in 5.7 N HCl at 105° C for 24 h. Values are averages of three to five measurements with s.m.e. and expressed as molar ratios. Values in parenthesis indicate integral numbers which were obtained by counting fraction .5 and over as a unit and cutting away the rest (see text).

* Value was corrected by assuming that phenylalanine was degraded during the acid hydrolysis.

thermolytic digestion. On the other hand, the amino acid composition of the purified peptide from peak 13 was clearly different from the peptides purified from peaks 17 or 19. Based on the amino acid analysis of these purified peptides and the primary structure of the Ca-ATPase established from cDNA analysis by MacLennan et al.(2,3), following conclusion was obtained. The peptide purified from Peak 13 contains relatively large amount of D/N, S, E/Q, G, A, L, and R with a roughly estimated molar ratio of 1:1:1:2:1:1:1, respectively. This amino acid composition is in fair agreement with the sequence of ---^{609}GSIQLCRDAG^{618} --- in the peptide chain of the Ca-ATPase, while all the other Cys-containing sequences widely differ from it in the amino acid compositions. On the other hand, both the peptides from Peaks 17 and 19 contain relatively large amount of D/N, S, E/Q, G, L, but low amount of A and R with a molar ratio of about 1 or 2:1:1:1:0:0, respectively. In addition, it is assumed that the low recovery of Phe residue in these peptides might be caused by its degradation during their acid hydration. On these assumptions, among the 24 Cys-containing peptide regions in the ATPase protein, the sequence of ---- ^{374}GDFCSLNE^{381} --- can be considered to be one of the most probable candidates for the peptides from Peaks 17 and 19. However, another possibilities can not be excluded because the impurity of the tested samples significantly lowered the accuracy of the data in Table II.

DISCUSSION

The Ca-ATPase of skeletal SR contains several reactive SH groups which are readily modified by a variety of SH reagents under mild conditions (10,25-28). Some of these SH groups play important roles in the Ca-transport across the membrane or the coupled ATPase reaction (29-32). There have been few reports concerning modification of the SH groups by a bifunctional reagent in order to demonstrate interaction between the ATPase molecules on the SR membrane. Recently, we observed that 1,4-phenylene bis maleimide (PBM) cross-linked the ATPase molecules in the SR membrane to form higher order oligomers under the ligand free condition. On the other hand, the binding of AMPPNP to the high affinity nucleotide binding site of the ATPase resulted in preferential accumulation of dimeric ATPase. In addition, we found that vanadate ions completely inhibited the cross-linking of the ATPase with PBM in the absence or presence of AMPPNP (16). It was assumed from these findings that there exist at least two distinct SH groups on the ATPase, both of which are involved in the intermolecular cross-linking with PBM. One SH group involved in the formation of dimeric ATPase is tentatively designated as SH_a and the other SH group involved in the further oligomerization of the ATPase is designated as SH_b. Based on the above assumptions, the experimental results of Figs. 4 and 5 can be interpreted as follows; binding of AMPPNP to the high affinity nucleotide binding site on the ATPase altered the conformation of the enzyme protein to make SH_b inaccessible without affecting the reactivity of SH_a. As a result, 1 mol ^{14}C-PBM was incorporated

into 1 mol of dimeric ATPase (Fig. 4), while 1 mol ^{14}C-NEM was incorporated into 1 mol of monomeric ATPase (Fig. 5). On the other hand, since both the SH_a and SH_b were accessible to the reagents when the enzyme was presented in the ligand-free condition, 2 mol ^{14}C-NEM was incorporated per mol of the ATPase (Fig. 5). The binding of 1 mol vanadate per mol of the enzyme also induced a conformational change such that SH_a and SH_b simultaneously became inaccessible to these reagents.

The reversible effect of vanadate on the PBM binding to SH_a and SH_b (see Figs. 1-3) enabled us to selectively label these SH groups with ^{14}C-PBM or ^{14}C-NEM as shown in Figs. 3 and 4. From the analysis of amino acid compositions of the ^{14}C-NEM labeled peptides which was purified from the thermolytic digest of the ATPase (Table II), we deduced that SH_a and SH_b are located in the primary structure of ATPase at the positions of Cys_{377} and Cys_{614}, respectively. The evidence for the involvement of Cys_{377} in the cross-linking of the ATPase agrees well with the previous conclusion that dimeric ATPase was formed by PBM via an SH group in the presence of AMPPNP (16). Under these conditions, it is easily assumed that Ca-ATPase molecules in the intact SR membrane are neighbors at a site near Cys_{377}, while under the ligand-free condition, the enzyme molecules are neighbors at two distinct sites near Cys_{377} and Cys_{614} as schematically shown in Fig. 9. The Asp_{351} residue, which is located very close to Cys_{377} on the linear map of the ATPase, can be phosphorylated by ATP as well as Pi to form a key intermediate of the ATPase reaction (13). Vanadate ion is suggested to bind near the phosphorylation site as an analogue of Pi under Ca-free condition to form the

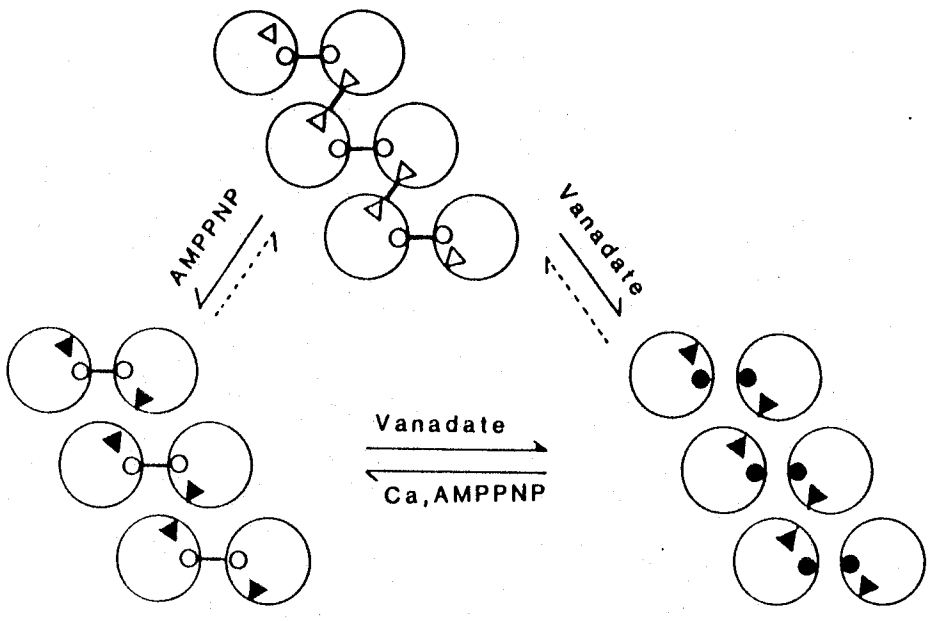

Fig. 9. Scheme proposed for the effects of AMPPNP, vanadate, and AMPPNP + Ca^{2+} on the PBM-induced cross-linking between Ca-ATPase molecules in the SR membrane.

Two kinds of the PBM binding site, Cys_{377} and Cys_{614} are represented by small circle and triangle, respectively. Open and closed symbols indicate conformations of the ATPase which lead the binding sites accessible and inaccessible to PBM, respectively.

E_2.vanadate complex (23). This raises the possibility of the Ca-ATPase molecules may exist in intact SR membrane with their phosphorylation sites facing each other to form half of the reaction site. The functional role of the ATPase-ATPase interaction in the SR membrane is unknown but the interaction between the ATPase molecules may play an important role in strictly maintaining the order of the ATPase reaction by controlling the binding or release of substrates or products at the catalytic site of the enzyme.

REFERENCES

1. Yamamoto,T., Takisawa,H., & Tonomura,Y. (1979) Curr.Top.Bioenerg. 9, 179-236
2. MacLennan,D.H., Brandl,C.J., Korczak,B., & Green,N.M. (1985) Nature 316, 696-700
3. Brandl,C.J., Green,N.M., Korczak,B.. & MacLennan,D.H. (1986) Cell 44, 597-607
4. Maruyama,K. & MacLennan,D.H. (1988) Proc.Natl.Acad.Sci.US 85, 3314-3318
5. Clarke,D.M., Loo,T.W., Inesi,G., & MacLennan,D.H. (1989) Nature 339, 476-478
6. Andersen,J.P., Vilsen,B., Leberer,E., & MacLennan,D.H. (1989) J.Biol.Chem. 264, 21018-21023
7. Vilsen,B., Andersen,J.P., Clarke,D.M., & MacLennan,D.H. (1989) J.Biol.Chem. 264,21024-21030
8. Suzuki,H., Obara,M., Kuwayama,H., & Kanazawa,T. (1987) J.Biol.Chem. 262,15448-1545
9. Saito-Nakatsuka,K., Yamashita,T., Kubota,I., & Kawakita,M. (1987) J.Biochem. 101, 365-376
10. Yasuoka-Yabe,K. & Kawakita,M. (1983) J.Biochem. 94, 665-675
11. Saito,K., Imamura,Y., & Kawakita,M. (1984) J.Biochem. 95, 1297-1304
12. Yamashita,T., & Kawakita,M. (1987) J.Biochem 101,377-385
13. Allen,G., & Green,N.M. (1976) FEBS Lett. 63, 188-192
14. Mitchinson,C., Wilderspin,A.F., Trinnaman,B.J., & Green,N.M. (1982) FEBS Lett. 146, 87-92

15. Keresztes,T., Jona,I., Pikula,S., Vegh,M., Mullner,N., Papp,S., & Martonosi,A. (1989) Biochim.Biophys.Acta 984, 326-338

16. Yamasaki,K. & Yamamoto,T. (1989) J.Biochem. 106, 1114-1120

17. Yamada,S., Yamamoto,T., & Tonomura,Y. (1970) J.Biochem. 67, 789-794

18. Goodno,C.C. (1979) Proc.Natl.Acad.Sci.US 76, 2620-2624

19. Wells,J.A. & Yount,R.G. (1982) Methods Enzymol. 85, 93-116

20. Nishimura,J.S., Petrich,J.A., Milne,A.F., & Mitchell,T. (1978) J.Biochem. 9, 93-96

21. Laemmli,U.K. (1970) Nature 227, 680-685

22. Meissner,G. & Fleischer,S. (1974) Methods Enzymol. 32, 475-481

23. Varga,S., Csermely,P. & Martonosi,A. (1985) Eur.J.Biochem. 148,119-126

24. Medda,P. & Hasselbach,W. (1983) Eur.J.Biochem. 137, 7-14

25. Coan,C. & Inesi,G.(1977) J.Biol.Chem. 252, 3044-3049

26. Guillain,F., Gingold,M.P., Buschelen,S., & Champeil,P.(1981) J.Biol.Chem. 256, 6140-6147

27. Yamada,S. & Ikemoto,N.(1978) J.Biol.Chem. 253, 6801-6807

28. Miki,K., Scott,T.L., & Ikemoto,N.(1981) J.Biol.Chem. 256, 9382-9385

29. Hasselbach,W. & Seraydarian,K.(1966) Biochem.Z. 345, 159-172

30. Murphy,A.J.(1978) J.Biol.Chem. 253, 385-389

31. Kawakita,M., Yasuoka,K., & Kaziro,Y.(1980) J.Biochem. 87, 609-617

32. Baba,A., Nakamura,T., & Kawakita,M.(1986) J.Biochem. 100, 1137-1147

BIBLIOGRAPHY

1. Yamasaki,K., & Yamamoto,T. (1989)
Effects of Adenyl-5'-Imidophosphate and Vanadate Ion on the Intermolecular Cross-Linking of Ca^{2+}-ATPase in the Sarcoplasmic Reticulum Membrane with N,N'-(1,4-Phenylene) bismaleimide
J.Biochem. 106, 1114-1120

2. Yamasaki,K., Sano,N., Ohe,M., & Yamamoto,T. (1990)
Determination of Primary Structure of Intermolecular Cross-Linking Sites on the Ca^{2+}-ATPase of Sarcoplasmic Reticulum Using ^{14}C-Labeled N,N'-(1,4-Phenylene)bismaleimide or N-Ethylmaleimide
J.Biochem. 108, 918-925

3. Yamasaki,K, & Yamamoto,T. (1991)
Existance of High- and Low-Affinity Vanadate Binding sites on Ca^{21+}-ATPase of the Sarcoplasmic Reticulum
J.Biochem. 110, 915-921

4. Yamasaki,K, & Yamamoto,T.
Effects of Vanadate binding to High- and Low-Affinity Sites on the Phosphorylation of Sarcoplasmic Reticulum Ca^{2+}-ATPase by Phosphate
in preparation

ACKNOWLEDGEMENTS

I wish to express my sincere thanks to Professor Takao Nakamura and Associate Professor Taibo Yamamoto of Osaka University for their helpful guidance and valuable advices throughout this work. I am greatly indebted to Dr. Haruhiko Takisawa for his excellent advices and valuable suggestions. I am grateful to Drs. Akio Inoue and Toshiaki Arata for their helpful suggestions and discussions.

I am indebted to Dr. Masato Ohe of Dokkyo University, School of Medicine, for analysis of amino acid composition. I would like to thank Mr. Naoto Sano for his great assistance to study of part IV.

I am also grateful to the members of Professor Nakamura's laboratory for their kind help during this study.